6-2021

Deposition and Diagenesis of the Blossom Sand, Panola County, Texas

Hannah Chambers
hchambers@jacks.sfasu.edu

Deposition and Diagenesis of the Blossom Sand, Panola County, Texas

Creative Commons License

Deposition and Diagenesis of the Blossom Sand, Panola County, Texas

By

Hannah C. Chambers, Bachelor of Science

Presented to the Faculty of the Graduate School of
Stephen F. Austin State University
In Partial fulfillment
Of the Requirements

For the Degree of
Master of Science

Stephen F. Austin State University
May 2021

Deposition and Diagenesis of the Blossom Sand, Panola County, Texas

By

Hannah C. Chambers, Bachelor of Science

APPROVED:

Dr. Julie Bloxson, Thesis Director

Dr. LaRell R. Nielson, Committee Member

Dr. Melinda Faulkner, Committee Member

Dr. Robert Friedfeld, Committee Member

Pauline M. Sampson, Ph.D.
Dean of Research and Graduate Studies

ABSTRACT

The Late Cretaceous Blossom Sand within the Austin Group is a historic gas reservoir in the East Texas basin, located at depths of approximately 2,000 ft below the surface. Since the discovery of the Carthage Field in 1918 in the East Texas Basin, the Blossom Sand has produced approximately 26 BCF of gas with minor amounts of oil. Despite its notoriety in the Carthage Field, there is very little research that has been conducted on this unit, although it crops out in northeast Texas and is found in the subsurface of southwest Arkansas, western Louisiana, and the East Texas Basin. The origin of its sediments, clay minerals, and depositional style have gone largely unknown. This study provides insights into the depositional environment and diagenetic history of the Blossom Sand using thin section analysis, x-ray diffraction (XRD), x-ray fluorescence (XRF), scanning electron microscopy (SEM), and porosity and permeability measurements. Each of these methods were used to identify clay minerals and their associations and variability, and correlated with porosity/permeability throughout the core to determine controls.

The major minerals found in this formation include quartz, calcite, and illite; accessory minerals include, plagioclase, muscovite, biotite, hematite, and siderite. Despite the literature stating that glauconite is common, it was not detected in any of the analyses. The Blossom Sand is composed of two major sand facies that contain planar lamination, wavy bedding, bioturbation, pellets, casts and molds of *Inoceramus sp.*

bivalves and one specimen of *Exogyra sp*. These sand facies are interbedded with shales and siltstones throughout. The porosity varies from 2.6-33.7% with an average of 23.8%, while the permeability varies from 0.0002-146 mD, with an average of 25.4 mD. The porosity and permeability are inversely correlated with calcite content based upon Ca from the XRF data, indicating that calcite cement is the main controlling factor on porosity and permeability within the Blossom. The fine sands and sedimentary structures indicative of multidirectional currents and shallow marine fossils suggest that the sands were deposited in nearshore environments. The presence of trace fossils such as casts and molds indicate that dissolution and redistribution of local biogenic carbonate resulted in the calcite cement that controls the porosity and permeability of the Blossom Sand. Gaining a better understanding of the nature of porosity and permeability in sandstone reservoirs like the Blossom Sand can improve success in oil and gas exploration, secondary recovery, or carbon capture and storage.

PREFACE

This thesis has previously been accepted for publication at the South Texas Geological Society Bulletin in March 2021. This manuscript will be published in the GCAGS Journal in 2022. The original manuscript submitted to the South Texas Geological Society Bulletin was a short research summary and diagenetic history, while the new manuscript includes more data and a more detailed depositional and diagenetic history. Further details on stratigraphy and methods are also found in the appendices for further reference.

ACKNOWLEDGEMENTS

I would like to thank my thesis advisor Dr. Julie Bloxson and the rest of my thesis committee for their guidance and support throughout this project. I would also like to thank the Stephen F. Austin State University Department of Geology and the South Texas Geological Society for providing funding that made this project possible.

TABLE OF CONTENTS

LIST OF FIGURES

LIST OF TABLES

1. Introduction

The Late Cretaceous Blossom Sand of the Austin Group consists primarily of fine to medium grained quartz sandstones deposited in a nearshore, tidally influenced, shallow marine environment, with secondary clay minerals precipitated throughout. It is found in the subsurface of east Texas, southwest Arkansas, and western Louisiana with outcrops located in northeast Texas (Stephenson, 1918). In Panola County, Texas, the Blossom Sand is a well-known gas reservoir within the Carthage Gas Field. As of August 2019, it had produced 26 BCF of gas since 1961 (Enverus, 2020).

Despite its notoriety in the Carthage Gas Field, there has been very little research conducted on this unit. Numerous AAPG Bulletins from as early as the 1920's note oil and gas production from the Blossom Sand in various fields within northern Louisiana parishes, yet descriptions of the Blossom only give vague descriptions, stating that it is a fine to medium grained quartz sandstone with glauconite throughout. However, research on the Blossom specifically is scarce. The lack of in-depth research is partially because most literature that mentions this formation was published prior to widespread use of advanced analytical methods such as x-ray diffraction (XRD), x-ray fluorescence (XRF), and scanning electron microscopy (SEM). The Blossom is also primarily found in the subsurface, is relatively thin (50-90 feet), and produces exclusively within the East Texas Basin.

In order to gain a better understanding of the Blossom Sand, here we study the mineralogy, geochemistry, grain size, and sedimentary structures from core sourced from Panola County, TX, in order to determine the depositional and diagenetic history, and controls on porosity and permeability on this gas sand reservoir in East Texas.

2. Geologic Setting

This research focuses on the Blossom Sand in the Carthage Gas Field of Panola County, Texas (Figure 1). The Carthage Gas Field is located on the east flank of the East Texas Basin on top of the Sabine Uplift. The Sabine Uplift is a structural high that bestrides the border of Texas and Louisiana. It is bound to the west by the East Texas Basin and to the east by the Minden and Winnfield Basins of Louisiana.

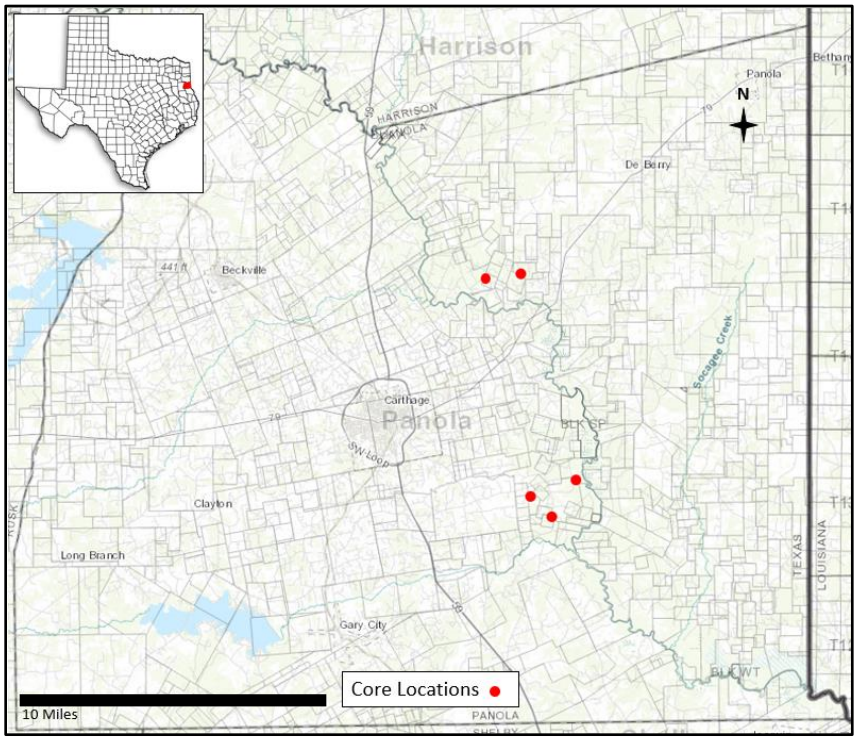

Figure 1. Study area and core locations.

Since the Paleozoic, the Sabine Uplift has been a positive anomaly. This mid-rift horst is the result of tensional forces that are also responsible for the formation of the East

Texas Basin (Adams, 2009). During this time the study area was located at 10-15°N and rifting of the region resulted in steeply dipping normal faults throughout the East Texas Basin. This was a period of thermal uplift that resulted in sea level retreat that prompted deposition of the Werner Anhydrite, Louann Salt and the clastic sediments of the Norphlet. Thinning of inner shelf deposits of the Louann Group across the Sabine Uplift followed by shoaling facies in the Cotton Valley Lime on the western flank indicate a period of uplift during the Late Jurassic. The Sabine Uplift experienced no vertical movement from the Late Jurassic through the Early Cretaceous. During this time, a southeast sloping basin existed on top of the Sabine Uplift. In East Texas and North Louisiana, the presence of an angular unconformity indicates upwarping that occurred across the Sabine Uplift during the Late Albian. At the beginning of the Late Cretaceous, the Sabine Uplift began to slowly subside while maintaining elevation higher than the East Texas Basin (Jackson and Laubach, 1988). As the Late Cretaceous Austin Group was being deposited, regional subsidence of the Sabine Uplift combined with minor warping resulted in sea level fluctuations in the area. Sedimentation during this time was largely uninterrupted with the exception of minor hiatuses. As upwarping led to a minor fall in sea level, sands were deposited in the resulting shallow areas (Figure 2). These were likely the conditions in which the Santonian Blossom Sand was deposited (Rogers, 1968; Young, 1963).

As Gulfian deposition drew to a close, regional uplift resumed, causing sea level to retreat from the north. During the Early Cenozoic, the Sabine Uplift continued to rise

very slowly. The depositional environments at this time consisted of continental, lagoonal and likely deltaic settings. By the end of the Miocene, severe erosion over the Sabine Uplift removed overlying sediments down to the Wilcox Group (Rogers, 1968).

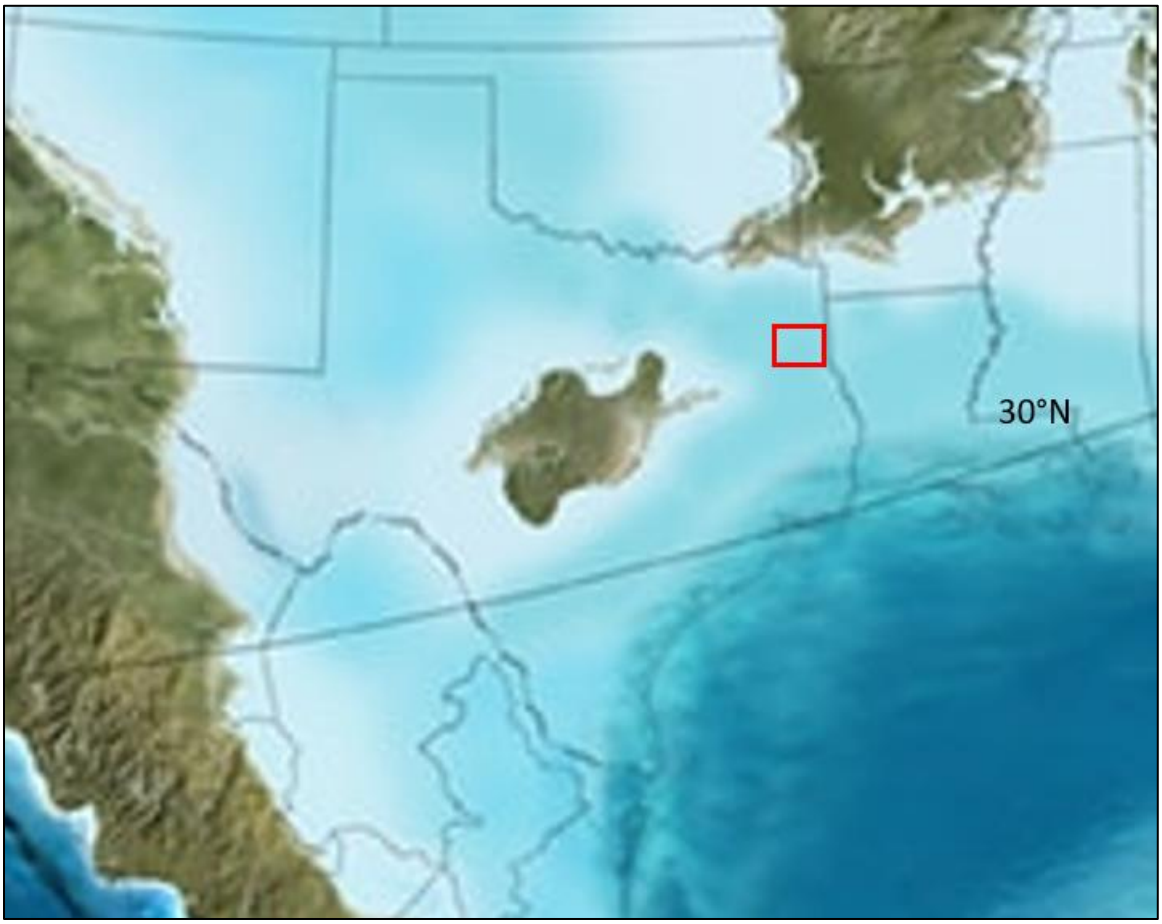

Figure 2. The study area during the Santonian (Modified from Blakey Maps, 2020). Shallow seas covered the area, resulting in fine to medium grain siliciclastic deposits across the area.

3. Stratigraphy

In Panola County, the Austin Group can be divided into four separate formations (Rogers, 1968). These formations include the Ector, Bonham Clay, Blossom Sand and the Brownstown Marl (Figure 3.). This study focuses on the Blossom Sand.

The Santonian Blossom Sand conformably overlies the Bonham Clay (Young, 1963; Rogers, 1968). These shallow marine sandstones range in thickness from 50 to 90 feet. This unit consists of greyish-green, medium to fine-grained, illitic, calcareous sandstones interbedded with dark green shales (Rogers, 1968). Though the Blossom Sand is sparsely fossiliferous, it is known to contain two genera of sharks and more than thirty species of mollusks. *Inoceramus deformis* and *Exogyra ponderosa* fossils are common mollusks, and fossilized teeth from sharks, *Corax* and *Otodus* are found in the Blossom Sand (Stephenson, 1918).

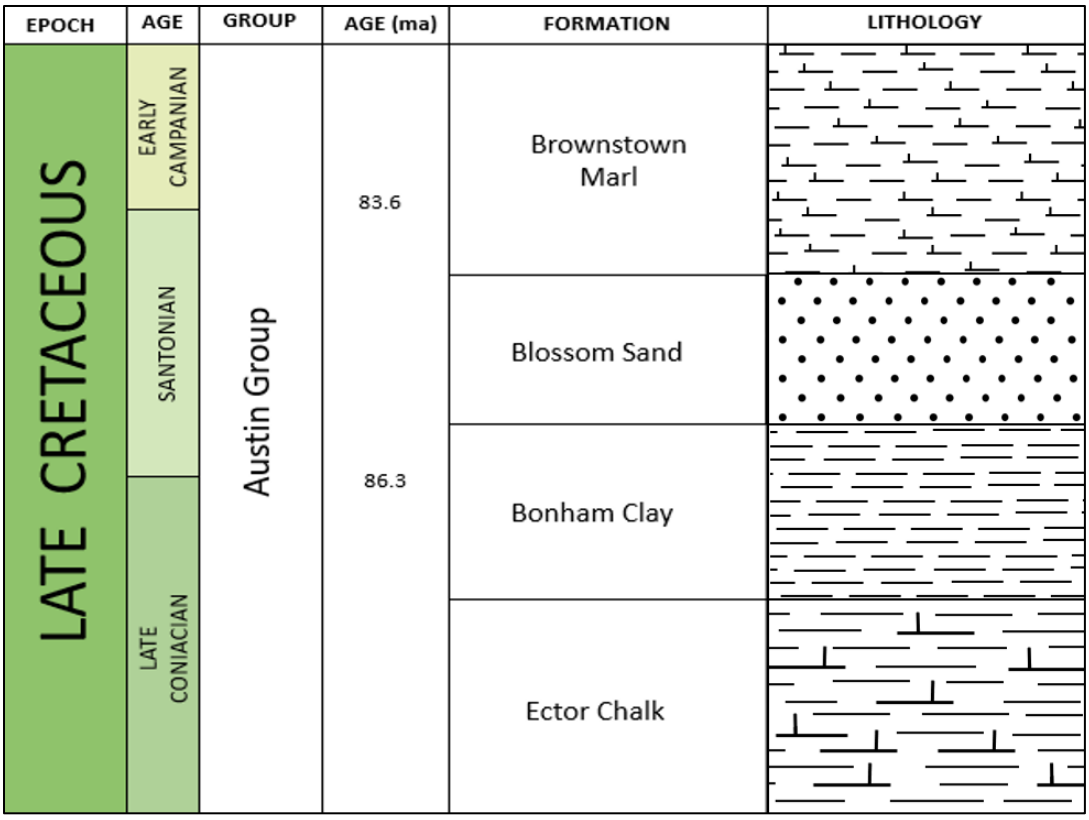

Figure 3. Stratigraphic Column of the Austin Group in Panola County, Texas.

4. Methodology

A combination of XRD, XRF, SEM, petrophysical analysis, and core analysis were used in this study to determine depositional and diagenetic history, along with controls on porosity and permeability. The primary source of data are five cores collected from Panola County, TX and archived in the East Texas Core Repository, Stephen F. Austin State University, Nacogdoches, TX (Table 1). The cores have a combined length of 216 feet. All five of the cores include butt ends, with one of the five containing an interval of seven slab packs.

Table 1. Details of the core used in this study.

Core No.	**API**	**Well Name**	**Top Depth (ft)**	**Bottom Depth (ft)**
146	4236530251	No.3-A Gena Williamson	2026	2062
150	4236534070	Carthage Gas Unit No. 9-4A	1985	2044
151	4236534131	Carthage Gas Unit No. 9-5A	1986	2014
153	4236534412	No.1 Werner Smith	2058	2098
156	4236534711	Borders Smith No. 1-A	2010	2064

A detailed description of each core noted sedimentary structures, grain sizes, fossils and lithologies, which were used to determine the Blossom Sand's depositional environment. Lithofacies were correlated across the five cores. Ten thin sections were made by National Petrographic to analyze grain size distribution, identify porosity types and sedimentary petrography. The thin sections were impregnated with blue epoxy to highlight porosity. The thin sections were analyzed using a Labomed Lx POL Polarizing microscope. Each thin section was analyzed under 400x magnification under cross polarized light and plane polarized light to observe primary and secondary porosity, verify mineralogy obtained by xrd, and observe relationships between minerals and pore spaces. To obtain grain size distributions, a photo of each thin section was taken under 400x magnification in cross polarized light. ImageJ was used to perform particle analysis with a 100point count on each of the photos.

XRD was used to identify the bulk mineralogy on four samples. Sample prep followed Eberl (2008). The samples were run on a Bruker D8 Advance diffractometer with an angle range from 5° to 65° 2Θ, a step size of 0.02° 2Θ, 2 seconds per step, and a voltage/amp of 40 kV/40 mA. The resulting data was analyzed for mineral content and quantity using RockJock from the USGS (Eberl, 2008).

Trace elemental analysis was conducted using the Thermo Fisher Scientific Niton XL3t GOLDD^{+} XRF Analyzer. The device was set to the Test All Geo setting and used to sample each of the five cores at a resolution of four inches for a total of 180 seconds (30 seconds main, low and high each, and 90 seconds on light). Cores were rinsed with

deionized water, and measured down core, avoiding anomalies such as lone body fossils, and small concretions (<10 cm in diameter). The resulting geochemical data was processed in Excel. Areas containing abundances of Fe, Al and Mg were identified as areas of high clay content. Areas containing high concentrations of Ca were identified as areas of high calcite content.

Eleven plugs were extracted from the core to obtain porosity and permeability measurements by Stratum Reservoir, Houston, TX. Locations for the plugs were chosen based on the varying amount of clay minerals throughout the core that were identified from the geochemical data. The eleven plugs were taken from areas exhibiting high, moderate and low clay content. Samples were convection dried at 140°C. The porosity and permeability were then taken at a net confining stress of 800 psi, following protocols at Stratum Reservoir. The permeability measurements were corrected using the Klinkenberg method.

Sampling locations for SEM were chosen based on the concentration of Fe, Ca, Al, Si and Mg from the XRF data. To obtain higher quality images, chips of samples were coated with gold and vanadium to increase their conductivity. Using a JEOL Scanning Electron Microscope, SEM was conducted on four samples to help provide insight as to the origin of the glauconite and the order of events that occurred as diagenesis progressed within the Blossom Sand. These images displayed the orientation of the sand grains, clay minerals, pore spaces, and any other clays that were present.

5. Results

5.1 XRD

XRD results indicate the presence of primarily quartz, calcite, siderite, biotite, and illite in the Blossom Sand. The mineral composition is similar across the four samples. However, calcite is present only in the clean, well-cemented sections of sandstone (Figure 4-A), compared to the samples containing abundant clay minerals (Figure 4-B).

Table 2. Cores and depths from which XRD samples were taken.

Sample Number	**Core Number**	**Depth (Ft)**
1	150	2012.07
2	153	2014.06
3	153	2029.04
4	150	2026.02

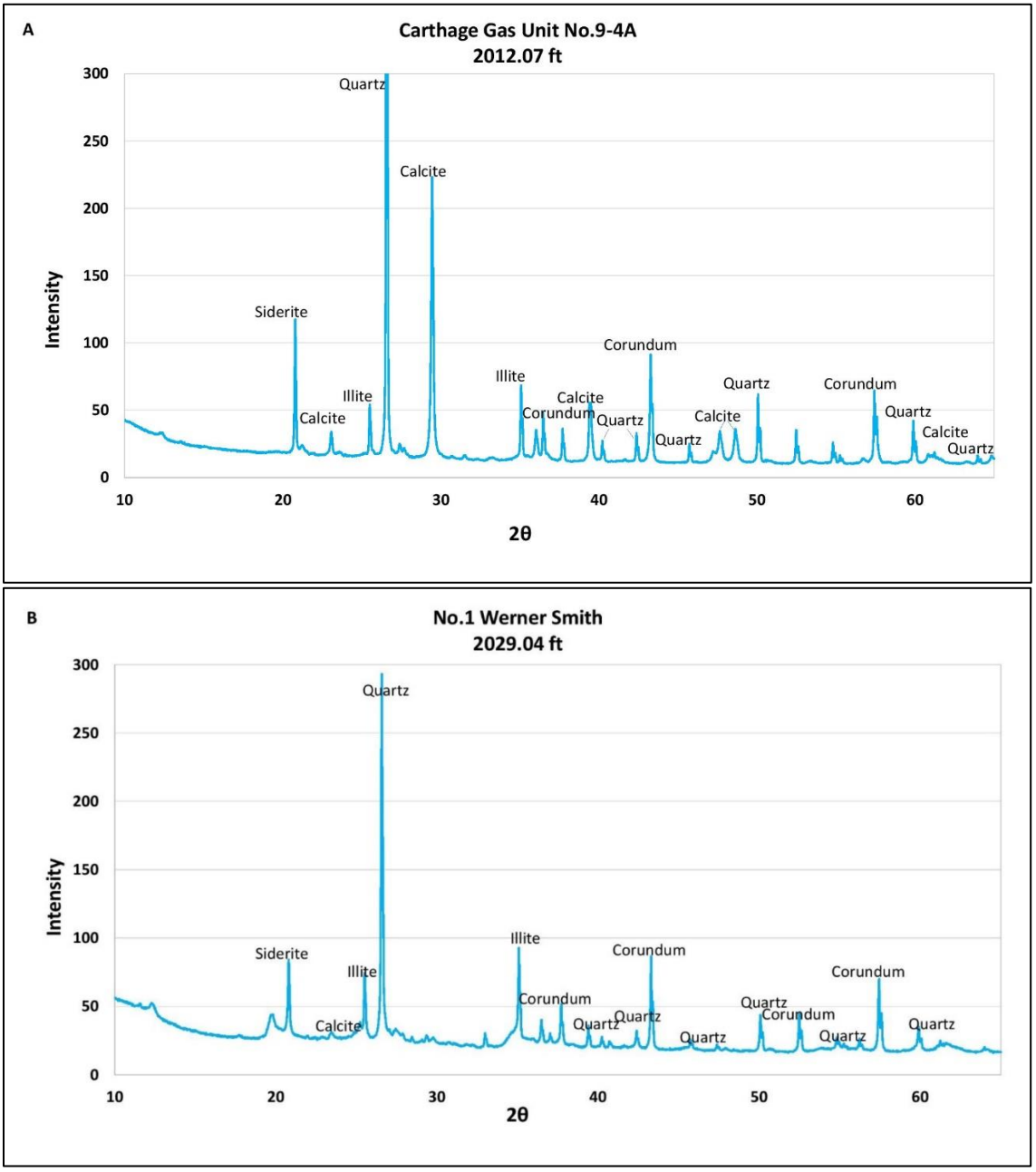

Figure 4. Diffractograms displaying the actual mineralogy of a (A) calcite cemented sandstone and (B) a sandstone containing no calcite with an abundance of authigenic illite. In the top right of each, are the actual samples from the core.

5.2 XRF

Ca, Fe, Al, and Mg were plotted with depth to observe variation in calcite (Ca) and illite (Fe, Al, Mg) content (Figure 5). In the plots for each core, it was noted that there were several depths at which Ca concentration increased, and concentrations of clay mineral components (Fe, A, Mg) decreased at these locations. Because few macrofossils were observed in the cores and only one *Foraminfera* was observed in thin section, high concentrations of Ca could not be attributed to calcite in body fossils. Therefore, depths with high concentrations of Ca were interpreted to be cemented with calcite.

5.3 Porosity and Permeability

To understand if porosity and permeability inhibition are linked to calcite cement or authigenic clays, samples for porosity and permeability testing were chosen based on the concentrations of Ca, Fe, Al and Mg. The resulting porosity and permeability data were plotted against Ca concentrations from the depths at which each individual sample for porosity and permeability was taken. The graphs for each display inversely proportional relationships between Ca and porosity as well as Ca and permeability (Figures 6 & 7). Regression statistics revealed an R^2 value of 0.84 for Ca-Porosity while Ca-Permeability resulted in an R^2 value of 0.11. The poor correlation with Ca and permeability is due to the wide range of permeability values, and the few points with extremely low permeabilities. The R^2 values indicate that calcite ultimately controls the porosity and permeability of the Blossom Sand.

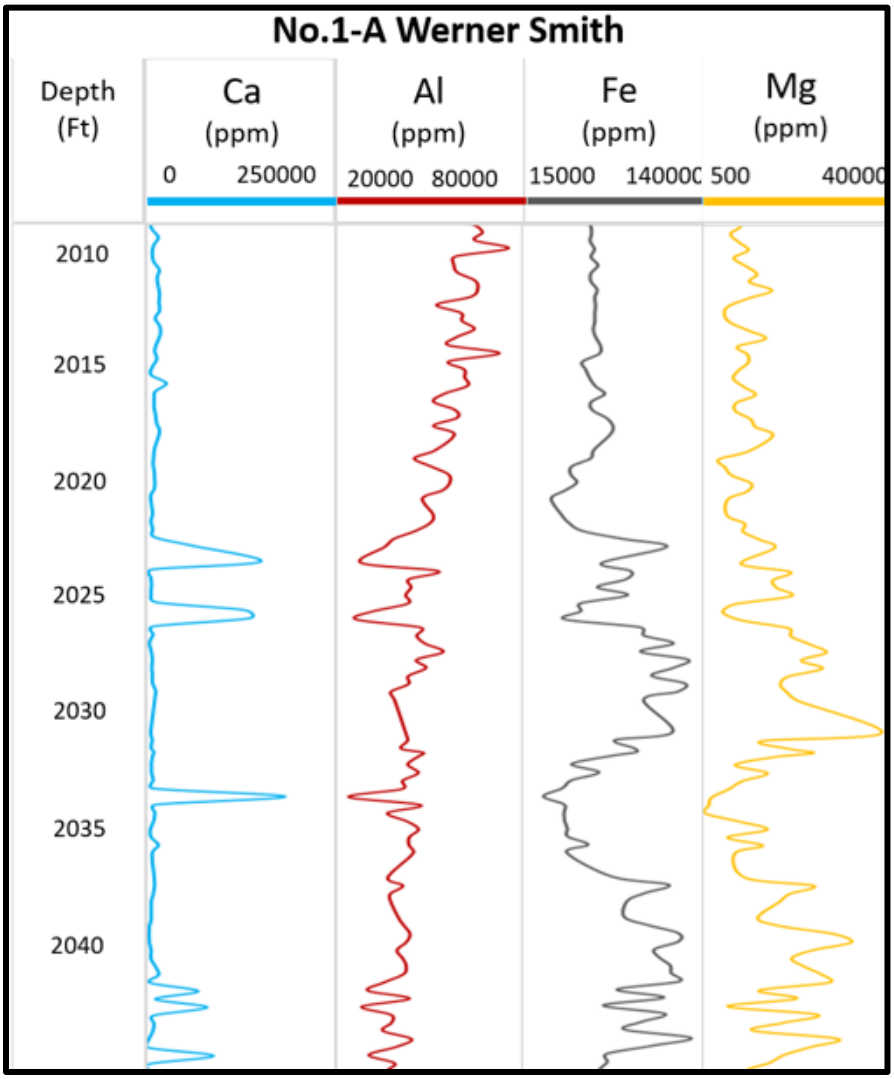

Figure 5. Variation of calcite (Ca) and illite (Fe, Al, Mg) with depth for an example core.

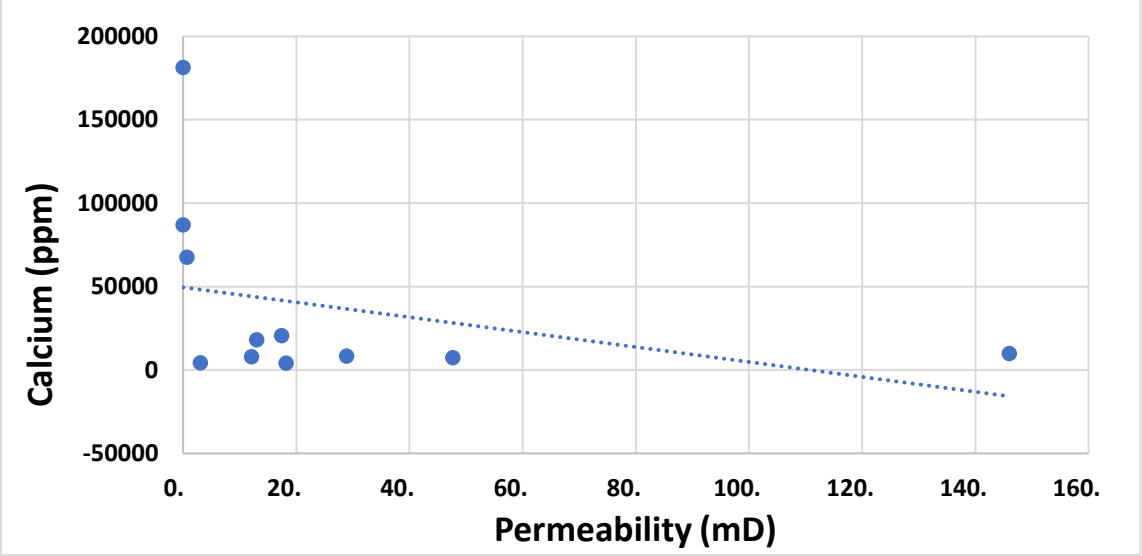

Figure 6. Relationship between calcium content and permeability in the Blossom Sand.

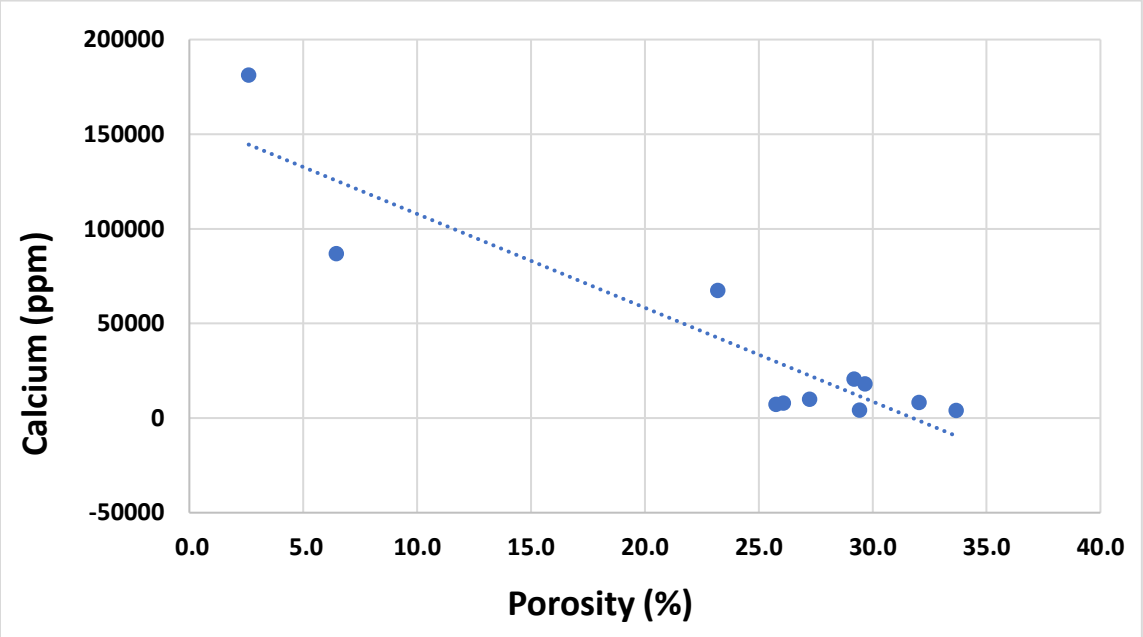

Figure 7. Relationship between calcium content and porosity in the Blossom Sand.

5.4 SEM

The SEM images display minerals and pore spaces that coincide with the findings from the porosity and permeability data. Figure 8 displays a calcite cemented interval (Figure 8(A)) compared to an illite cemented interval (Figure 9 (B)) at similar magnifications. In Figure 8 (A), the pore spaces between the calcite and chlorite are approximately 1-10 µm wide. Conversely, Figure 8 (B) displays a pore space typical of the illite cemented sandstones of the Blossom Sand. Even with considerable illite precipitated around each sand grain, the pore spaces are approximately 100 µm wide. In addition to supporting the porosity and permeability data, clay minerals that formed prior to the beginning of diagenesis are displayed as pellets that have undergone ductile deformation as the sands started to compact. Authigenic clays are displayed as groups of thin platelets and fibrous clusters that formed between the compacted sand grains. Fecal pellets often display ductile or brittle deformation that occurred as a result of physical compaction of the sands (Figure 10). The SEM also showed chlorite (Figure 8-A) and kaolinite (Figure 9), whose concentrations were too low to be detected by the XRD.

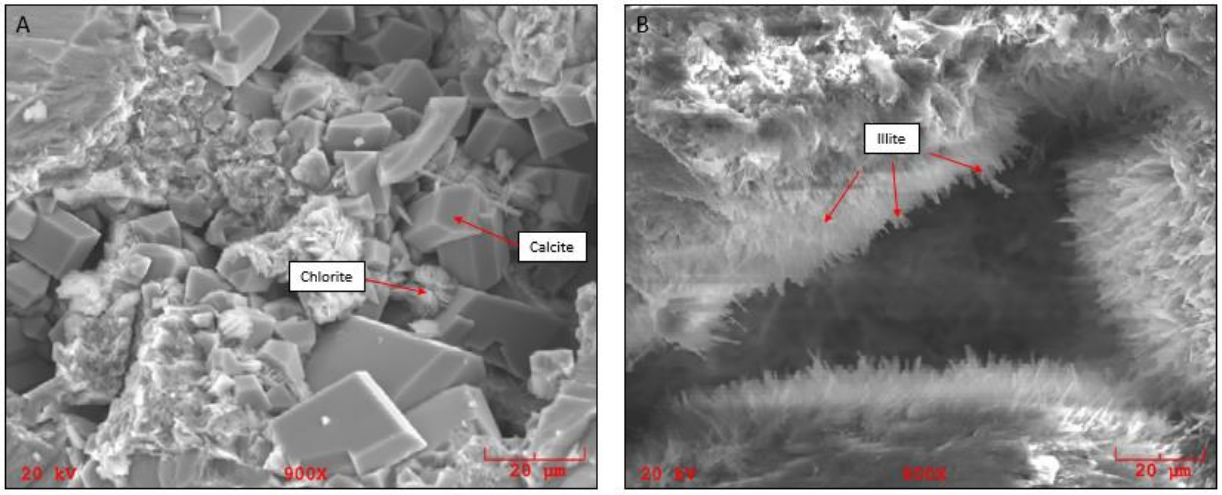

Figure 8. SEM images of the Carthage Gas Unit No.9-4A. (A) Calcite cemented sandstone at 2011.92 feet. (B) Pore space between three sand grains coated with fibrous crystals typical of authigenic clays from a sandstone with no calcite from 2016.62 feet.

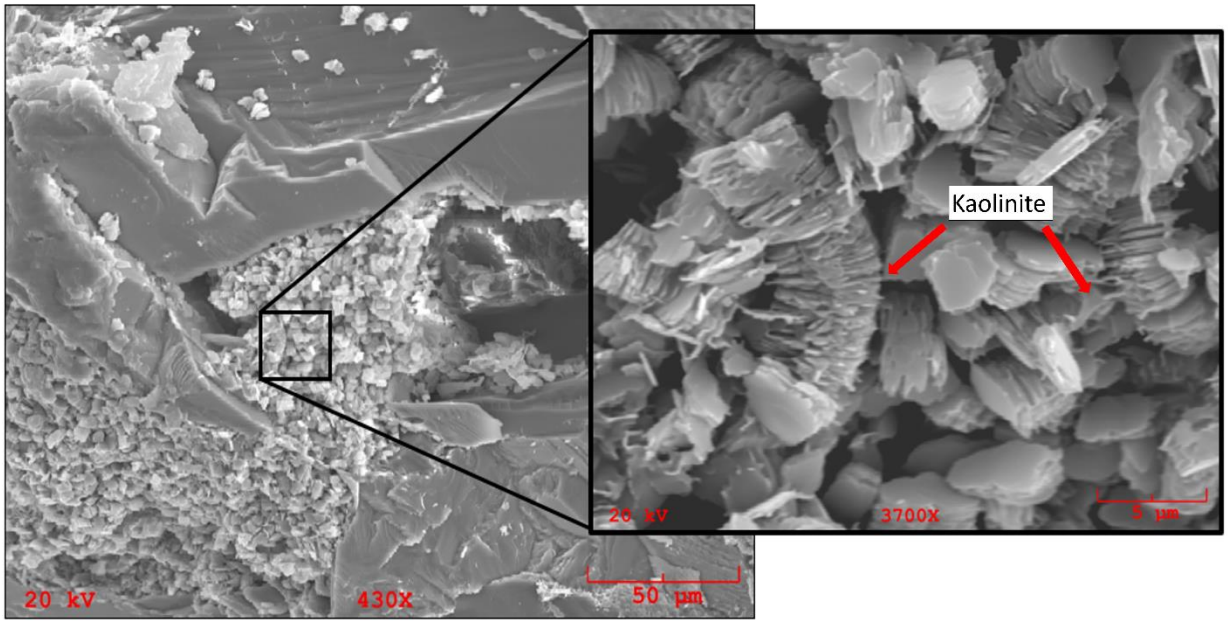

Figure 9. A pore space obstructed by kaolinite from a calcite cemented sandstone at 2011.92 ft in the Carthage Gas Unit No.9-4A.

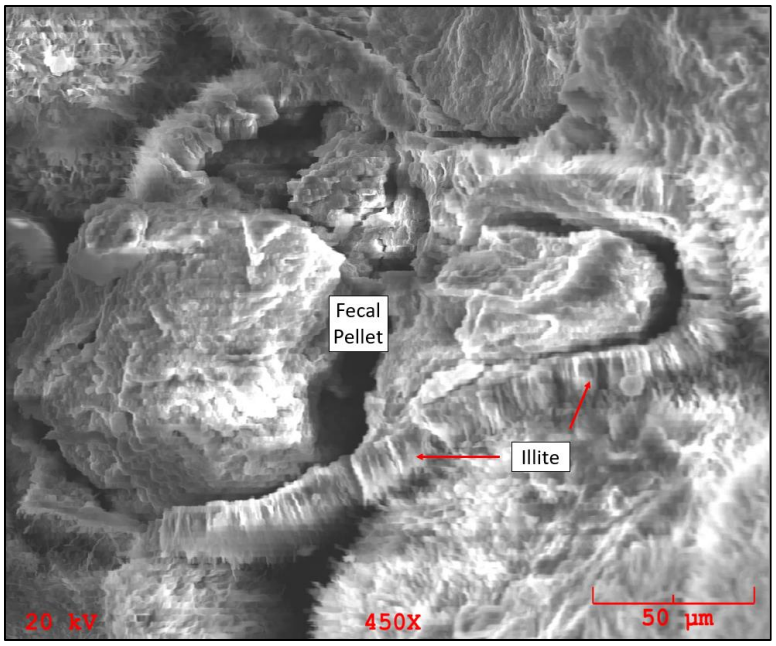

Figure 10. A fecal pellet deformed during compaction.

According to the particle analyses conducted on the thin sections, the grain size of the Blossom Sand varies from 1-7 ϕ (Figure 12). Due to the excess of fine silt found in the Blossom Sand, the histogram displays the sediments of this formation as slightly negatively skewed (Figure 11).

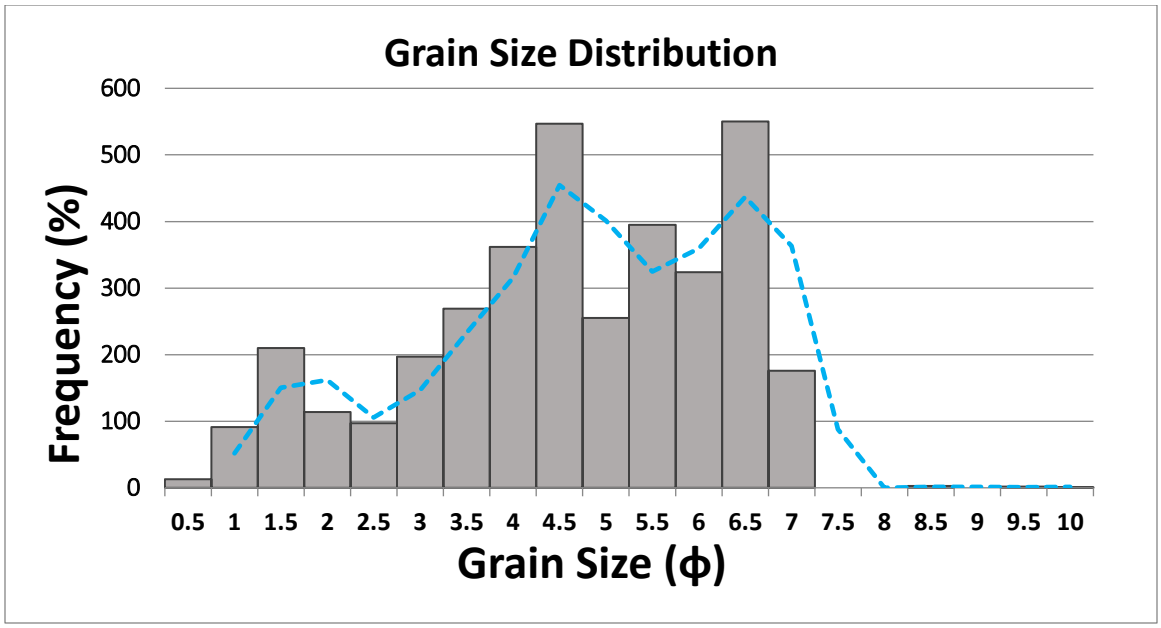

Figure 11. Grain size distribution of the Blossom Sand.

5.5 Thin Sections

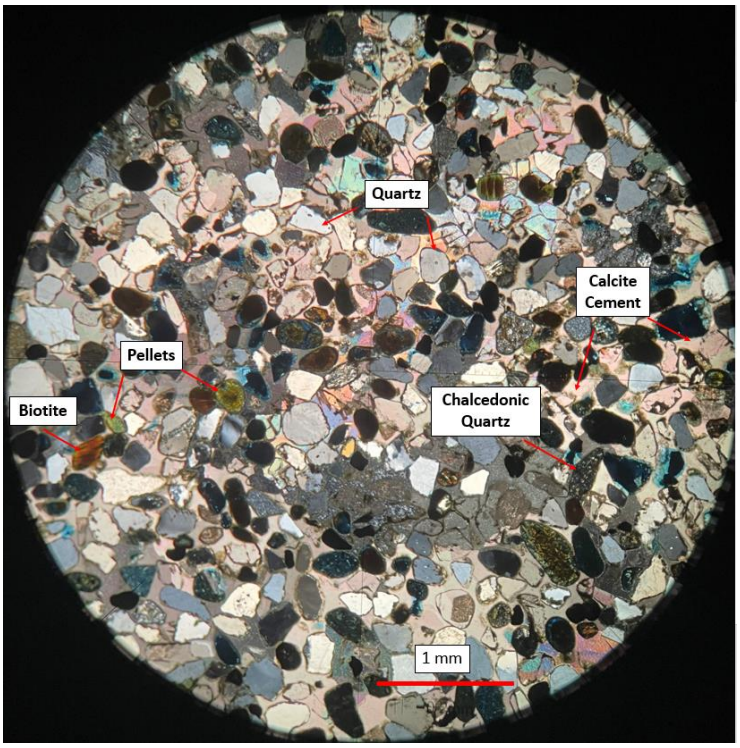

Figure 12. Thin Section A at 400x magnification under cross polarized light. Thin section A is from a calcite cemented sandstone at 2012 feet in the Carthage Gas Unit No.9-4A

Figure 12 is a quartz arenite and has an average grain size of 3.9 **ϕ**. The clasts found in this sample are subrounded to well-rounded and are moderately sorted (Figure 12, 13). Point counts indicate that this thin section is composed of 42% quartz grains, 1% chalcedonic quartz, 9% pellets and 35% calcite cement. SEM images display biotite and kaolinite clays in this sample as well. This sample has undergone mechanical compaction likely from the gradual addition of overlying sediments. Most sand grains are very close

together and touching at least one other. Additionally, the pellets display ductile deformation from being compressed between the harder quartz and chalcedonic quartz sand grains.

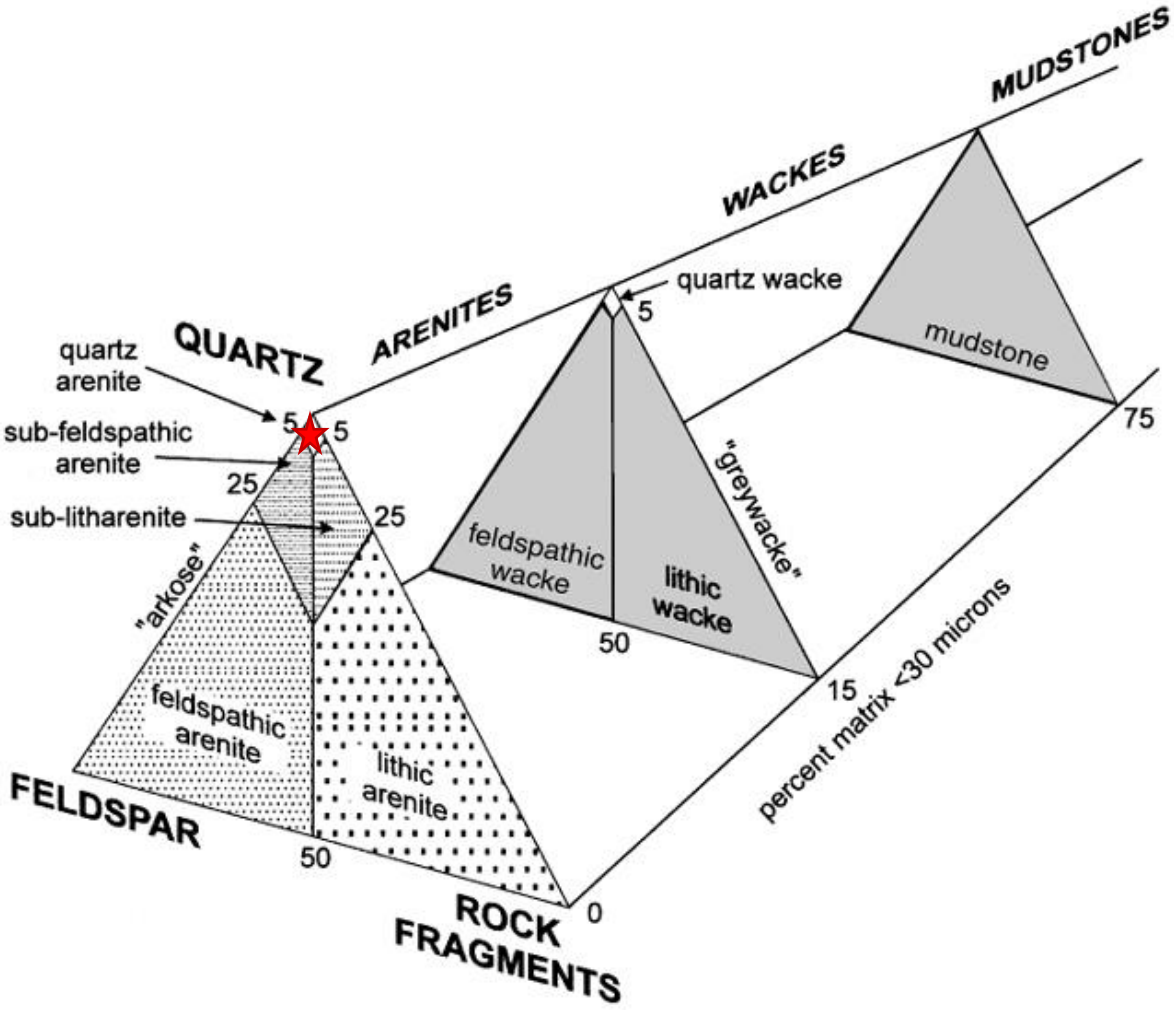

Figure 13. Composition of sample A places it within quartz arenite of the modified Dott classification noted by a red star, after Pettijohn et al., (1987).

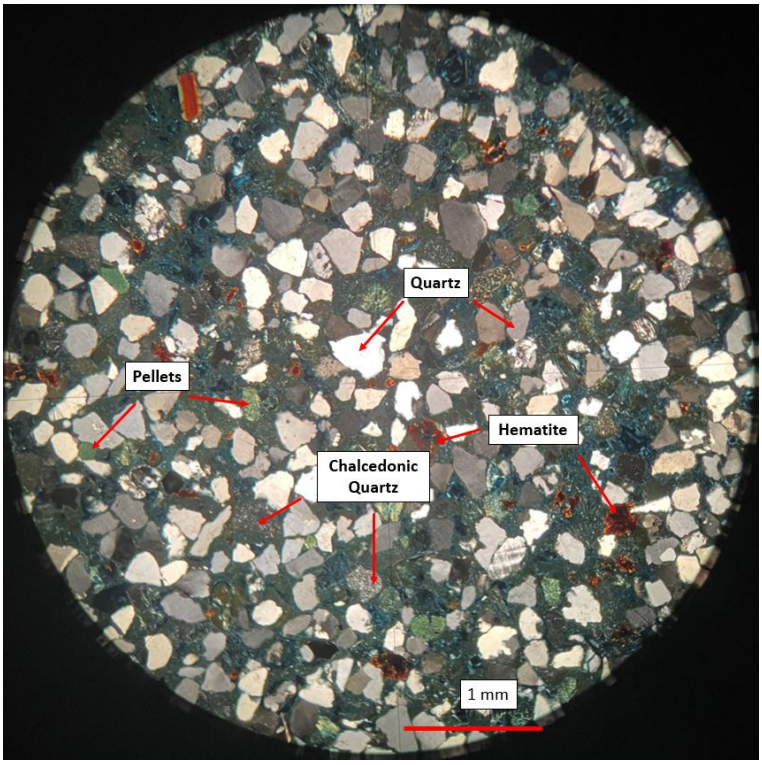

Figure 14. Thin Section B at 400x magnification under cross polarized light. Thin section B is from a sandstone at 2016 feet from the Carthage Gas Unit No.9-4A.

The quartz wacke found at 2016 in the Carthage Gas Unite No. 9-4A well has an average grain size of 3.9 **ϕ**. The clasts found in this sample are angular to subrounded and are well sorted. The sandstone displayed in this thin section is composed of 61% quartz, 1% chalcedonic quartz, 4% pellets, 2% hematite and 25% matrix. This sample has undergone a considerable amount of mechanical compaction as most of the pellets display ductile deformation and the quartz and chalcedonic quartz grains are closely compacted (Figure 14, 15).

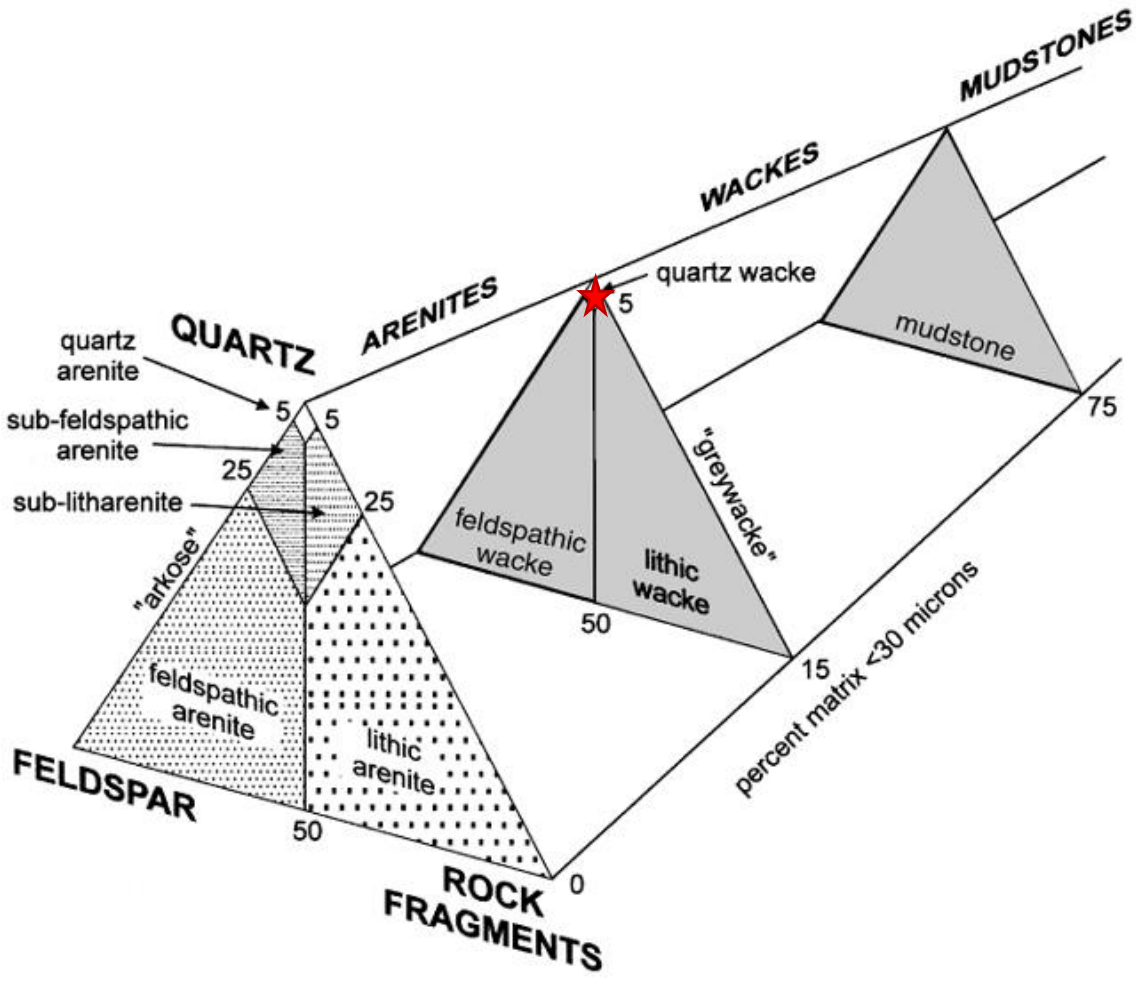

Figure 15. Composition of sample B places it within quartz wacke of the modified Dott classification noted by a red star, after Pettijohn et al., (1987).

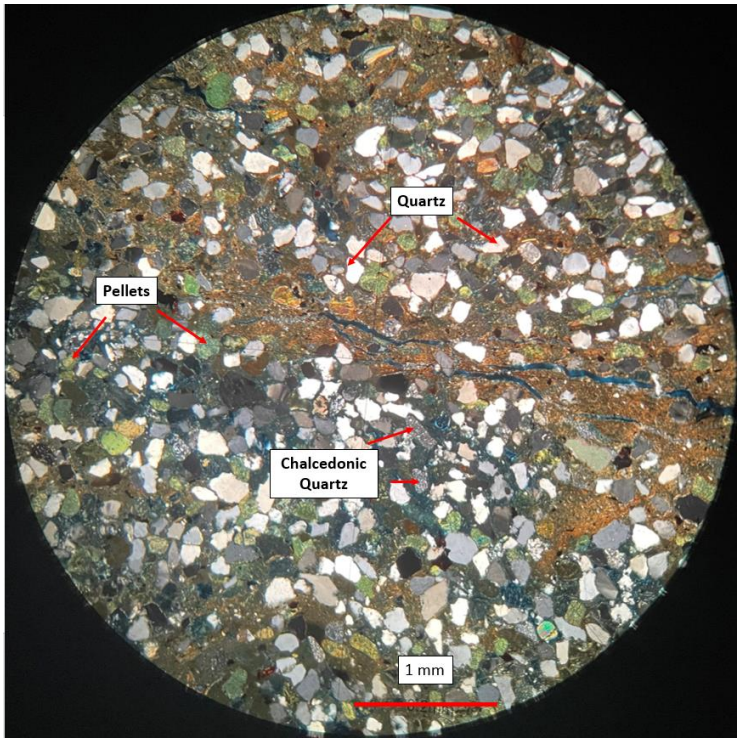

Figure 16. Thin Section C at 400x magnification under cross polarized light. Thin section C is from a sandstone at 2022 feet from the Carthage Gas Unit No. 9-4A.

The quartz wacke from 2022 feet from the Carthage Gas Unite No. 9-4A well has an average grain size of 1.2 **ϕ** (Figure 16, 17). The clasts found in this sample are angular to subrounded and well sorted. The sandstone displayed in this thin section is composed of 50% quartz, 10% chalcedonic quartz, 8% pellets 13 hematite and 16% matrix. This sample is very well compacted as there is very little to no space between grains and pellets display ductile deformation from being compressed amongst quartz grains. There is secondary porosity exhibited by the fractures in the reddish-brown detrital clays.

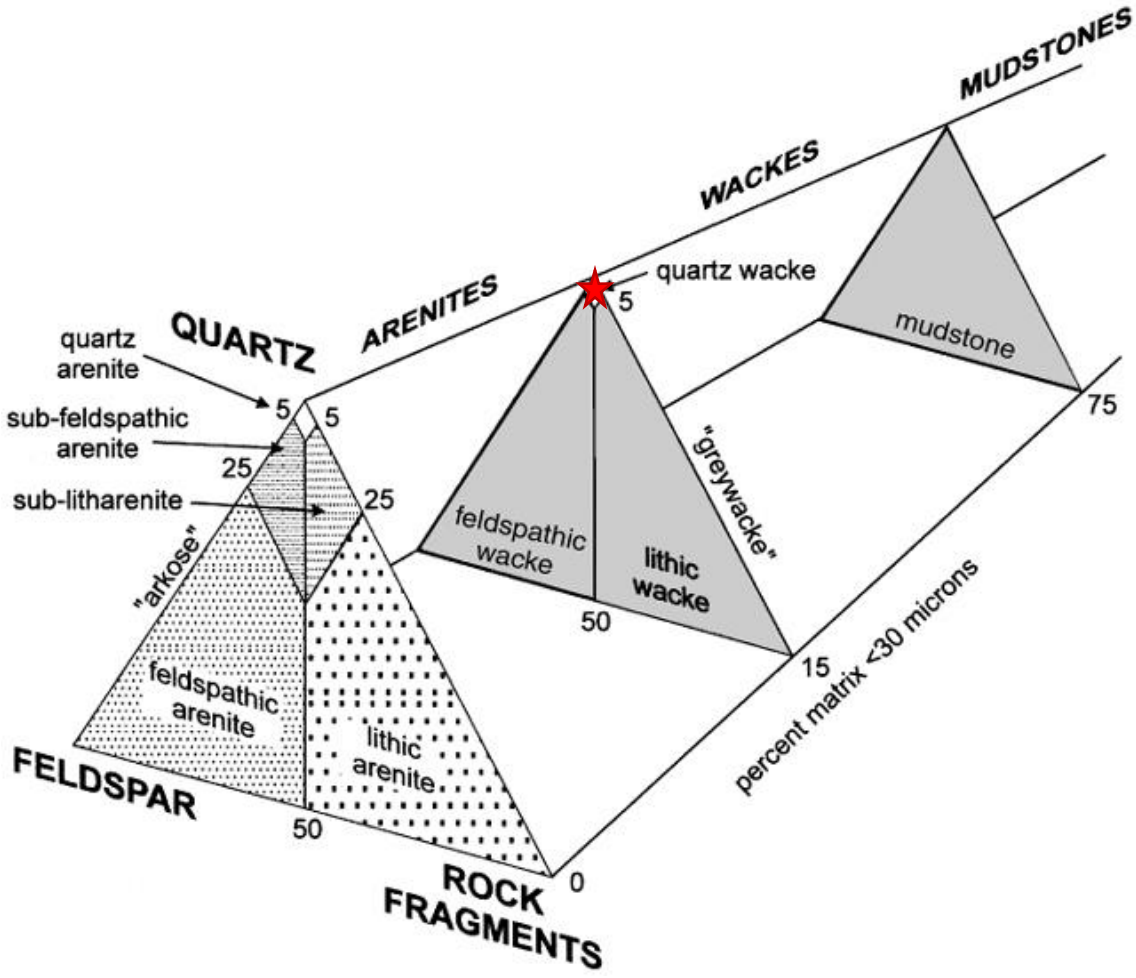

Figure 17. Composition of sample C places it within quartz wacke of the modified Dott classification noted by a red star, after Pettijohn et al., (1987).

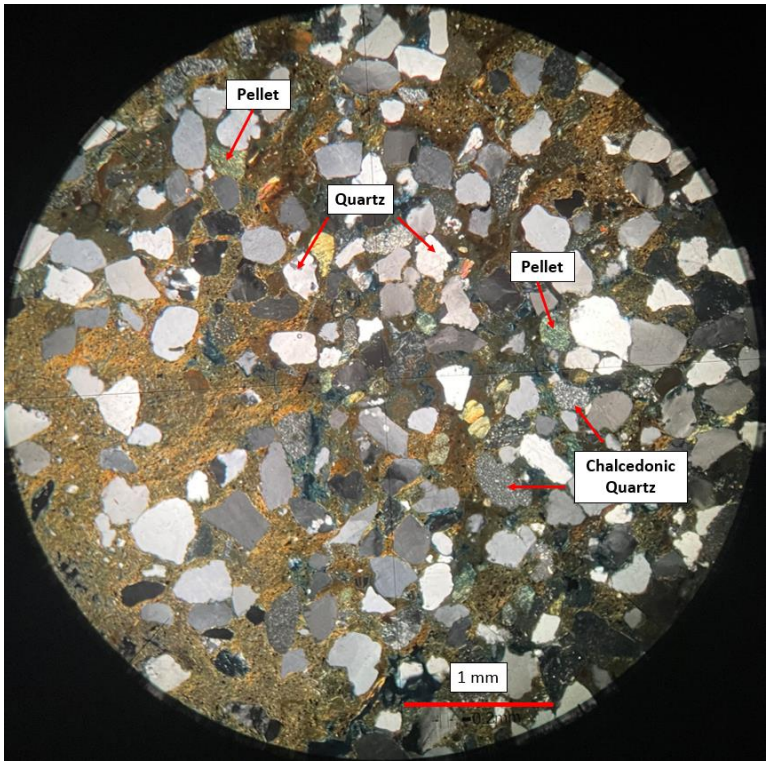

Figure 18. Thin Section D at 400x magnification under cross polarized light. Thin section D is from a sandstone at 2037 feet from the Carthage Gas Unit No. 9-4A.

The quartz wacke from 2037 feet has an average grain size of 4 **ϕ** (Figure 18, 19). The clasts found in this sample are subangular to subrounded and are moderately sorted. The sandstone displayed in this thin section is composed of 44% quartz, 11% chalcedonic quartz, 2% pellets and 43% matrix. This sample is very well compacted as there is little to no space between grains, and pellets display ductile deformation from being compressed between quartz grains.

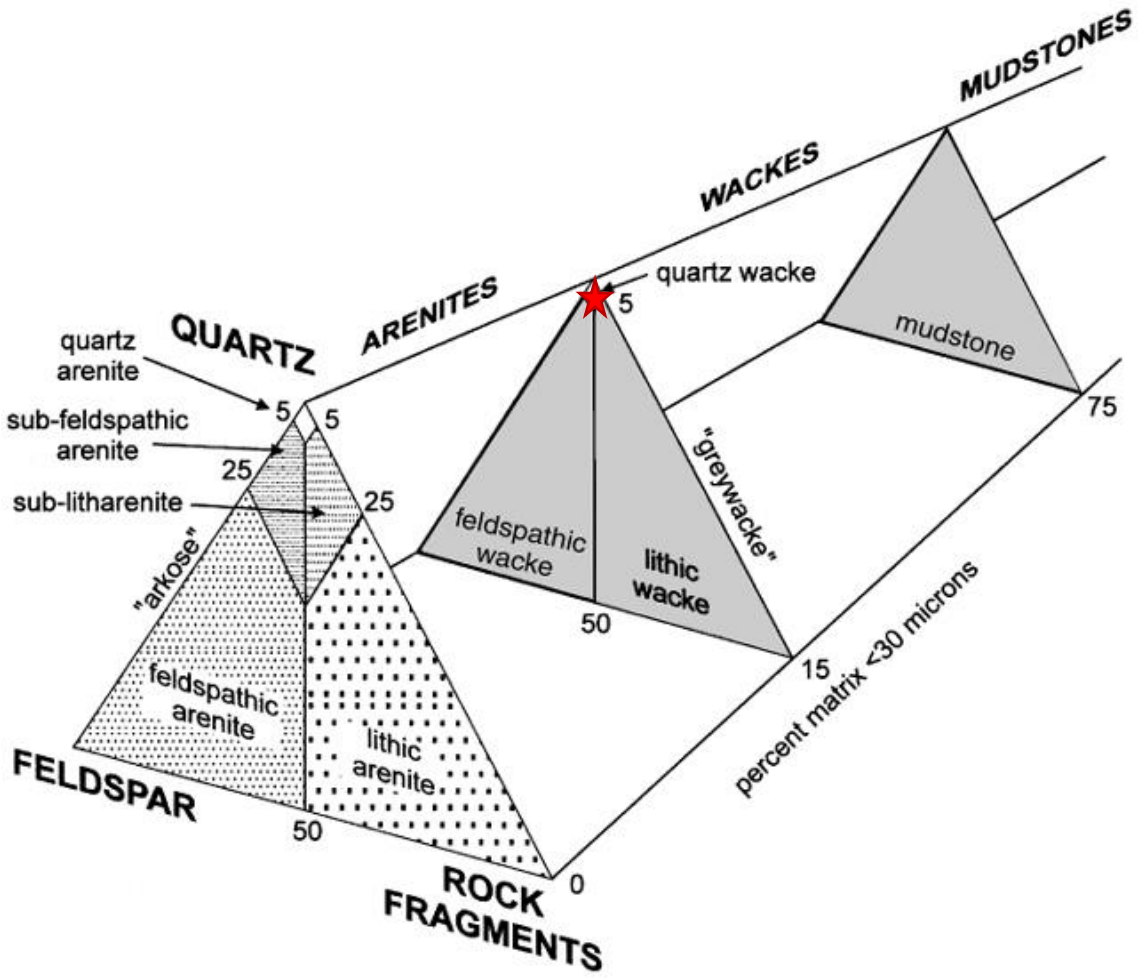

Figure 19. Composition of sample D places it within quartz wacke of the modified Dott classification noted by a red star, after Pettijohn et al., (1987).

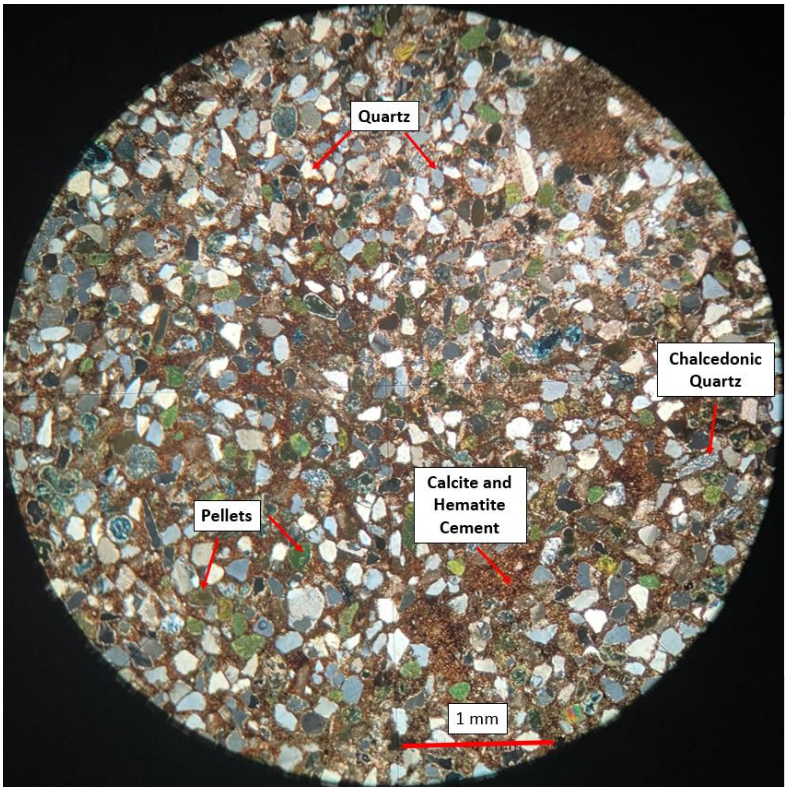

Figure 20. Thin Section E at 400x magnification under cross polarized light. Thin section E is from a calcite cemented sandstone at 2043 feet from the Carthage Gas Unit No. 9-4A.

The quartz arenite from 2043 feet from the Carthage Gas Unit No. 9-4A well has an average grain size of 5.5 **ϕ**. The clasts found in this sample are angular to subrounded and are poorly sorted. The sandstone displayed in this thin section is composed of 53% quartz, 3% chalcedonic quartz, 13% pellets and 32% calcite and siderite cement. This sample is very well compacted both chemically and mechanically. The pellets display signs of ductile deformation from being compressed between quartz grains and the lack of porosity is due to calcite and siderite filling former pore spaces (Figure 20, 21).

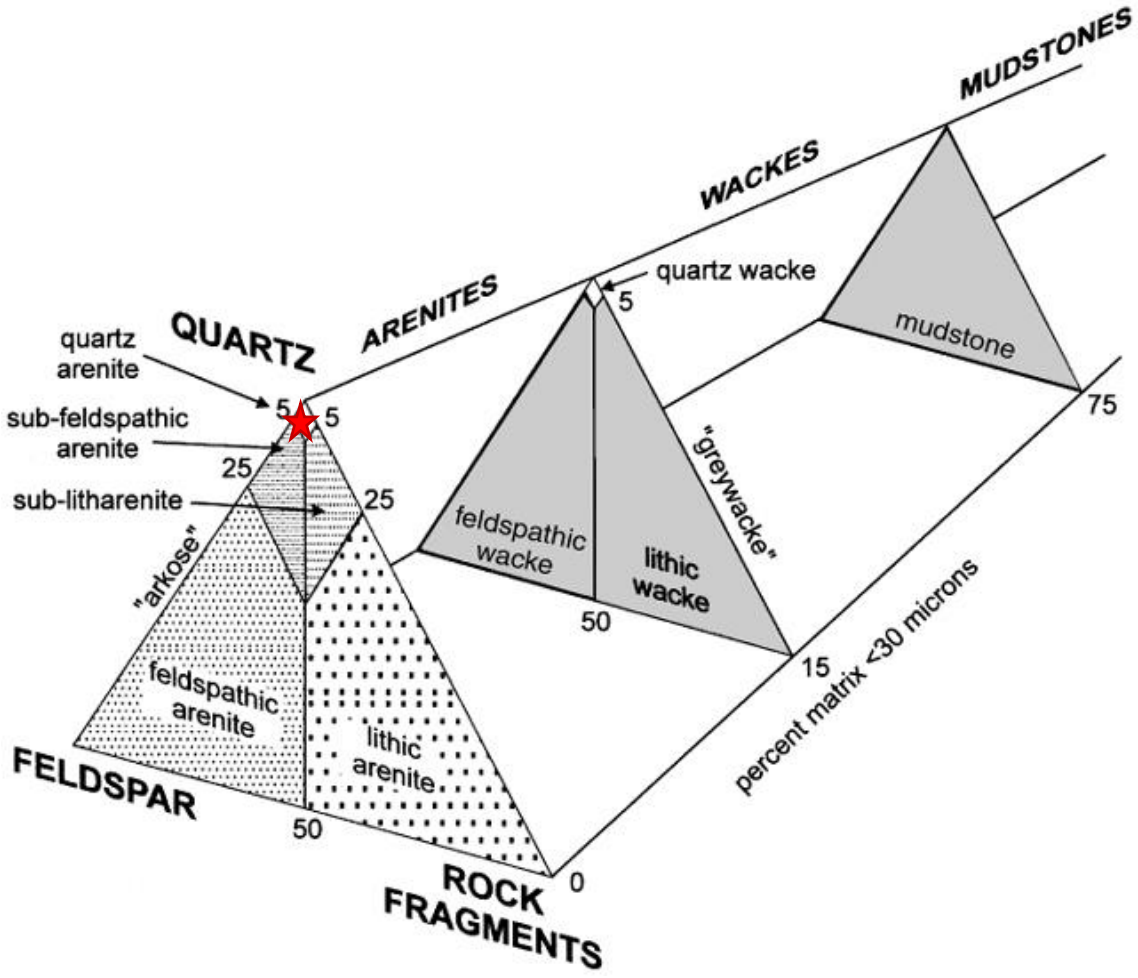

Figure 21. Composition of sample E places it within quartz arenite of the modified Dott classification noted by a red star, after Pettijohn et al., (1987).

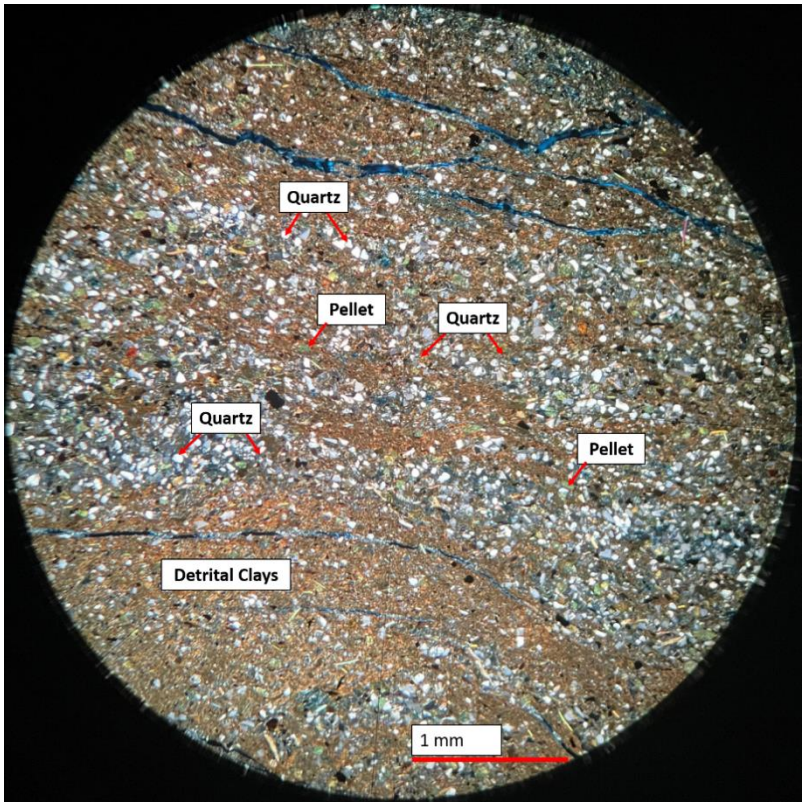

Figure 22. Thin Section F at 400x magnification under cross polarized light. Thin section F is from a section of a siltier wavy bedded sandstone at 2011 feet from the No.1 Werner Smith.

The quartz wacke from 2011 feet from the No. 1 Werner Smith well has an average grain size of 4.1 **ϕ** (Figure 22, 23). The clasts found in this sample are subangular and are moderately sorted. The sandstone displayed in this thin section is composed of 62% quartz, 3% pellets, and 35% matrix. This sample is very well compacted as there is little to no space between grains, and pellets display ductile deformation from being compressed between quartz grains. There is some secondary porosity exhibited by the fractures in the reddish-brown detrital clays.

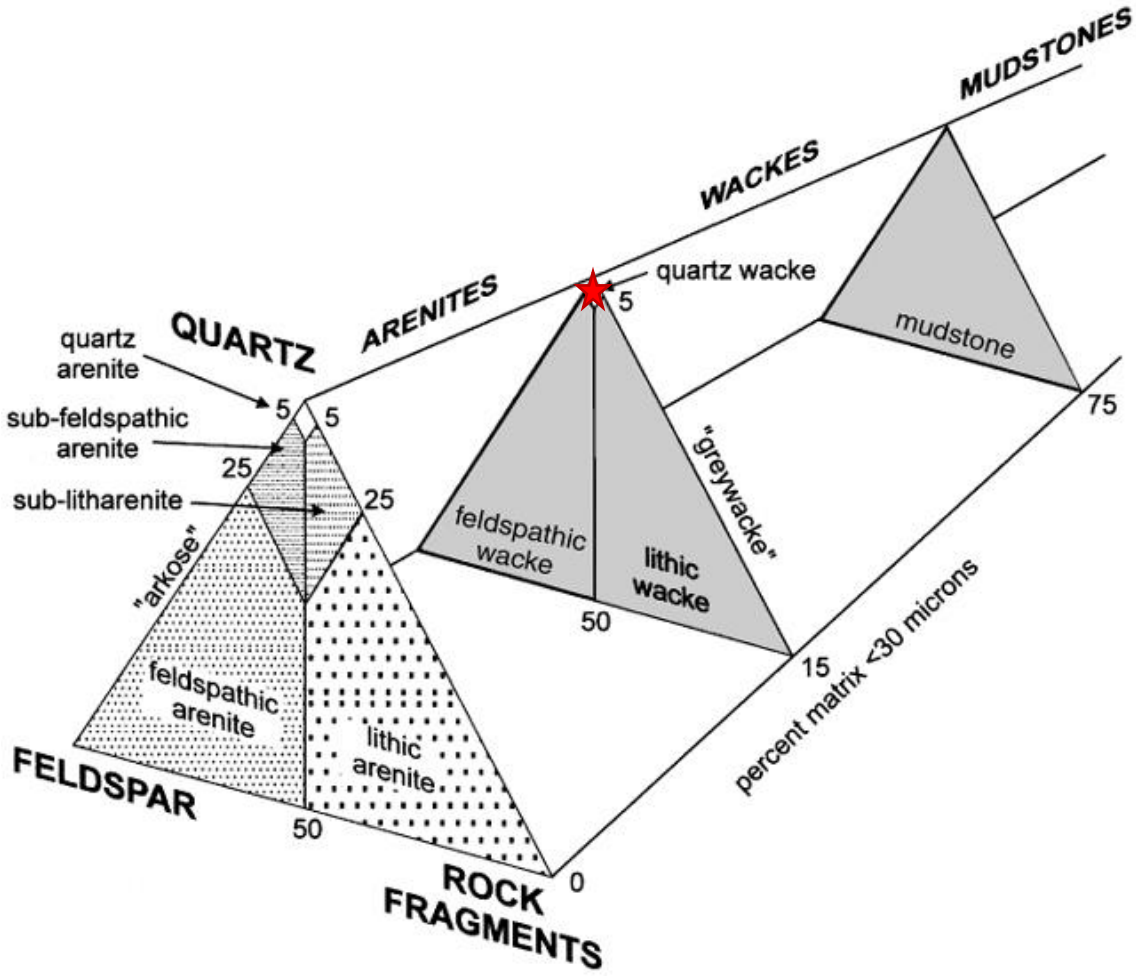

Figure 23. Composition of sample B places it within quartz wacke of the modified Dott classification noted by a red star, after Pettijohn et al., (1987).

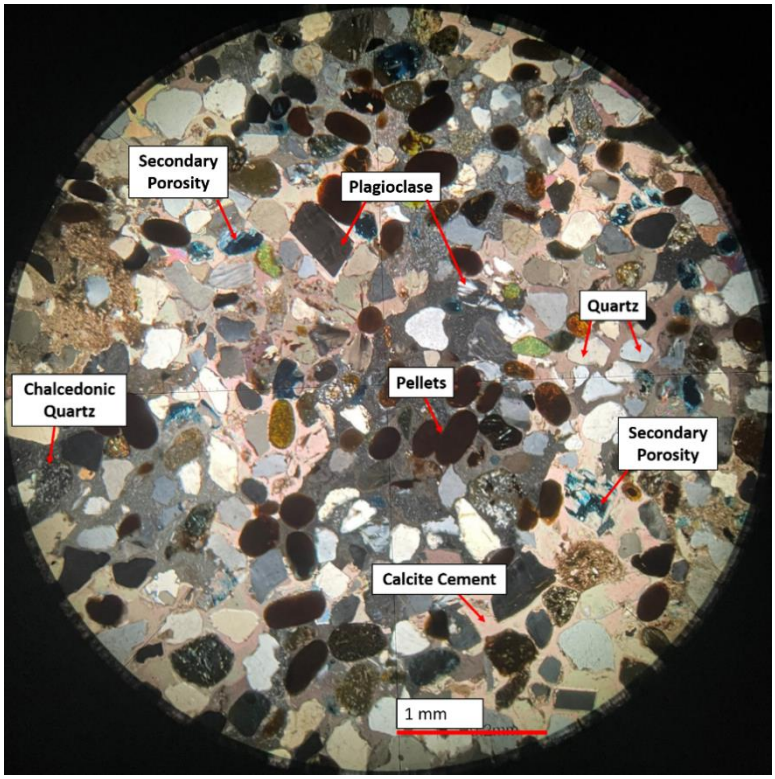

Figure 24. Thin Section G at 400x magnification under cross polarized light. Thin section G is from a sandstone at 2026 feet from the No.1 Werner Smith.

The quartz arenite from 2026 feet from the No. 1 Werner Smith has an average grain size of 5.5 **ϕ** (Figure 24, 25). The clasts found in this sample are subrounded to well rounded and are well sorted. The sandstone displayed in this thin section is composed of 30% quartz, 2% chalcedonic quartz, 20% pellets, 3% plagioclase, 45% calcite cement. This sample has undergone less mechanical compaction compared to our other sands as few of the pellets display ductile deformation and the quartz and chalcedonic quartz grains are close together without being tightly compacted. A considerable amount of the porosity is secondary via dissolution of what appears to have been feldspar (Figure 18).

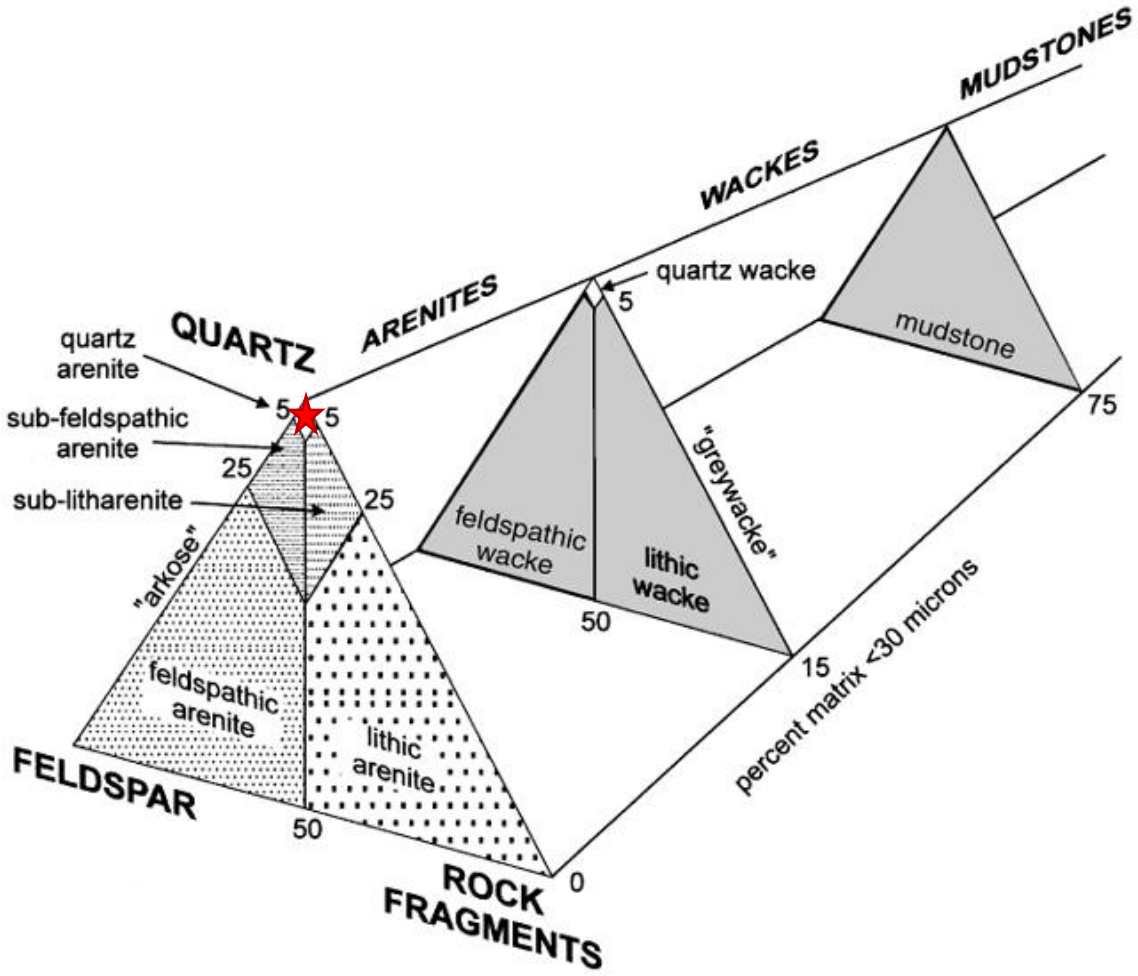

Figure 25. Composition of sample G places it within quartz arenite of the modified Dott classification noted by a red star, after Pettijohn et al., (1987).

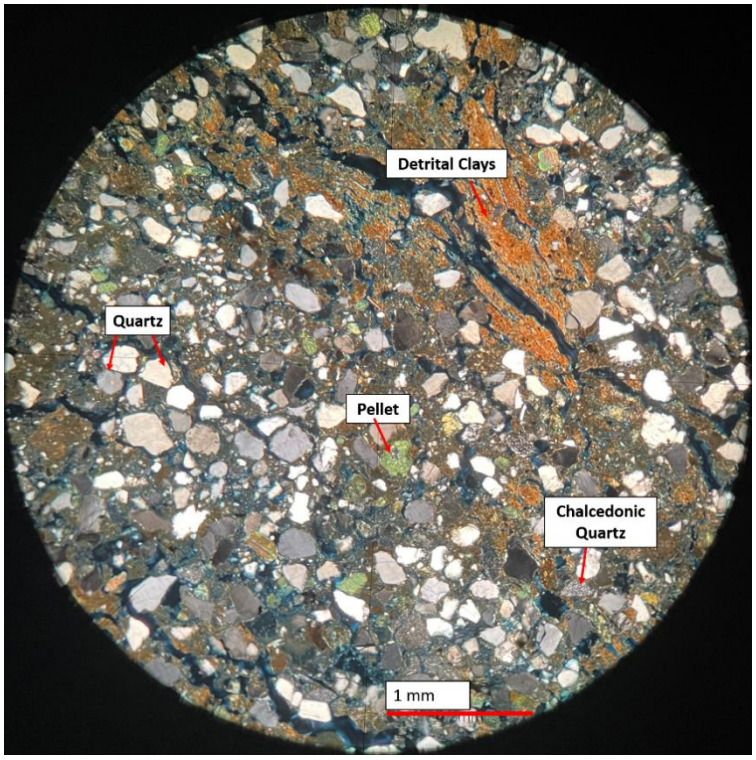

Figure 26. Thin Section H at 400x magnification under cross polarized light. Thin section H is from a wavy bedded sandstone at 2028 feet from the No.1 Werner Smith.

The quartz wacke from 2028 feet from the No. 1 Werner Smith has an average grain size of 5.7 **ϕ** (Figure 26, 27). The clasts found in this sample are angular to subangular and are poorly sorted. The sandstone displayed in this thin section is composed of 51% quartz, 3% chalcedonic quartz, 4% pellets, 4% plagioclase, and 38% matrix. This sample is very well compacted. The pellets display signs of ductile deformation from being compressed between quartz grains. There is secondary porosity exhibited by the fractures in the red-ish brown detrital clays (Figure 19).

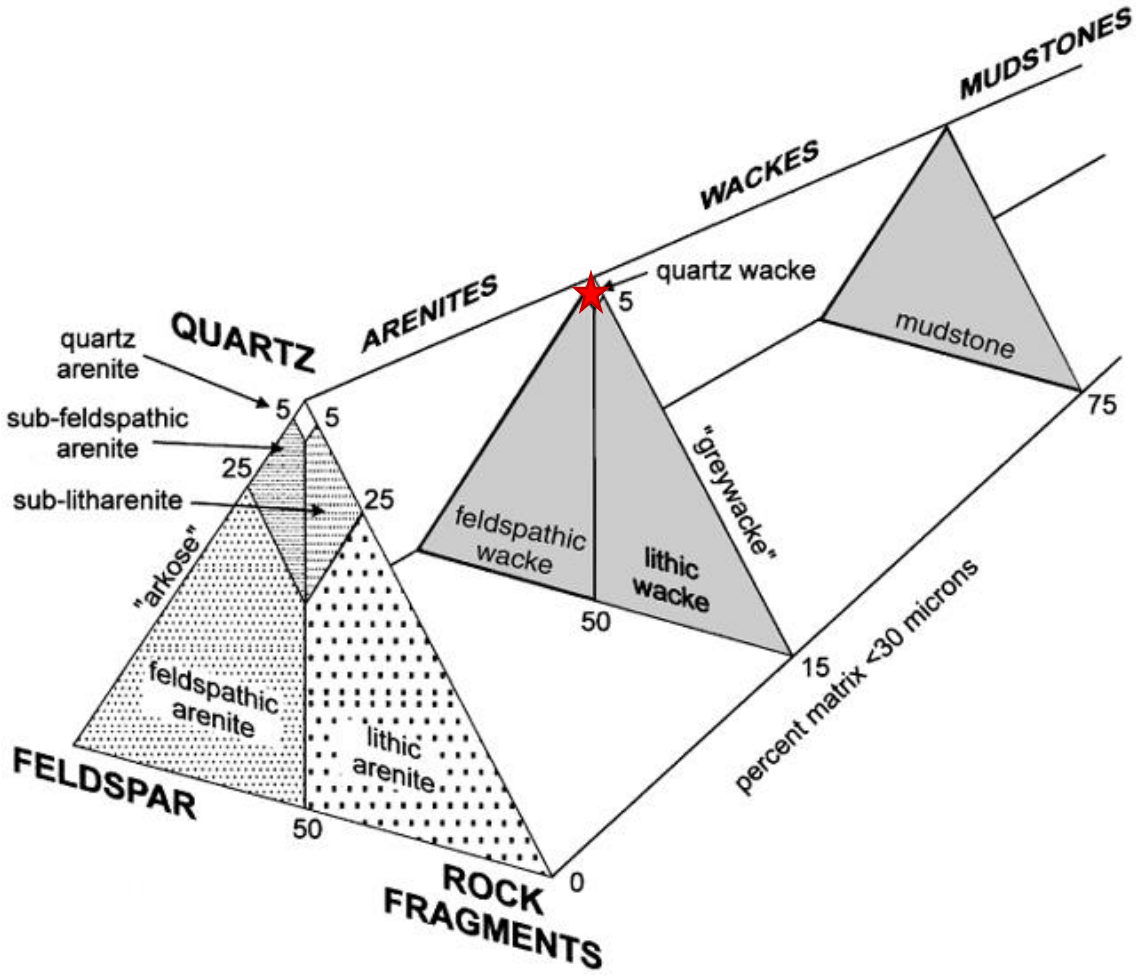

Figure 27. Composition of sample B places it within quartz wacke of the modified Dott classification noted by a red star, after Pettijohn et al., (1987).

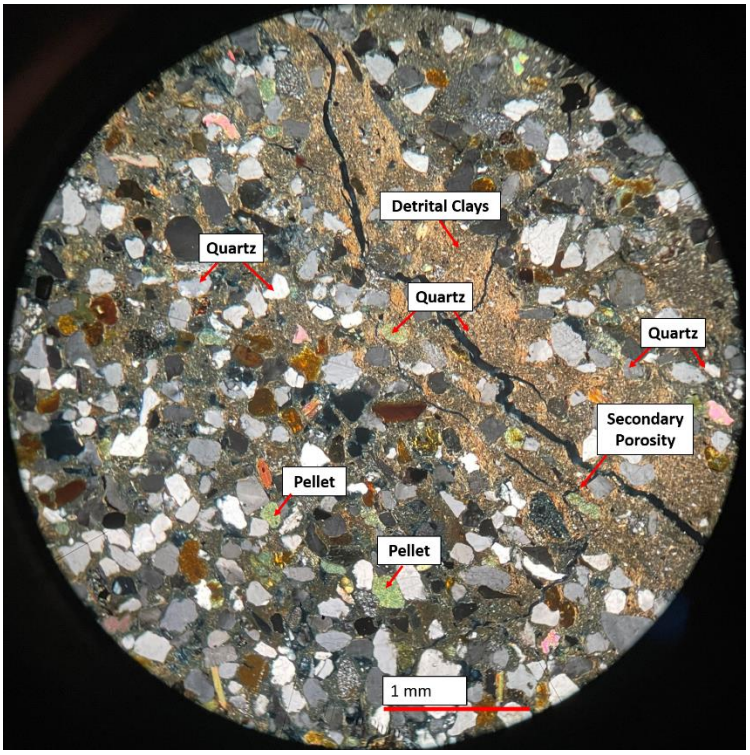

Figure 28. Thin Section I at 400x magnification under cross polarized light. Thin section I is from a wavy bedded sandstone at 2037 feet from the No.3-A Gena Williamson.

The quartz wacke from 2037 feet from the No.3-A Gena Williamson well has an average grain size of 18 **ϕ** (Figure 28, 29). The clasts found in this sample are angular to subangular and are poorly sorted. The sandstone displayed in this thin section is composed of 54% quartz, 2% chalcedonic quartz, 2% pellets, 42% matrix. This sample is very well compacted. The pellets display signs of ductile deformation from being compressed between quartz grains.

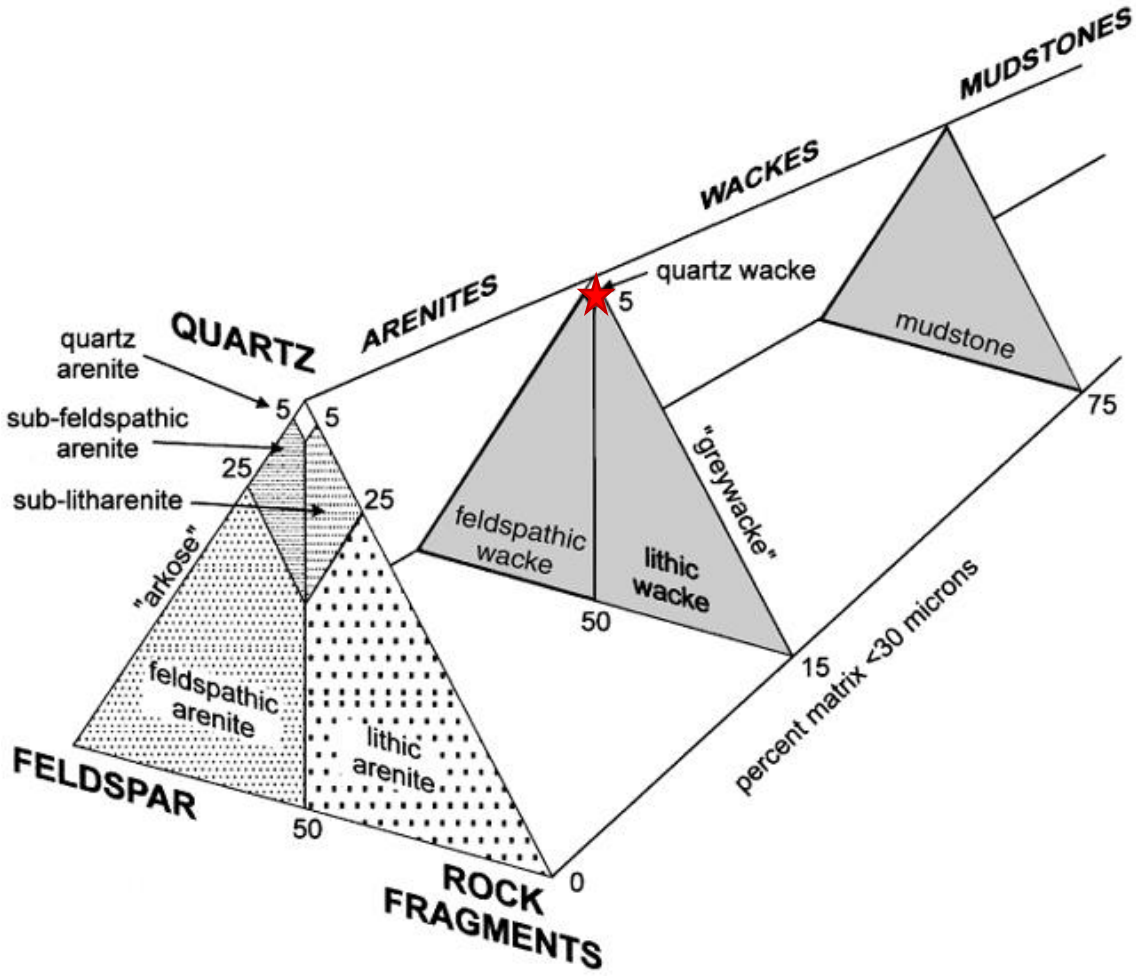

Figure 29. Composition of sample I places it within quartz wacke of the modified Dott classification noted by a red star, after Pettijohn et al., (1987).

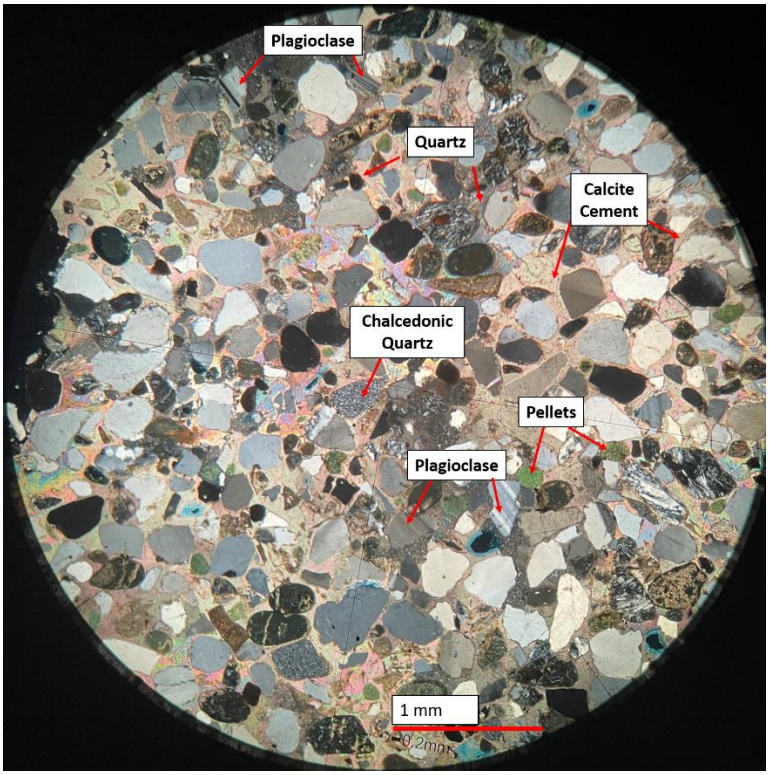

Figure 30. Thin Section J at 400x magnification under cross polarized light. Thin section J is from a wavy bedded sandstone at 2059 feet from the Borders Smith No.1-A.

The quartz arenite from 2059 feet from the Borders Smith No.1-A well has an average grain size of 5.6 **ϕ**. The clasts found in this sample are subangular to subrounded and are poorly sorted. The sandstone displayed in this thin section is composed of 55% quartz, 13% chalcedonic quartz, 4% pellets, 2% plagioclase, and 24% calcite cement. This sample is very well compacted. The pellets display signs of ductile deformation from being compressed between quartz grains. Due to precipitation of calcite, this samples exhibits little to no porosity (Figure 30, 31).

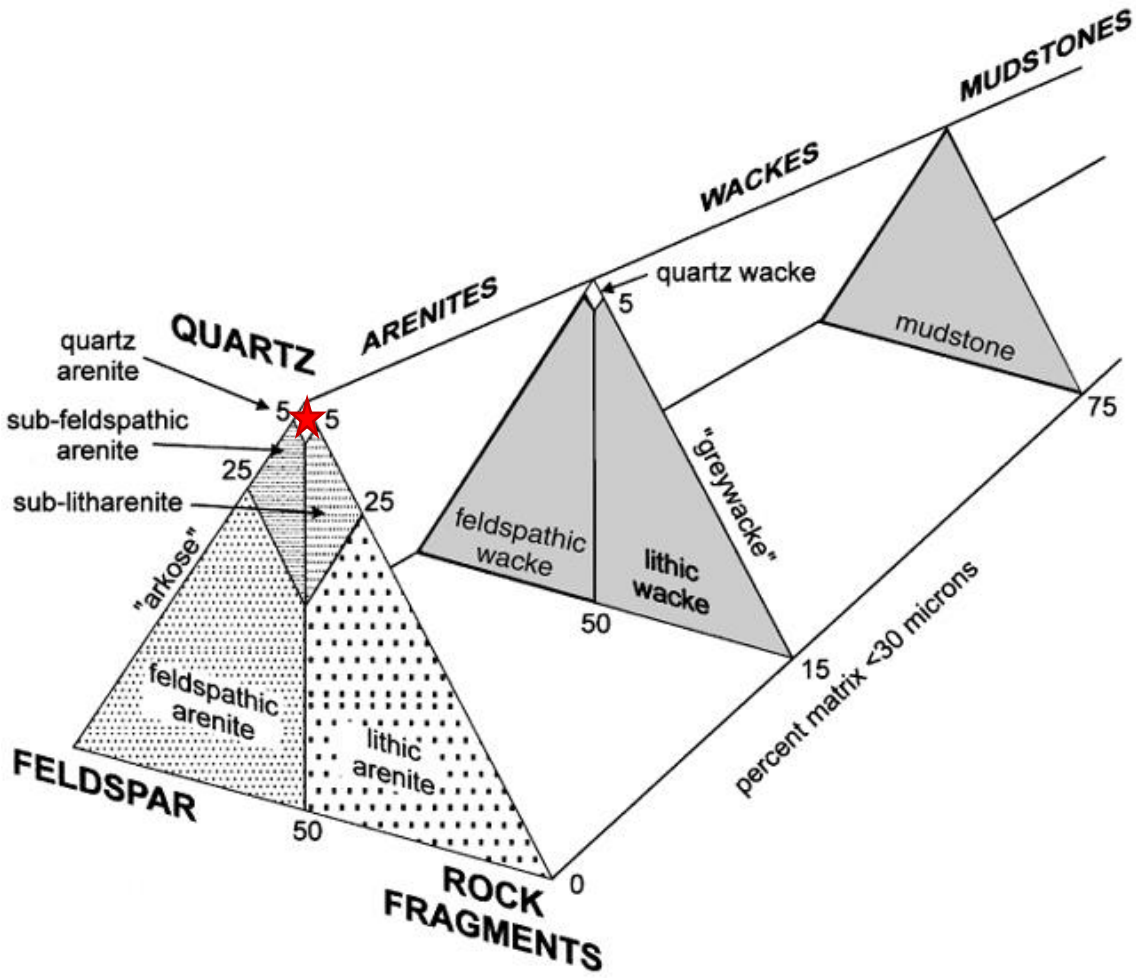

Figure 31. Composition of sample J places it within quartz arenite of the modified Dott classification noted by a red star, after Pettijohn et al., (1987).

5.6 Core Descriptions

The Blossom Sand contains two major sandstone facies (Figure 34). The first is wavy bedded sandstone that is composed of alternating layers of fine sand and thinner layers of clay (Figure 34-B). The second sandstone facies is composed of fine sandstones that display faint planar lamination (Figure 34-A). The thin sections from the areas that display wavy bedding showed the most detrital clays (Figure 35-C). The wavy bedding seen in these sandstones is often severely deformed by intense bioturbation. The thin sections from the cleanest sands displayed the most authigenic illite and calcite cement (Figure 35-A&B). The wavy bedding indicates a bidirectional current influenced by tidal fluctuations while the planar lamination is indicative of multidirectional combined flows. Valves belonging to shallow marine bivalves, *Inoceramus sp.* and *Exogyra sp.* were found in the cores over the course of this study. The presence of these bivalves indicates that the Blossom Sand would have been deposited in a shallow marine environment in normal marine salinity. Ichnofossils observed in the cores include extensive burrows and casts and molds of bivalves.

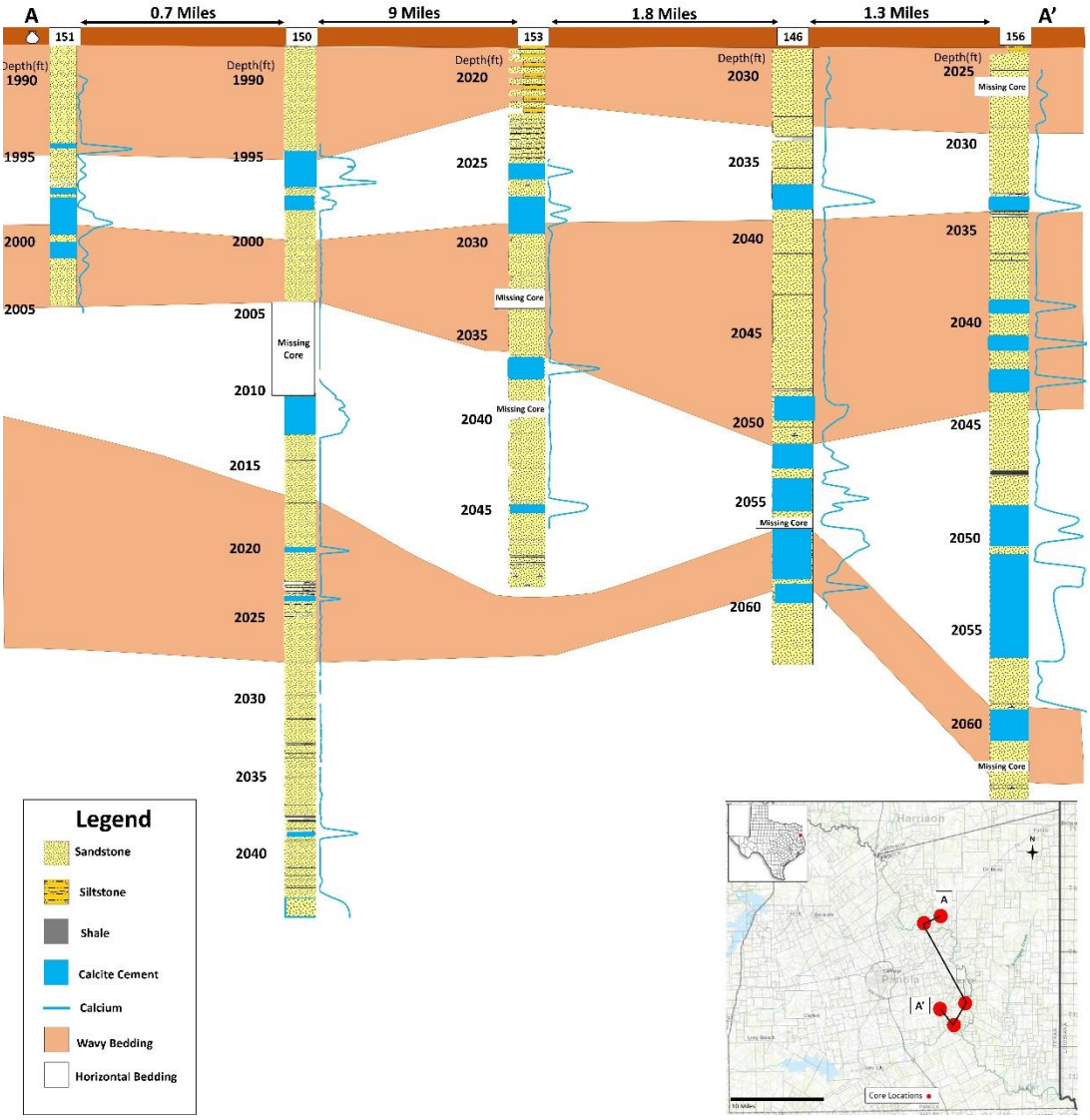

Figure 32. The descriptions of the four cores used in this study. The Blossom Sand is flattened on its contact with the overlying Brownstown Marl. Lithofacies correlations of the Blossom Sand showing the depths at which calcite cement occurs according to the Ca curves derived from the XRF data

The flooding surfaces found in the cores do not correlate well with one another (Figure 32). Though it should be noted that core 150 and 153 are missing several feet of

core that could contain another flooding surface. The thicknesses of the sands between the flooding surfaces also vary significantly for which the missing sections could also be responsible. Regardless of missing sections, there is one consistent flooding surface in red that appears in four of the cores that could indicate the last large-scale flooding event before the one that ended Blossom Deposition and began deposition of the Brownstown Marl.

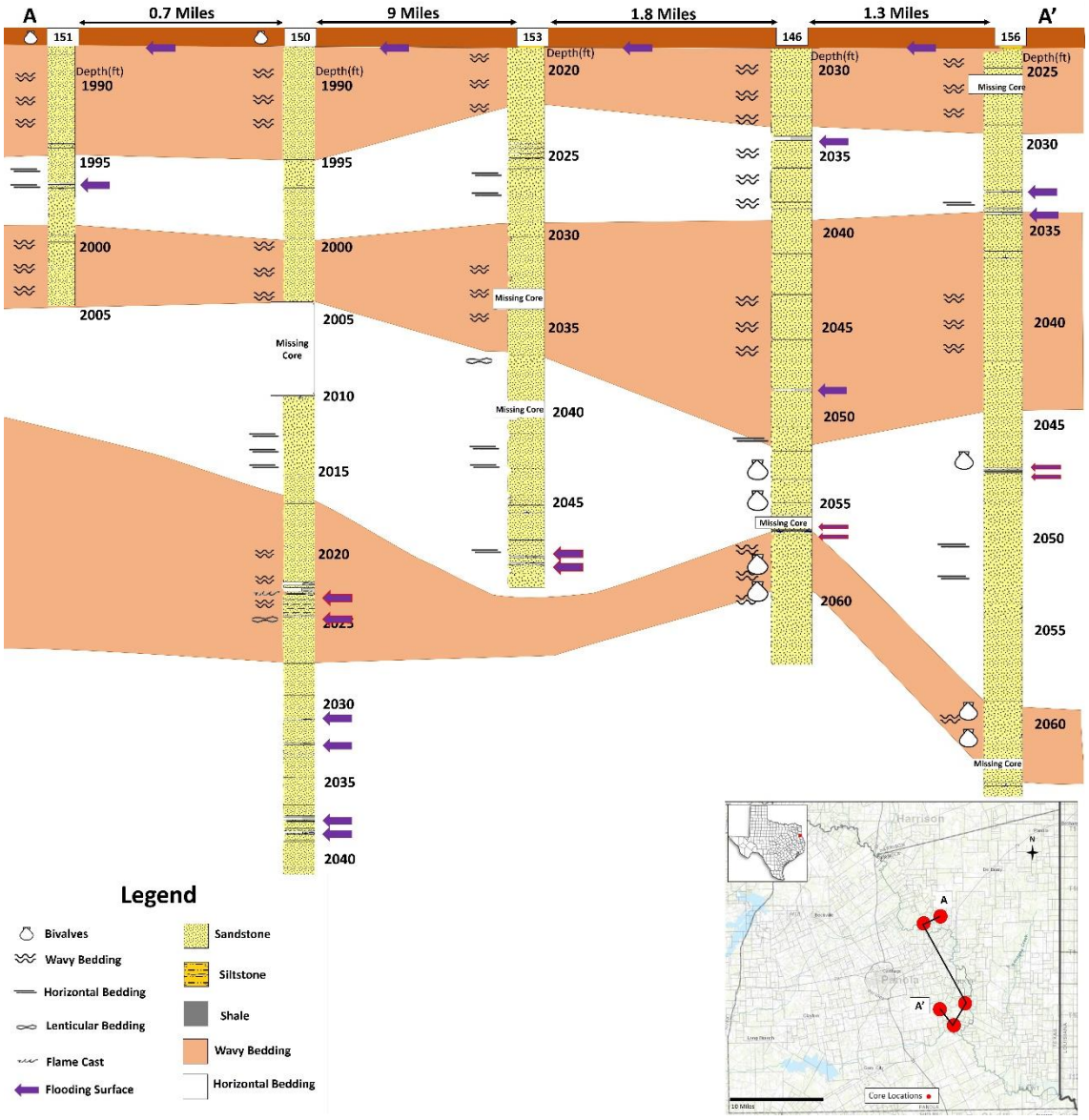

Figure 33. The descriptions of the four cores used in this study. The Blossom Sand is flattened on its contact with the overlying Brownstown Marl. Correlations of wavy bedded sandstones and planar bedded sandstones. Flooding surfaces are denoted with the purple arrows. Purple arrows outlined in read denote the only consistent flooding surface found in the cores.

The inconsistencies in subsequent flooding surfaces could indicate that core 150 and 153 would have received a more consistent sediment supply than the other cores. The consistent sediment supply could have come from the output of a nearby river delta indicating that the sediments of the Blossom could be deltaic sands.

Figure 34. Core of the Blossom Sand from the Carthage Gas Unit No.9-4A displaying planar bedding (A) and wavy bedding altered by bioturbation (B).

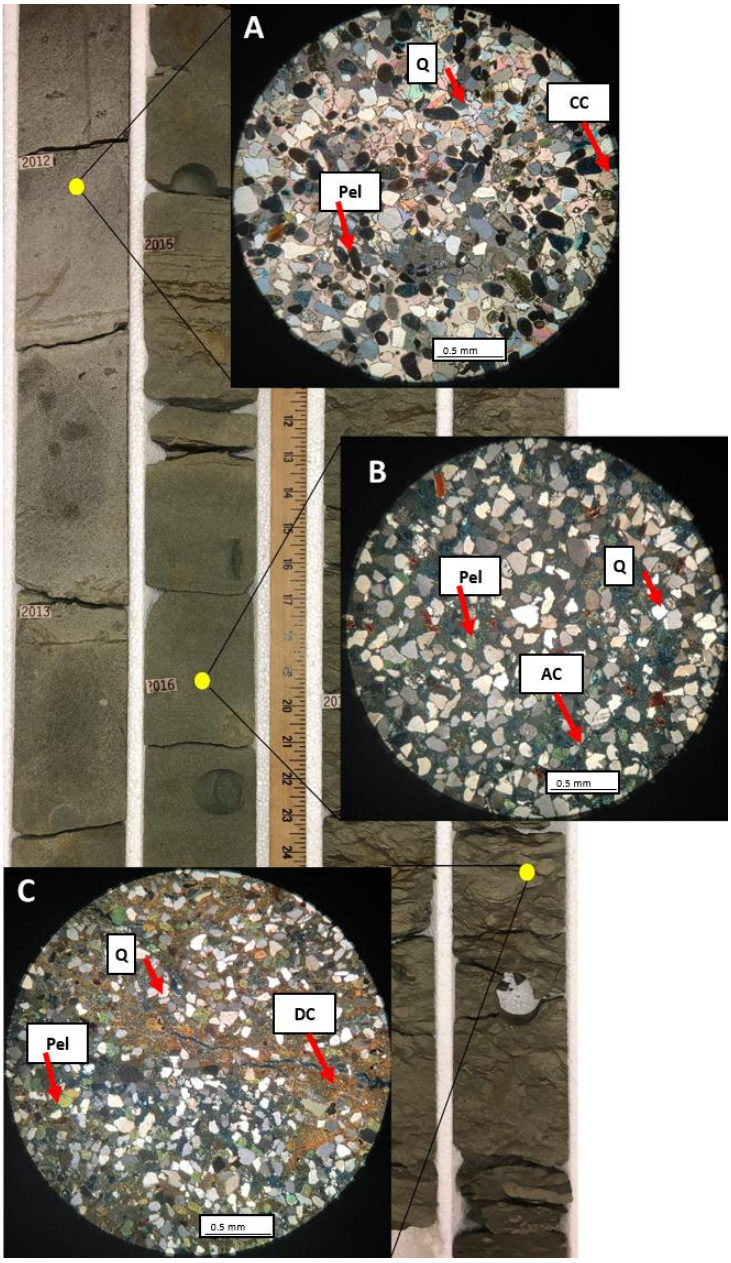

Figure 35. Core from the Carthage Gas Unit No.9-4A with photos of thin sections under 40x magnification in cross polarized light. Pel indicates pellets, Q indicates quartz, CC indicates calcite cement, AC indicates authigenic clay, DC indicates detrital clay. (A) calcite cemented sandstone, (B) planar bedded sandstone with authigenic illite and (C) wavy bedded sandstone with reddish brown detrital clays.

6. Discussion

6.1 Clay Mineralogy

Contrary to previous research, there is no detectable glauconite in the Blossom Sand amongst any of the XRD results. No peaks in any of the diffractograms were comparable to glauconite spectra at low 2Θ. The long, fibrous crystals of illite seen coating the sand grains in the SEM indicate that the green hue that inspired previous researchers' interpretation of glauconite can instead be attributed to illite (Figure 8-B), combined with no detectable amounts of glauconite in the XRD (Figure 4). The illite in this formation appears to be authigenic and not detrital because it is displayed as fibrous crystals that coat sand grains and deformed fecal pellets (Figures 8-B, 10 & 14-B). The illite also would have been precipitated after deposition and compaction as it does not display any deformation due to compaction (Figures 8-B). Some models indicate that glauconitization favors environments with low sedimentation rates while illite prefers low sedimentation rates and hypersaline environments (Meunier and El Albani, 2007), while others suggest that the occurrence of glauconite depends on diffusion of K ions (Meunier and El Albani, 2007). This study found that the Blossom Sand has porosity and permeability that would allow for adequate diffusion rates. The lack of glauconite in this formation could be attributed to low concentrations of K in the pore waters. However,

conditions that are believed to favor glauconitization or illite precipitation continue to be highly disputed.

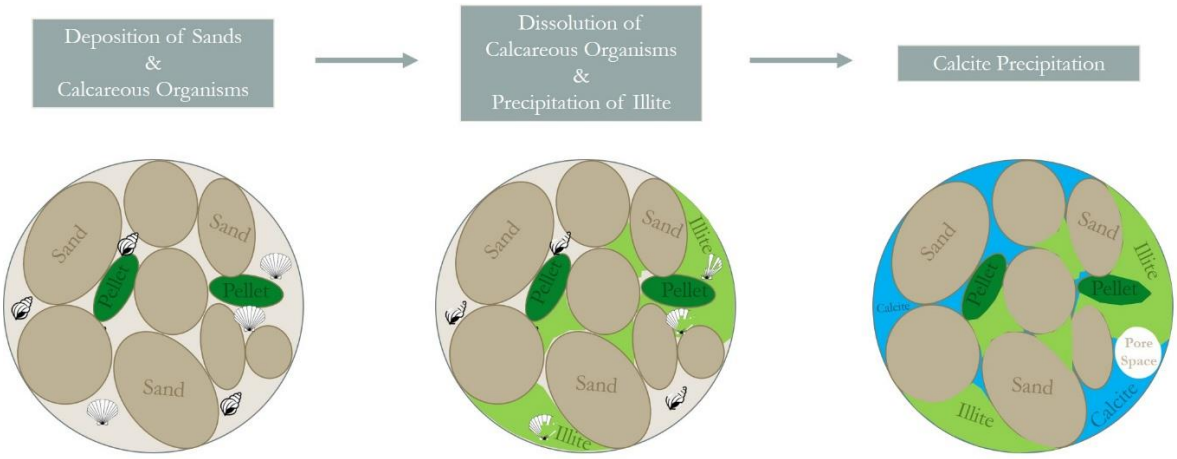

Figure 36. Diagenetic model of the Blossom Sand displaying deposition of sands and calcareous organisms followed by precipitation of illite and finally precipitation of calcite.

6.2 Depositional Environment and Diageneis

The grain sizes, sedimentary structures, fossils and bioturbation found in the core indicate that these sandstones were deposited in two separate shallow marine settings in normal marine salinity. The wavy bedding and such intense bioturbation in the muddy sands of this formation point to a depositional setting depositional setting that would have experienced bidirectional flow, fluctuating currents and sediment supply such as a lower shoreface (Figure 34-B). The lower shoreface would have been far enough below fair-weather wave-base for deposition of detrital clays. The faint planar bedding exhibited by the coarser, cleaner sands would have been deposited in much shallower waters such as those of the foreshore (Figure 34-A). A depositional setting on the upper shoreface would

have supplied the higher flow velocity and multidirectional flow necessary to form planar bedding and work out any detrital clays to be deposited in the offshore transition. Here, bivalve organisms like *Inoceramus* sp. and *Exogyra* sp. would have flourished. Following their burial, they would have begun dissolution in the pore fluids. Once the pore fluids became saturated, calcite would have begun exsolving from the pore fluids and precipitating in the voids between the sands and pellets (Figure 36). Since the calcite cement is not laterally continuous and instead occurs in lenses, the pore fluids likely became saturated before they could transport the dissolved calcite any considerable distance.

6.3 Controls on Porosity

Calcite cement appears to be the controlling factor on porosity and permeability throughout the formation, rather than precipitation of clay minerals (Figures 7 & 8). The presence of casts and molds and abundance of trace fossils in the Blossom Sand suggests that the calcite cement is the result of dissolution and redistribution of local biogenic carbonates. The depths at which the calcite cement occurs are not continuous through all of the cores (Figure 32), which suggests that the calcite cemented intervals are not laterally continuous. The lack of support for lateral continuity indicates that the Blossom Sand is divided into compartments of high porosity and permeability that are separated from one another by the calcite cement.

7. Conclusions

The Blossom Sand was found to exhibit very high porosities and permeabilities constrained primarily by calcite cement. The calcite cement was found to lack lateral continuity and was found to occur in lenses instead. Combined with the sparse fossils of the Blossom Sand, the lenticular behavior indicates that the calcite cement is the result of dissolution of local calcareous organisms and precipitation of calcite. Though it is uncommon, in thin sections where calcite is seen in conjunction with illite, calcite is seen precipitated around the fibrous illite crystals which indicates that the illite would have begun nucleation on the sands and pellets prior to calcite dissolution, redistribution and precipitation (Figure 37).

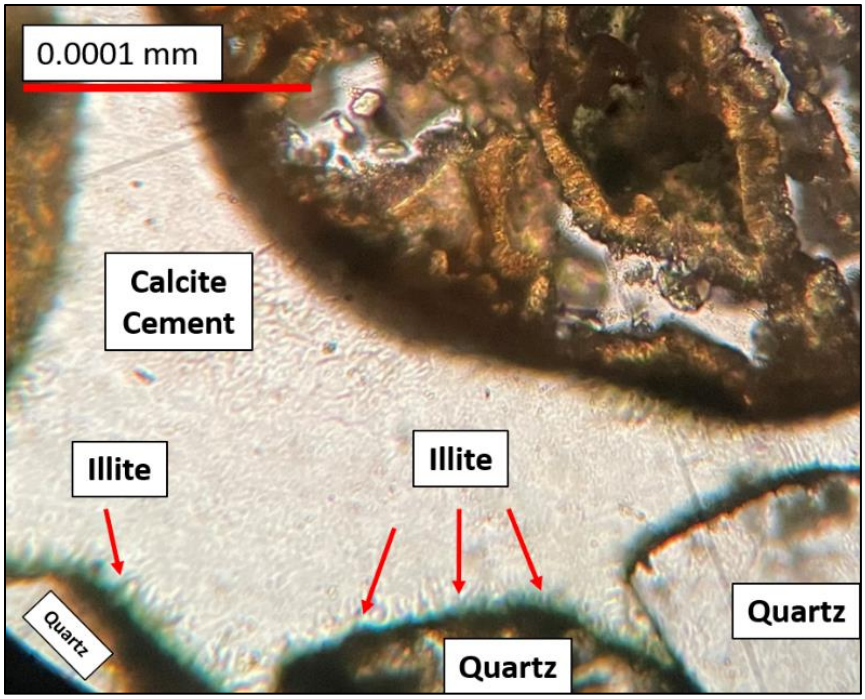

Figure 37. Illite precipitated around sand grains in a calcite cemented sandstone at 400x magnification under cross polarized light.

As indicated by the XRD results, this study found that the long believed glauconitic sandstones of the Blossom Sand were found instead to be illitic sandstones. Though the Blossom Sand contains bright green fecal pellets, the pore fluids evidently either did not contain enough K to alter them to the glauconite typically seen in green fecal pellets or the flow rate through the formation was not adequate for the diffusion of K. As a result, the pellets instead were altered to illite.

The Blossom Sand was found to be the deposits of nearshore to foreshore environments. The wavy bedding indicated that the muddy sands of Blossom Sand were deposited in a nearshore setting while the planar bedding of the cleaner sands indicated that they were deposited under the higher velocities of the foreshore. In each of these environments, they hosted a variety of marine fauna including bivalves and extensive burrowers.

8. References

Adams, R., 2009, Basement Tectonics and Origin of the Sabine Uplift: Gulf Coast Association of Geological Societies Transactions, v. 59, p. 3-19.

Albertson, M., 1923, Possible Explanation of the Large Initial Production of Some Wells of the Haynesville Field, Louisiana: American Association of Petroleum Geologists, v. 7, p. 295-296.

Berryhill, R. A., Champion, W. L., Meyerhoff, A. A., Sigler, G. C., 1968, Stratigraphy and Selected Gas Field Studies of North Louisiana: Natural Gases of North America, v. 1, p. 1103-1137.

Brantly, J. E., 1924, Résumé of the Geology of the Gulf Coastal Plain: American Association of Petroleum Geologists, v. 8, p. 21-28.

Deep Time Maps, 2020, North American Key Time-slices Series. http://deeptimemaps.com/north-american-key-time-slices-series/

Enverus, 2020, Drilling Info. https://www.enverus.com/

Ewing, T. E., 2009, The Ups and Downs of the Sabine Uplifts and the Northern Gulf of Mexico Basin: Jurassic Basement Blocks, Cretaceous Thermal Uplifts, and Cenozoic Flexure: Gulf Coast Association of Geological Societies Transactions, v. 59, p. 253-269.

Gordon, C. H., 1911, Geology and Underground Waters of Northeastern Texas: Water Supply Paper: USGS, no. 276, p. 1-78.

Holman, E., Campbell, R. B., 1923, The Bellevue Oil Field, Louisiana: American Association of Petroleum Geologists, v. 7, p. 645-652.

Hull, J.P.D., 1922, Webster Parish Gas Fields, Louisiana: Geological Notes: American Association of Petroleum Geologists, v. 6, no. 3, p. 251-252.

Hull, J. P. D., Spooner, W. C., 1922, A Review of Oil and Gas Pools in North Louisiana Territory: American Association of Petroleum Geologists, v. 6, no. 3, p. 179-192.

Jackson, M. L. W., Laubach, S. E., 1988, Cretaceous and Tertiary Compressional Tectonics as the Cause of the Sabine Arch, East Texas and Northwest Louisiana: Bureau of Economic Geology: Gulf Coast Association of Geological Societies, v. 38, p. 245-256.

Meunier, A., El Albani, A., 2007, The Glauconite-Fe-illite-Fe-smectite Problem: A Critical Review: Terra Nova, v. 19, no. 2, p. 95-107.

Pearson, K., 2012, Geologic Models and Evaluation of Undiscovered Conventional and Continuous Oil and Gas Resources-Upper Cretaceous Austin Chalk, U.S. Gulf Coast: USGS Scientific Investigations Report, p. 1-26.

Pettijohn, F. J., P. E. Potter, and R. Siever, 1987, Sand and Sandstone: 2nd ed. Springer-Verlag, New York, 553 p.

Powers, S., 1920, The Sabine Uplift: American Association of Petroleum Geologists, v. 4, no. 2, p. 117-136.

Rogers, E. R., 1968, Carthage Field, Panola County, Texas: Natural Gases of North America, v. 1, p. 1020-1059.

Ross, J. S., 1930, Deep Sand Development in Cotton Valley Field, Webster Parish, Louisiana: U.S. Bureau of Mines, p. 983-995.

Short, D., 2018, Tectonics of the Texas portion of the Sabine Island: Gulf Coast Association of Geological Societies Transactions, v. 68, p. 493-516.

Stephenson, L. W., 1918, A Contribution to the Geology of Northeastern Texas and Southern Oklahoma: Shorter Contributions to General Geology: USGS, v. 120, p. 129-163.

Veatch, A. C., 1906, Underground Water Resources of Northern Louisiana and Southern Arkansas: USGS, no. 46, p. 1-422.

Young, K., 1963, Upper Cretaceous Ammonites from the Gulf Coast of the United States: The University of Texas: Bureau of Economic Geology, no. 6304 p. 1-382.

Appendices

Appendix A – XRF Graphs

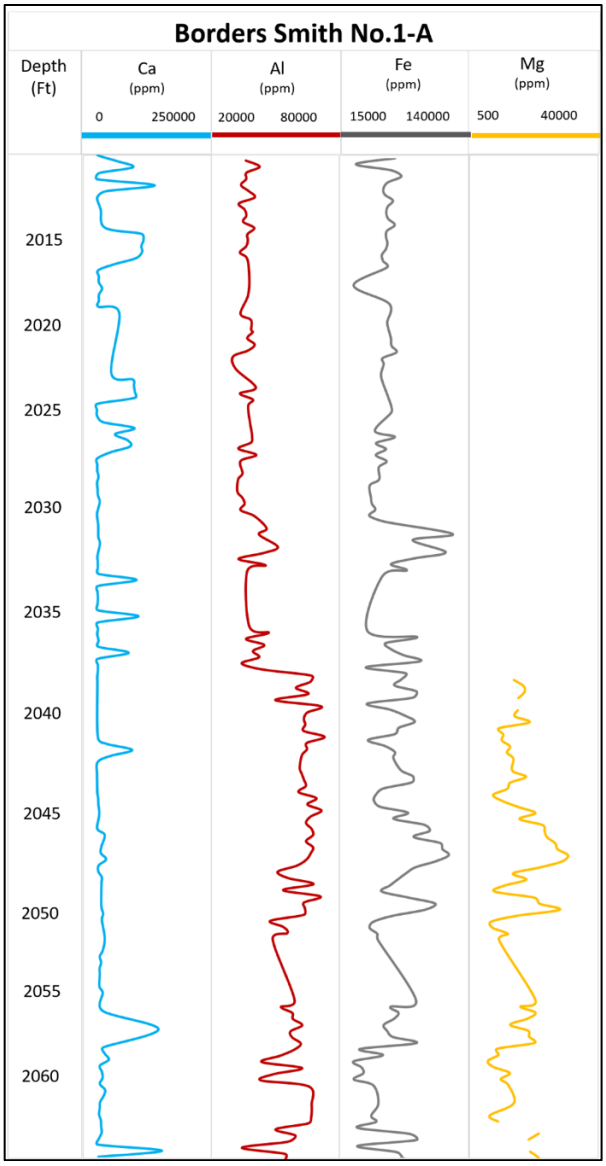

Figure 37. XRF data from core 156.

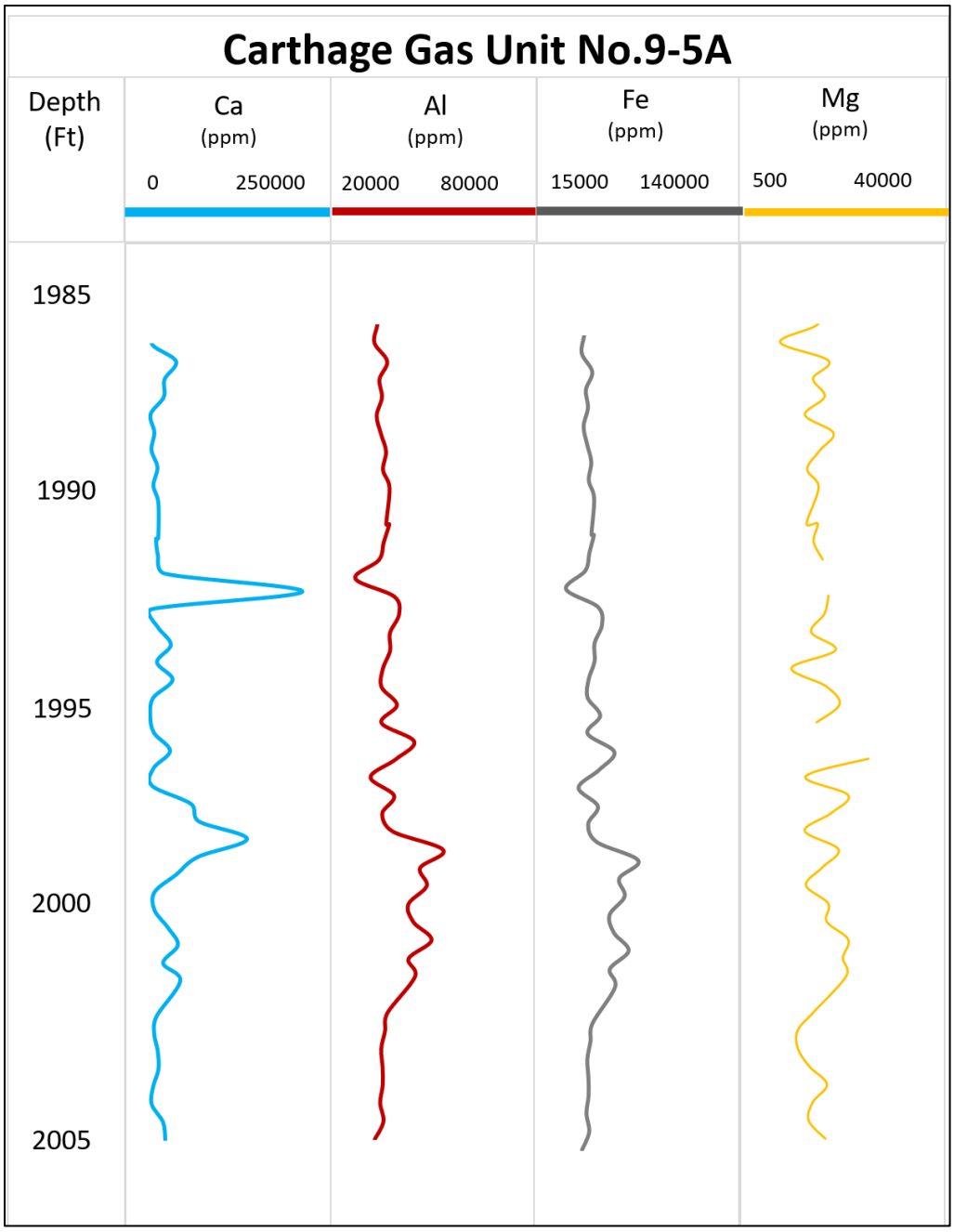

Figure 38. XRF data from core 151.

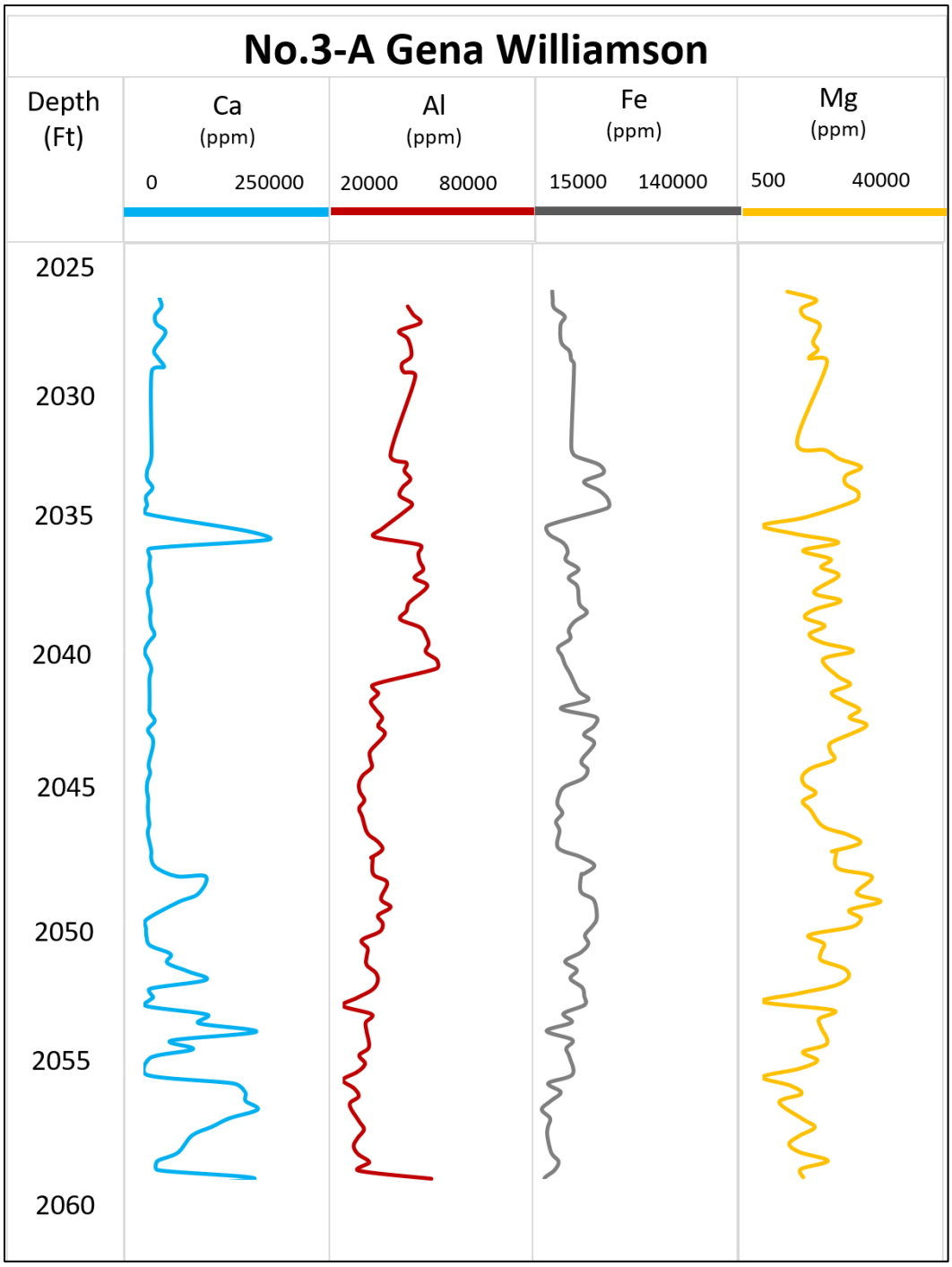

Figure 39. XRF data from core 146.

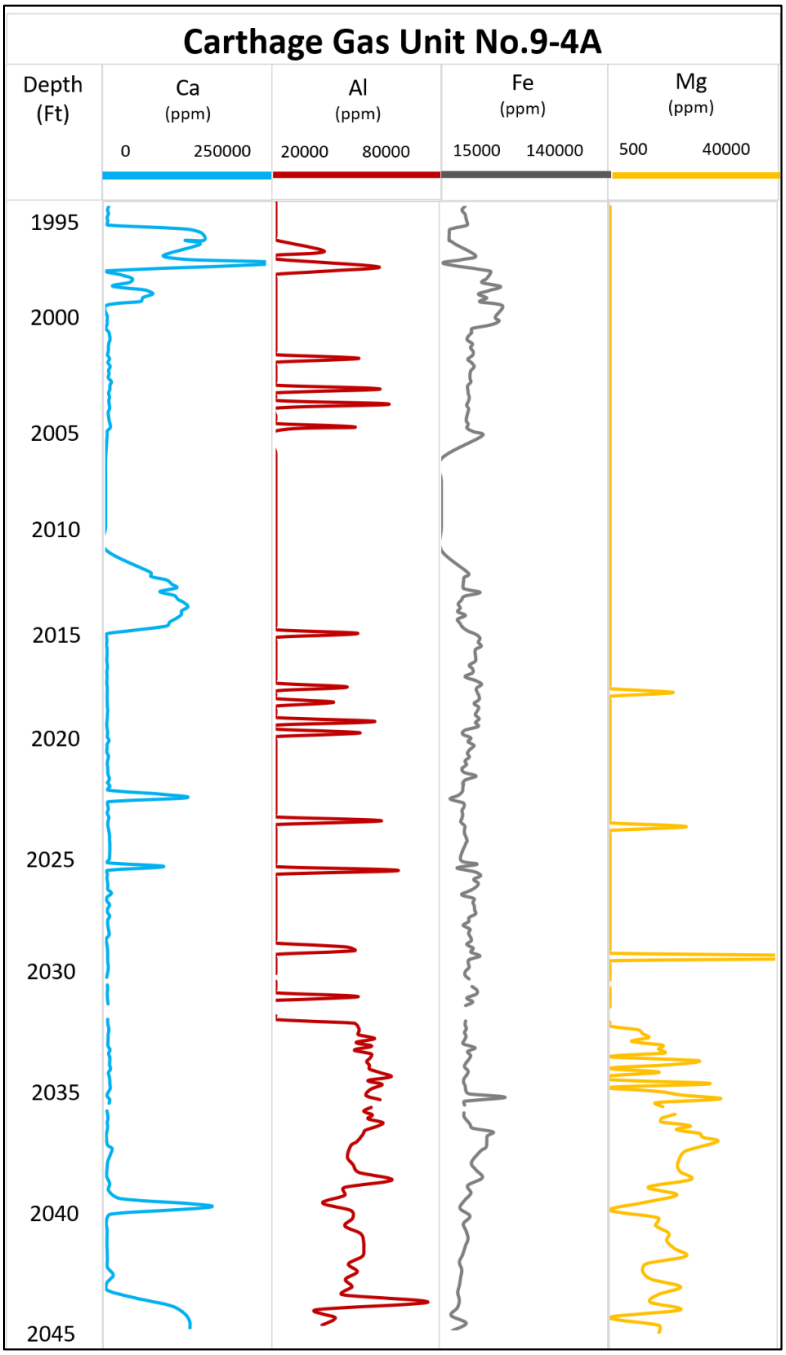

Figure 40. XRF data from core 150.

Appendix B – XRD Spectra

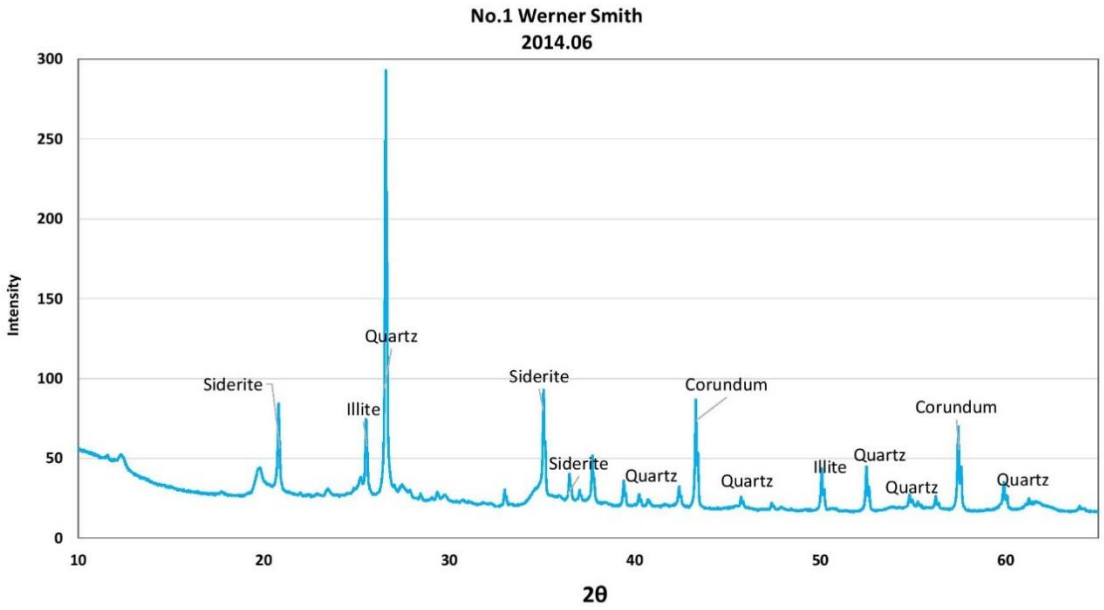

Figure 41. Diffractogram from core 153 (No.1 Werner Smith) displaying mineralogy found at the 2014.06 ft.

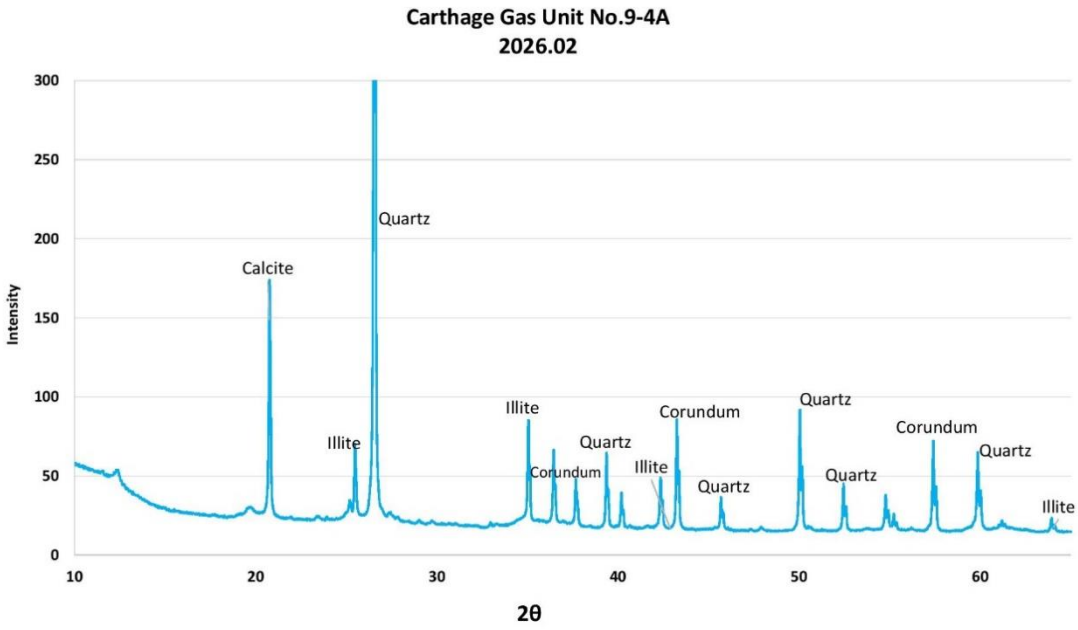

Figure 42. Diffractogram from core 150 (Carthage Gas Unit No.9-4A) displaying mineralogy found at the 2026.02 ft.

Appendix C – Porosity and Permeability Data

Table 3. Porosity and permeability data from 12 plugs from the cores. Porosity was measured at a net confining stress (NCS) of 800 psi. Permeability was adjusted with the Klingenberg method.

Well Name	Sample Depth (ft)	Porosity at NCS (%)	Permeability (mD)
Borders Smith No. 1-A	2026.80	29.19	17.4
Borders Smith No. 1-A	2027.65	29.43	3.06
Carthage Gas Unit No.9-4A	1990.90	29.67	13.0
Carthage Gas Unit No.9-4A	1992.40	27.24	146.
Carthage Gas Unit No.9-4A	2012.20	2.61	0.0002
Carthage Gas Unit No.9-4A	2015.00	33.67	18.2
Carthage Gas Unit No.9-4A	2032.90	25.76	47.7
No.1 Werner Smith	2023.50	23.20	0.695
No.1 Werner Smith	2029.10	32.04	28.9
No. 3-A Gena Williamson	2044.40	26.08	12.1
No. 3-A Gena Williamson	2055.85	6.46	0.0043
No. 3-A Gena Williamson	2057.30	20.12	17.3

Appendix D – Raw XRF Data

Table 4. Raw XRF data derived from the Carthage Gas Unit No.9-4A at a sampling interval of 4 inches. Elemental concentrations in parts per million.

Carthage Gas Unit No.9-4A				
Depth (ft)	**Ca (ppm)**	**Al (ppm)**	**Fe (ppm)**	**Mg (ppm)**
1991	18021.79	36235.2	18021.79	0
1991.167	10329.85	43796.73	10329.85	14963.77
1991.333	9695.93	0	9695.93	0
1991.5	6376.38	45288.88	6376.38	0
1991.667	20160.35	35511.54	20160.35	0
1991.83	36976.75	0	36976.75	0
1992	11139.76	0	11139.76	0
1992.167	10143.63	0	10143.63	0
1992.333	11447.19	0	11447.19	0
1992.5	6302.38	0	6302.38	0
1992.67	5236.18	0	5236.18	0
1992.83	7339.88	0	7339.88	0
1993	8293.82	0	8293.82	0
1992.167	9922.45	0	9922.45	0
1993.33	5581.11	0	5581.11	0
1993.5	6542.16	0	6542.16	0
1993.67	11370.79	0	11370.79	0
1993.83	8707.93	0	8707.93	0
1994	6567.18	0	6567.18	0
1994.167	8709.65	0	8709.65	0
1994.333	9835.19	0	9835.19	0
1994.5	7538.63	0	7538.63	0
1994.67	6812.09	38528.34	6812.09	0
1994.83	0	0	5597.57	0
1995	5597.57	0	7646.15	0
1995.167	7646.15	0	4789.88	0
1995.333	4789.88	0	7232.25	0
1995.5	7232.25	0	3803.81	0

Carthage Gas Unit No.9-4A				
Depth (ft)	**Ca (ppm)**	**Al (ppm)**	**Fe (ppm)**	**Mg (ppm)**
1995.67	3803.81	0	5792.98	0
1995.83	5792.98	0	5360.24	0
1996	5360.24	0	198481.89	0
1996.167	198481.89	0	239715	0
1996.5	239715	0	246685.02	0
1996.67	199334.66	0	236622.39	0
1997.167	236622.39	25261.02	144560.19	0
1997.333	144560.19	0	204201.11	0
1997.5	204201.11	0	435748.59	0
1997.83	435748.59	52869.18	3524.43	0
1998	3524.43	31342.11	38048.88	0
1998.167	38048.88	0	67169.32	0
1998.333	67169.32	0	60590.03	0
1998.5	60590.03	0	17508.71	0
1998.67	17508.71	0	99131.68	0
1998.83	99131.68	0	118450.84	0
1999	118450.84	0	92926.05	0
1999.167	92926.05	0	87596.18	0
1999.333	87596.18	0	2777.35	0
1999.83	2777.35	0	4475.53	0
2000	4475.53	0	3771.23	0
2000.167	3771.23	0	3901.93	0
2000.333	3901.93	0	0	0
2000.5	7792.83	0	7792.83	0
2000.67	10092.25	0	10092.25	0
2000.83	10992.66	0	10992.66	0
2001	7640.76	0	7640.76	0
2001.167	6986.54	0	6986.54	0
2001.333	6846.63	0	6846.63	0
2001.5	4857.68	0	4857.68	0
2001.67	9781	0	9781	0
2001.83	5763.67	43182.63	5763.67	0
2002	11389.28	0	11389.28	0
2002.167	7319.46	0	7319.46	0
2002.333	8493.98	0	8493.98	0

Carthage Gas Unit No.9-4A				
Depth (ft)	**Ca (ppm)**	**Al (ppm)**	**Fe (ppm)**	**Mg (ppm)**
2002.5	6670.54	0	6670.54	0
2002.67	14909.92	0	14909.92	0
2002.83	10690.04	0	10690.04	0
2003.333	9611.77	0	9611.77	0
2003.5	7845.56	0	7845.56	0
2003.67	9025.35	0	9025.35	0
2003.83	10076.99	58952.94	10076.99	0
2004	6627.58	0	6627.58	0
2004.333	8482.57	0	8482.57	0
2004.5	10676.71	0	10676.71	0
2004.67	12050.66	0	12050.66	0
2004.83	3752.52	41342.27	3752.52	0
2005	3959.19	0	3959.19	0
2006	113451.91	0	0	0
2007	113211.16	0	0	0
2008	154210.36	0	0	0
2009	165408.61	0	0	0
2010	178009.27	0	0	0
2011	136036.81	0	113451.91	0
2011.167	172013.25	0	113211.16	0
2011.333	181323.2	0	154210.36	0
2011.5	198348.64	0	165408.61	0
2011.67	206425.34	0	178009.27	0
2011.83	190782.58	0	136036.81	0
2012	190137.41	0	172013.25	0
2012.167	177224.31	0	181323.2	0
2012.333	160234.89	0	198348.64	0
2012.5	153504.06	0	206425.34	0
2012.67	80558.98	0	190782.58	0
2012.83	3247.93	0	190137.41	0
2013	2775.12	0	177224.31	0
2013.167	3278.1	0	160234.89	0
2013.333	1807.07	0	153504.06	0
2013.5	3751.08	0	80558.98	0
2013.67	3425.02	0	3247.93	0

Carthage Gas Unit No.9-4A				
Depth (ft)	**Ca (ppm)**	**Al (ppm)**	**Fe (ppm)**	**Mg (ppm)**
2013.83	2628.2	42632.83	2775.12	0
2014	4108	0	3278.1	0
2014.167	4477.72	0	1807.07	0
2014.67	3691.52	0	3425.02	0
2014.83	3486.04	0	2628.2	0
2015	2932.1	0	4108	0
2015.167	4246.87	0	4477.72	0
2015.333	4039.79	0	2885.74	0
2015.5	3880.32	0	3691.52	0
2015.67	3782.8	0	3486.04	0
2015.83	4068.69	0	2932.1	0
2016	4166.94	0	4246.87	0
2016.167	5420.27	37090.01	4039.79	15364.46
2016.333	4565.71	0	3880.32	0
2016.5	4261.12	0	3782.8	0
2016.67	3460.34	0	4068.69	0
2016.83	2657.55	30066.74	4166.94	0
2017	3934.09	0	5420.27	0
2017.167	5214.88	0	4565.71	0
2017.333	4230.62	0	4261.12	0
2017.5	8454.26	0	3460.34	0
2017.67	3736.56	51471.59	2657.55	0
2017.83	3959.42	0	3934.09	0
2018	2558.37	0	5214.88	0
2018.167	7175.12	43759.01	4230.62	0
2018.33	5657.43	0	8454.26	0
2018.5	4008.79	0	3736.56	0
2018.67	5360.6	0	3959.42	0
2018.83	5635.16	0	2558.37	0
2019	6299.99	0	7175.12	0
2019.167	9327.28	0	5657.43	0
2019.333	5129.38	0	4008.79	0
2019.5	4369.4	0	5360.6	0
2019.67	10738.06	0	5635.16	0
2019.83	6151.21	0	6299.99	0

Carthage Gas Unit No.9-4A				
Depth (ft)	**Ca (ppm)**	**Al (ppm)**	**Fe (ppm)**	**Mg (ppm)**
2020	135518.23	0	9327.28	0
2020.167	202023.2	0	5129.38	0
2020.167	6847.75	0	4369.4	0
2020.333	5662.22	0	10738.06	0
2020.5	6741.27	0	6151.21	0
2020.67	3883.91	0	135518.23	0
2020.83	7875.02	0	202023.2	0
2021	6381.64	0	6847.75	0
2021.167	5502.82	0	5662.22	0
2021.333	6908.95	0	6741.27	0
2021.5	8407.22	0	3883.91	0
2021.67	9897.66	0	7875.02	0
2021.83	9542.14	0	6381.64	0
2022	10485.12	54856.28	5502.82	18544.41
2022.167	11632.53	0	6908.95	0
2022.333	0	0	8407.22	0
2022.5	8610.15	0	9897.66	0
2022.67	9418.19	0	9542.14	0
2022.83	5068.11	0	10485.12	0
2023.5	146006.91	0	9418.19	0
2023.67	4346.55	0	5068.11	0
2023.83	4728.8	0	146006.91	0
2024	3326.78	0	4346.55	0
2024.167	4848.1	63725.29	4728.8	0
2024.333	5788.84	0	3326.78	0
2024.5	5574.9	0	4848.1	0
2024.67	14866.49	0	5788.84	0
2024.83	3658.38	0	5574.9	0
2025	3035.89	0	14866.49	0
2025.167	10026.12	0	3658.38	0
2025.333	5165.75	0	3035.89	0
2025.5	4773.85	0	10026.12	0
2025.67	10043.75	0	5165.75	0
2025.83	5494.78	0	4773.85	0
2026	5327.6	0	10043.75	0

Carthage Gas Unit No.9-4A				
Depth (ft)	**Depth (ft)**	**Depth (ft)**	**Depth (ft)**	**Depth (ft)**
2026.167	6313	0	5494.78	0
2026.333	8076.89	0	5327.6	0
2026.5	8490.67	0	6313	0
2026.67	1227.36	0	8076.89	0
2026.83	2614.89	0	8490.67	0
2027	4180.64	0	1227.36	0
2027.167	5039.28	0	2614.89	0
2027.333	5266.25	0	4180.64	0
2027.5	5276.31	36173.62	5039.28	0
2027.67	5401.77	40709.98	5266.25	75032.39
2027.83	6776.39	0	5276.31	0
2028	6637.2	0	5401.77	0
2028.167	4695.39	0	6776.39	0
2028.333	2892.25	0	6637.2	0
2028.5	0	0	4695.39	0
2028.67	4415.73	0	2892.25	0
0	5269.86	0	0	0
2029	4117.4	0	4415.73	0
2029.167	4489.64	0	5269.86	0
2029.333	5086.34	0	4117.4	0
2029.5	6250.01	0	4489.64	0
2029.67	0	42854.74	5086.34	0
2029.83	6011.95	0	6250.01	0
2023.167	5367.42	0	6011.95	0
0	5421.24	0	0	0
2030.5	7258.14	0	5367.42	0
2030.67	7981.59	0	5421.24	0
2030.83	6349.62	40521.83	7258.14	6890.06
2031	6419.28	42822.98	7981.59	7961.81
2031.167	6044.34	43300.78	6349.62	9408.62
2031.333	6013.52	42949.41	6419.28	5258.49
2031.5	10860.22	51339.12	6044.34	12803.04
2031.67	7298.08	41673.99	6013.52	11786.86
2031.83	10463.5	49813.97	10860.22	13292.68
2032	10155.36	40756.81	7298.08	0

Carthage Gas Unit No.9-4A				
Depth (ft)	**Depth (ft)**	**Depth (ft)**	**Depth (ft)**	**Depth (ft)**
2032.167	9898.04	49530.36	10463.5	21278.2
2032.333	12485.54	49147.15	10155.36	15606.24
2032.5	6845.57	47228.45	9898.04	0
2032.67	9087.55	48680.39	12485.54	11942.56
2032.83	10327.12	48711.73	6845.57	0
2033	10518.61	54751.63	9087.55	0
2033.167	11800.07	59845.58	10327.12	24324.78
2033.333	7124.9	47902.59	10518.61	0
2033.5	3462.6	55261.83	11800.07	11401.88
2033.67	9975.97	50256.64	7124.9	17655.52
2033.83	8702.19	47546.15	3462.6	26800.23
2034	0	47071.59	9975.97	11093.19
2034.167	3360.51	54201.11	8702.19	12826.06
0	5276.4	0	0	0
2034.5	6137.47	49598.34	3360.51	15802.68
2034.67	3919.64	45697.2	5276.4	12575.7
2034.83	5324.37	50158.37	6137.47	12429.4
2035	4228.5	47959.81	3919.64	19464.43
2035.167	1769.76	55642.44	5324.37	16153.27
2035.333	1756.5	52349.39	4228.5	21747.1
2035.5	5011.26	46508.04	1769.76	22505.92
2035.67	16305.85	45304.25	1756.5	26198.61
2036	6022.82	42096.27	5011.26	20057.95
2036.167	3891.25	38997.66	16305.85	17738.9
2036.67	2442.8	37197.39	6022.82	16409.06
2037	10021.98	40138.46	3891.25	17073.26
2037.333	7974.7	43006.03	2442.8	19659.36
2037.67	38122.14	60337.82	10021.98	9276.27
2038	267371.56	35411.13	7974.7	16262.78
2038.333	13875.86	35857.91	38122.14	8326.72
2038.67	1781.33	24270.76	267371.56	0
2039	3703.56	39022.16	13875.86	11645.9
2039.333	3578.27	39960.74	1781.33	11056.92
2039.67	3294.36	35798.37	3703.56	14279.93
2040	4046.5	43956.7	3578.27	13777.42

Carthage Gas Unit No.9-4A				
Depth (ft)	**Depth (ft)**	**Depth (ft)**	**Depth (ft)**	**Depth (ft)**
2040.333	4489.39	45561.3	3294.36	15639.37
2040.67	4667.72	45745.36	4046.5	18424.28
2041	19167.7	44904.6	4489.39	8797.56
2041.333	3406.56	37686.4	4667.72	7946.07
2041.67	4765.48	42356.58	19167.7	10045.74
2042	75690.47	36128.84	3406.56	17154.24
2042.333	162866.7	39625.05	4765.48	11759.3
2042.67	197054.58	34564.82	75690.47	9810.72
2043	210414.81	78930.67	162866.7	17044.21
2043.333	211336.28	20802.3	197054.58	0
2043.67	0	30884.96	210414.81	11811.25
2044	0	23967.01	211336.28	11871.29

Table 5. Raw XRF data derived from the No.3-A Gena Williamson at a sampling interval of 4 inches. Elemental concentrations in parts per million.

No.3-A Gena Williamson				
Depth (ft)	**Ca (ppm)**	**Al (ppm)**	**Fe (ppm)**	**Mg (ppm)**
2026.67	19393.11	47753	40138.96	9749.02
2027	22008.96	34696.8	59046.55	10476.82
2027.33	38155.17	40126.61	51749.18	14301.64
2028	18068.2	42179.02	53108.82	12629.45
2028.33	25354.29	36418.41	67355.42	13797.11
2028.67	35182.32	37650.22	70511.78	11634.36
2028.83	13485.78	44667.06	75484.12	16102.6
2032	13344.75	29348.41	70619.79	8625.21
2032.33	11056.94	39028.14	77047.73	15698.02
2032.67	5222.94	37942.84	119272.5	19142.31
2033	5548.64	41619.97	126860.1	24604.84
2033.33	14914.49	36812.69	92991.02	20864.92
2033.67	3169.86	35095.25	120169.6	20727.66
2034	5308.01	42659.84	135176.2	23900.22
2034.33	3765.22	37661.37	134174.8	23256.13
2035	184302	24406.17	29339.18	10794.17
2035.33	221345.1	19378.91	31278.1	0
2035.67	10277.36	47677.46	56752.75	8321.57
2036	10713.36	46513.37	64379.63	18912.88
2036.33	9225.86	47420.57	60981.4	10139.18
2037	12123.15	44136.42	65892.09	14675.78
2037.33	6310.29	52014.07	81250.38	18987.53
2038	11796.62	40859.98	85053.16	12852.11
2038.33	10393.32	39234.09	98092.17	19484.89
2038.67	12386.56	35306.31	76516.16	13183.21
2039	18170.15	47537.34	66204.64	10595.17
2039.33	6732.51	51084.18	68591.69	15502.19
2039.67	1069.39	52855.34	47421.22	11705.96
2040	8068.2	51121.5	54377.29	14934.52
2040.33	12861.28	57984.48	59745.72	22574.17
2040.67	9548.13	57583.93	68608.56	15114
2041.33	9764.45	18639.25	83397.48	18639.25

No.3-A Gena Williamson				
Depth (ft)	**Ca (ppm)**	**Al (ppm)**	**Fe (ppm)**	**Mg (ppm)**
2041.67	9754.54	21859.89	100041.9	21859.89
2042	10128.89	17275.43	52145.66	17275.43
2042.33	18727.26	20241.04	113950	20241.04
2043.33	15304.06	25886.32	111114.4	25886.32
2044	7977.84	17030.64	88288	17030.64
2044.33	10688.43	16950.99	99366.93	16950.99
2044.67	5728.48	17816.71	91364.71	17816.71
2045	4731.73	12286.98	58244.17	12286.98
2045.33	7234.21	9958.67	48890.76	9958.67
2045.67	6440.87	10514.85	46301.16	10514.85
2046	7255.84	13285.79	54838.02	13285.79
2046.33	9281.24	10062.22	43722.64	10062.22
2046.67	6395.67	11932.17	49893.34	11932.17
2047.33	12645.38	15098.75	47531.55	15098.75
2047.67	12819.25	21386.33	86572.13	21386.33
2048	21781.95	24328.13	111311.2	24328.13
2048.33	58724.36	17379.67	92059.48	17379.67
2049	96429.76	18775.89	87368.47	18775.89
2049.33	60042.09	27269.14	110273.1	27269.14
2050	3937.04	23500.66	115455.7	23500.66
2050.33	3346.94	29445.36	107466.7	29445.36
2050.67	4287.82	21696.99	94685.51	21696.99
2051	10718.24	24585.64	100554.9	24585.64
2051.33	47247.78	22558.96	87159.03	22558.96
2051.67	41078.85	11589.28	59727.04	11589.28
2052	78245.35	15290.11	80422.67	15290.11
2052.33	109728.2	14674.56	69104.71	14674.56
2052.67	10350.91	14656.64	89886.31	14656.64
2053	16037.91	20390.08	93427.24	20390.08
2053.33	2957.42	21525.57	94245.96	21525.57
2053.67	112732.6	18262.46	56775.1	18262.46
2054	96990.98	8892.42	71284.49	8892.42
2054.33	199510.5	0	27206.02	0
2054.67	48355.25	17781.08	72362.15	17781.08

No.3-A Gena Williamson				
Depth (ft)	**Ca (ppm)**	**Al (ppm)**	**Fe (ppm)**	**Mg (ppm)**
2055	86961.02	14158.13	61794.35	14158.13
2055.33	11275.58	14534.74	67493.77	14534.74
2056	5935.5	16072.12	72473.89	16072.12
2056.33	160061.3	10103.04	29964.08	10103.04
2057.33	202258.6	0	18567.39	0
2057.67	151799.3	6974.48	33210.3	6974.48
2058	120344.7	9712.09	29505.79	9712.09
2058.33	85452.88	4212.67	28383.28	4212.67
2059	59761.34	9974.32	35630.56	9974.32
2059.33	23112.96	13048.02	48290.34	13048.02
2059.67	24528.38	9248.83	40571.89	9248.83
2060	196859.2	6663.1	23025.43	6663.1
2060.33	12140.02	9319.11	41738.76	9319.11
2060.67	4955.52	16306.72	46695.88	16306.72
2061	19146.23	9586.83	44541.71	9586.83
2061.33	15388.98	54548.98	54424.18	10172.39

Table 6. Raw XRF data derived from the No.1 Werner Smith at a sampling interval of 4 inches. Elemental concentrations in parts per million.

No.1 Werner Smith				
Depth (ft)	**Ca (ppm)**	**Al (ppm)**	**Fe (ppm)**	**Mg (ppm)**
2007	12136.74	64533.32	54371.56	15111.98
2007.33	37626.91	48151.67	53384.22	11864.86
2008	47232.09	44384.25	53085.8	5950.28
2008.33	24456.04	53999.82	53568.64	12135.5
2008.667	18048.83	53770.91	63182.79	12300.74
2009	23634.48	55902.02	56516.96	13490.7
2009.33	9258.82	59131.96	55426.21	14145.88
2009.67	36188.83	41312.88	52230.94	8915.04
2010	7537.35	63877.36	55759.41	12085.54
2010.33	7542.68	67471.93	56681.01	10182.39
2010.667	17495.05	65094.4	55520.42	11707.23
2011	10069.37	75520.78	58834.73	13582.12
2011.33	7738.86	59222.65	56197.22	10821.2
2011.667	10122.63	58606.39	61604.89	13148.39
2012	18883.29	59748.01	56082.14	15269.37
2012.33	15503.39	65168.31	55956.81	13805.13
2012.67	17088.61	66033.77	60923.34	18098.37
2013	19544.48	63992.56	59128.09	13662.72
2013.33	18308.24	53257.31	59744.49	9761.74
2013.67	19605.51	60871.32	59199.39	9020.94
2014	12574.95	61180.2	59289.18	10132.17
2014.33	19908.47	64999.68	57938.96	13550.7
2014.67	20487.62	59448.08	59991.05	16881.16
2015	15303.21	56871.4	63539.17	11494.08
2015.33	11684.03	72727.95	62752	13447.8
2015.67	15143.83	57062.63	49298.13	13548.21
2016	8025.64	61848.52	52156.99	11644.04
2016.33	6034.68	61997.46	54968.5	10729.74
2016.67	29937.84	62947.15	59408.89	12760.75
2017	12761.7	55811.15	66791.24	14971.34
2017.33	10593.87	52317.61	56240.91	11315.04
2017.67	10766.82	58928.89	57208.38	11143.18

No.1 Werner Smith				
Depth (ft)	**Ca (ppm)**	**Al (ppm)**	**Fe (ppm)**	**Mg (ppm)**
2018	13282.14	59652.63	68524.47	14036.03
2018.33	14882.61	52261.1	73427.98	14956.42
2018.67	19357.38	58781.68	71347.77	18299.05
2019.33	11772.15	53021.88	58239.36	13706.09
2019.67	10135.98	46380.54	55813.64	7920.94
2020	9360.33	51323.4	41072.8	9159.3
2020.33	11220.52	56892.57	40213.92	10395.66
2020.67	11861.65	57402.05	45043.22	14168.57
2021	11310.88	55102.66	35622.3	13343.86
2021.33	5431.25	48895.55	24999.15	9658.27
2022	8407.73	52204.18	32997.54	9535.57
2022.33	5994.51	51429.59	38626.27	12869.15
2022.67	8628.4	46856.77	49384.77	12613.42
2023	11394.11	40062.84	80717.9	15819.36
2023.33	67547.62	37251.47	115574.95	18643.81
2024	177957.5	29923.1	64471.31	12191.51
2024.33	6788.78	53745.36	87092.14	21619.42
2024.67	5959.01	44705.34	83764.14	18291.56
2025	6865.36	45359.11	61027.83	19063.99
2025.33	6195.26	43682.64	84829.16	21773.84
2025.67	13208.83	44432.3	47862.6	10966.18
2026	153148.95	33479.91	48188.09	8686.91
2026.33	160850.75	28337.74	35279.08	12181.15
2026.67	9078.83	48413.18	95159.06	21356.94
2027	9272.37	47075.41	97353.73	21700.18
2027.33	3602.15	49665.63	120815.48	25321.55
2027.67	6099.47	55361.02	94946.88	28492.04
2028	8206.06	47036.7	132202.13	23647.77
2028.33	7142.27	50047.8	121560.38	27747.62
2028.67	8083.7	44516.34	103604.13	21112.96
2029	8363.96	44552.16	130136.7	19703.83
2029.33	13220.31	38986.7	124115.46	21046.39
2029.67	11884.16	40259.11	97329.46	23059.97
2031	5676.34	43631.99	120210.3	39077.39

No.1 Werner Smith				
Depth (ft)	**Ca (ppm)**	**Al (ppm)**	**Fe (ppm)**	**Mg (ppm)**
2031.33	7839.15	44302.26	75182.89	16256.01
2031.67	6218.89	42247.31	90129.84	21600.31
2031.833	10530.81	49085.8	91686.73	26067.64
2032	8464.09	47509.29	71067.85	18571.6
2032.33	6399.08	44302.71	40916.02	11057.44
2032.67	6625.41	47611.32	62478.9	17249.62
2033	9622.05	42687.76	40880.28	12396.8
2033.33	9070.45	42792.3	33704.23	9876.8
2033.67	216177.33	25988.36	18874.12	6596.84
2034	12533.65	48383.87	35062.58	6066.04
2034.33	12192.47	38027.31	35077.48	5381.24
2034.67	10212.05	44022.85	35355.29	11801.08
2035	5181.11	47683.56	37677.77	17208.28
2035.33	5968.43	44815.19	37860.9	9622.2
2035.67	17685.25	44728.15	53918.88	16322.58
2036	7788.7	45945.95	37242.6	10971.06
2037	11038.55	38135.39	73188.75	13018.03
2037.33	11554.89	42821.7	117117.32	26068.71
2037.67	9694.97	38922.68	98575.2	21463.71
2038	6352.35	39065.43	84587.6	19496.51
2038.67	6417.06	41503.23	82300.95	15385.13
2039	3458.66	43261.85	100969.59	19745.12
2039.33	2874.67	45030.08	124509.27	29973.6
2039.67	3493.94	43880.33	125065.11	33281.95
2040	6365.84	40960.6	105919.34	25824.54
2040.33	5829.69	42742.28	109394.19	21860.01
2040.67	13227.85	43885.19	118291.71	24176.3
2041	17926.39	42948.81	119168.66	27528.79
2041.33	5307.11	37004.6	125608.73	29177.92
2041.67	79786.38	31946.31	76506.36	15594.86
2042	12926.67	44879.8	113284.76	22848.71
2042.33	93707.05	30066.51	65704.93	9625.44
2042.67	10265.56	39155.85	113978.81	26795.96
2043	10718.56	39266.38	96154.29	20386.87

No.1 Werner Smith				
Depth (ft)	**Ca (ppm)**	**Al (ppm)**	**Fe (ppm)**	**Mg (ppm)**
2043.33	8802.34	36602.61	82487.88	14428.92
2043.67	2495.15	45535.65	134502.75	30678.86
2044	2808.83	40628.55	103967.44	25649.13
2044.33	103966.4	32211.03	68550.19	20507.75
2044.67	2574.26	40267.17	68910.32	17590.34
2045	7739.38	37557.05	62237.2	13197.87
2045.67	64676.83	33752.97	52525.1	14592.83
2046	136841.11	23408.1	27435.34	0
2046.33	186921.64	25928.86	36484.41	10288.1
2046.67	190155.16	22557.22	23406.14	0

Table 7. Raw XRF data derived from the No.1 Borders Smith at a sampling interval of 4 inches. Elemental concentrations in parts per million.

No.1 Borders Smith				
Depth (ft)	**Ca (ppm)**	**Al (ppm)**	**Fe (ppm)**	**Mg (ppm)**
2010	409.26	15029.83	65089.59	0
2010.04	543.88	0	20197	0
2010.08	515.22	12123.28	60977.84	0
2011	375.06	19076.03	72151.78	0
2011.04	525.79	12455.09	56721.7	0
2011.08	533.95	12335.81	51710.97	0
2012	539.07	9700.94	53142.48	0
2012.04	356.08	13608.3	62412.71	0
2012.08	520.6	16635.6	56509.28	0
2013	402.56	8638.91	54980.02	0
2013.04	520.43	11501.93	57044.76	0
2013.08	376.87	12368.75	64599.91	0
2014	498.09	10806.61	55660.33	0
2014.04	515.12	16383.68	54642.03	0
2014.08	410.3	12963.34	56242.55	0
2015	429.32	13136.26	54486.84	0
2015.04	406.22	12305.14	49832.45	0
2015.08	555.75	9171.31	51427.92	0
2016	411.94	12792.17	55873.72	0
2017	471.35	13875.84	17570.8	0
2018	431.25	13247.82	58161.04	0
2019	517.15	9452.79	56065.62	0
2019.04	520.58	14689.9	57029.19	0
2019.08	527.61	14831.23	60107.06	0
2020	487.54	15624.08	60443.49	0
2020.04	470.17	12856.18	60986.61	0
2020.08	501.88	16581.48	66653.77	0
2021	493.57	13145.7	50714.73	0
2021.04	509.03	5642.87	51922.41	0
2022	343.51	7093.66	49030.02	0
2023	336.96	17159.96	56035.47	0
2023.04	355.76	9205.16	58476.28	0

No.1 Borders Smith				
Depth (ft)	**Depth (ft)**	**Depth (ft)**	**Depth (ft)**	**Depth (ft)**
2023.08	447.3	15774.39	60721.93	0
2024	504.72	13325.5	60444.04	0
2025	454.55	14351.3	41897.77	0
2025.04	482.34	14925.95	64784.59	0
2025.08	408.05	15290.26	43265.63	0
2026	316.31	14711.27	54473.09	0
2026.04	453.53	8369.04	42998.83	0
2026.08	484.02	17367.95	55348.63	0
2027	442.61	9496.11	46441.7	0
2027.08	510.79	10453.49	46749.64	0
2028	437.95	8253.06	36057.45	0
2028.08	437.59	7904.46	37414.03	0
2029	475.86	10392.48	38448.24	0
2029.04	459.73	11522.78	42389.35	0
2029.08	392.8	9516.41	35624.1	0
2030	441.36	16530.18	53798.82	0
2030.08	406.89	22610.64	130721.49	0
2031	528.13	18819.01	85145.41	0
2031.08	540.83	20660.15	73929.91	10.35
2032	489.08	21074.22	87927.02	0
2032.04	520.75	8462.98	60325.54	0
2032.08	444.04	22122.01	78413.91	0
2033	502.21	12794.36	50322.5	0
2036	495.62	13915.42	33311.68	0
2036.04	533.44	23711.5	90084.06	0
2036.08	405.06	12223.84	54311.7	0
2037	480.49	21399.71	60105.54	0
2037.04	281.94	15697.49	74398.12	0
2037.08	294.68	18758.98	93379.3	0
2038	286.24	10030.59	31678.67	0
2038.04	463.67	20312.42	76995.12	0
2038.08	10246.65	45319.45	72034.55	13092.53
2039	4304.58	44688	64448.63	16146.32
2039.04	7093.66	37400.15	89497.58	16475.85

No.1 Borders Smith				
Depth (ft)	**Depth (ft)**	**Depth (ft)**	**Depth (ft)**	**Depth (ft)**
2039.08	6251.64	43519.32	85196.7	14489.74
2040	194684.94	27046.14	33189.05	0
2040.04	7549.51	49971.15	59279.68	14326.85
2040.08	5546.34	43166.09	76646.54	13356.5
2041	7102.25	41418.35	87346.03	18076.95
2041.04	5607.58	42102.09	69055.85	8279.97
2041.08	6500.52	41245.57	64951.97	9695.94
2042	185342.56	51851.65	34030.42	9221.32
2042.04	10082.63	42809.41	53412.71	11847.79
2042.08	6583.03	42956.65	64821.57	10862.11
2043	6460.83	40416.32	63085.24	12912.41
2043.08	5350.31	39280.59	71811.17	12598.97
2044	16580.84	40307.19	85406.49	16942.34
2044.04	9315.4	41440.5	84043.3	11901.89
2044.08	8569.2	42371.43	51411.69	10928.85
2045	8488.92	38729.3	43133.63	6450.68
2045.04	4939.23	47660.21	40742.38	9316.3
2045.08	3262.31	43167.38	47696.28	14538.14
2046	10562.86	50244.77	79662.86	19961.32
2046.04	15602.1	44771.54	63216.67	14897.46
2046.08	6825.45	42500.5	98744.85	22397.96
2047	5692.67	45272.26	104417.75	22921.99
2047.04	3299.84	46016.88	86192.71	23667.66
2047.08	9703.51	42472.56	116570.74	26346.95
2048	4086.33	46022.86	119039.16	27088.04
2048.04	4179.52	44822.86	126308.63	30436.88
2048.08	3547.14	42640.54	111437.57	28512.1
2049	64624.48	37770.38	88265.64	21396.62
2049.04	156825.75	28190.28	77486.9	12799.06
2049.08	145056.88	33378.39	68001.41	17018.4
2050	86613.61	46213.02	59026.81	10073.67
2050.04	175799.64	30940.5	49755.82	6949.41
2050.08	30800.13	49694.87	80607.51	19747.06
2051	3354.48	41445.33	110884.52	21294.47

No.1 Borders Smith				
Depth (ft)	**Depth (ft)**	**Depth (ft)**	**Depth (ft)**	**Depth (ft)**
2051.04	2810.26	41941.91	99486.59	27737.75
2051.08	3147.5	41314.21	62306.52	13884.79
2052	178742.38	24420.73	40043.77	5663.8
2052.04	177481.75	31035.63	35856.77	6292.39
2052.08	173572.16	33027.95	44789.89	11169.36
2053	168266.88	25659.94	45415.86	8327.66
2056.04	69335.94	36719.8	88945.78	20013.72
2056.08	105690.71	29835.2	60043.72	15175.26
2057	8909.55	35535.54	68889.59	19983.82
2057.04	11877.01	35878.98	63818.68	17491.88
2057.08	11886.1	40584.57	51977.7	11900.61
2058	26427.14	34713.7	55848.5	17649.52
2058.04	11615.39	35473.9	62218.27	17953.96
2058.08	11370.49	39851.9	89154.94	19658.9
2059	8932.14	36528.93	24668.79	7614.2
2059.04	83569.91	29423.13	51204.16	8165.35
2059.08	182924.78	20114.35	17744.61	4710.31
2059.08	211206.08	25932.78	19517.28	0
10000	0	661.79	253071.69	26518.41
2059.08	184033.97	21348.95	17030.47	7462.3
2060	207787.69	40516.09	26547.2	6563.91
2060.04	217756.5	26208.55	28693.64	11776.14
2060.08	208169.23	19766.23	17903.86	8876.77
2061	40257.71	43895.19	40217.38	11313.69
2062	20104.04	45315.24	45894.92	13043.15
2062.08	4230.25	45091.06	37699.61	5354.48

Table 8. Raw XRF data derived from the Carthage Gas Unit No.9-5A at a sampling interval of 4 inches. Elemental concentrations in parts per million.

Carthage Gas Unit No.9-5A				
Depth (ft)	**Ca (ppm)**	**Al (ppm)**	**Fe (ppm)**	**Mg (ppm)**
1986.33	13179.38	45260.37	55199.39	5044.89
1986.67	4590.42	66027.22	55360.02	14835.43
1987	18214.18	57788.35	58559.83	14089.33
1987.33	6402.57	54965.87	52826.43	9479.89
1987.67	6466.37	48130.61	44115.37	9841.48
1988	17586.25	40360.23	49382.9	0
1988.33	5286.19	54144.3	42488.35	7771.65
1988.67	32326.35	48427.78	45119.41	9169.42
1989	55508.63	24812.98	42109.68	0
1989.01	26079.49	43717.01	51504.7	12453.34
1989.33	7292.04	47129.53	61370.04	15659.51
1989.67	21758.59	41795.63	62618.52	12895.35
1990	5908.83	42824.47	57971.28	13481.04
1990.33	51203.35	27257.5	53507.14	4586.25
1990.67	29813.52	39035.62	72911.01	16008.48
1991	28468.32	38626.17	61155.12	12368.83
1991.33	3570.91	52047.35	64953.8	15095.89
1991.67	10711.57	46772.61	56967.67	10451.69
1992	5315.47	45675.88	63276.55	17149.76
1992.33	16458.09	45572.48	71143.64	13858.6
1992.67	9019.21	53733.78	66581.9	10981.95
1993	18208.6	42687.22	76443.27	13666.51
1993.67	17862.89	41881.51	71476.71	10839.71
1993.67	13846.05	47482.94	76002.46	13441.87
1994	17576.21	43816.54	67706.87	12475.85
1994.33	29821.39	49477.13	60161.3	14620.68
1994.67	287540.4	23986.7	24391.11	
1995	5877.07	49648.13	83484.09	15993.85
1995.33	16577.23	47872.54	90931.8	15043.3
1995.67	41534.45	44547.67	77180.04	11906.67
1996	15690.03	58324.52	77265.41	17678.09
1996.33	44733.13	42918.89	66336.05	7271.23
1996.67	8598.92	59591.06	64313.64	15478.46
1997	2853.56	53884.86	87694.87	18585.26
1997.33	9911.72	44922.99	64235.73	13202.93

Carthage Gas Unit No.9-5A				
Depth (ft)	**Depth (ft)**	**Depth (ft)**	**Depth (ft)**	**Depth (ft)**
1998	8916.37	42193.27	85771.41	25369.09
1998.33	6643.59	44021.43	47540.52	10543.95
1998.67	79194.84	40420.18	83365.63	20618
1999	94147.02	32775.3	65408.95	16670.79
1999.33	184173.9	20213.36	81499.97	10405.25
1999.67	91943.57	36590.25	158245.9	18345.23
2000	51812.63	32335.31	122964.4	14586.31
2000.33	11139.81	32226.8	133107.2	10675.28
2000.67	10910.45	44901.39	105076.1	15945.34
2001	35990.93	40569.78	112981.4	15561.43
2001.33	54683.48	44616.11	140393.7	20640.33
2001.67	27179.28	40529.45	105554.2	19384.35
2002	59246.21	36552	115276.8	20202.32
2002.67	14944.48	48949.31	73305.79	12466.45
2003	10401.33	39925.4	69669.22	8750.17
2003.33	17117.17	42542.59	63852.77	8718.58
2003.67	18373.37	51349.03	65860.29	11486.02
2004	8360.66	47162.86	66147.91	15636.77
2004.33	5730.58	50498.36	62195.61	12252.32
2004.67	27138.08	42812	67215.62	11344.91
2005	31134.97	51601.82	53902.6	15255.43

Appendix E - Particle Analysis Data

Table 9. Grain size derived from particle analyses on each thin section.

Thin Section #	**A**	**B**	**C**	**D**	**E**	**F**	**G**	**H**	**I**	**J**
Grain Size (ϕ)	3.92	3.85	1.23	3.99	5.52	4.07	5.51	5.71	18.14	5.60
	3.08	4.48	1.35	3.69	6.43	4.48	6.24	3.08	17.93	5.67
	4.19	3.08	1.50	3.40	6.32	4.19	5.70	6.29	19.93	6.42
	4.48	4.98	1.26	3.32	3.98	4.48	5.30	4.98	15.29	5.90
	3.08	3.69	0.84	2.25	6.11	3.98	6.16	5.63	22.16	5.73
	4.98	2.86	1.55	2.58	4.48	4.19	4.98	4.48	15.93	3.25
	4.48	4.98	1.56	2.19	4.48	4.19	2.98	3.03	22.23	4.48
	5.17	4.98	1.50	4.48	5.67	4.48	6.24	2.90	13.59	6.07
	3.08	2.86	1.54	2.55	4.19	3.98	6.53	5.76	22.06	5.83
	4.48	5.14	0.98	3.13	5.55	4.48	6.22	2.61	21.13	5.96
	2.66	3.40	1.53	3.98	5.50	3.82	5.28	5.90	21.06	2.94
	3.69	5.06	1.50	3.13	5.61	3.58	6.27	5.41	20.34	6.50
	3.58	4.98	0.94	3.03	6.10	3.98	6.36	5.29	12.53	5.93
	3.03	3.69	1.53	2.61	6.60	4.48	5.84	5.38	14.76	5.93
	2.36	2.75	1.50	3.98	6.39	4.19	5.28	6.26	12.32	5.09
	5.07	5.16	0.72	2.90	3.98	3.82	5.80	6.35	20.09	4.98
	2.69	4.48	1.35	5.23	4.48	4.48	6.55	2.61	21.71	5.73
	4.48	2.75	1.50	5.19	5.56	4.48	5.97	3.08	22.07	6.02
	3.82	3.98	1.35	2.58	3.98	3.98	5.97	4.48	8.32	6.12
	4.98	3.40	1.50	5.14	6.35	3.82	6.12	5.85	20.23	6.41
	3.25	3.03	1.20	3.25	5.15	4.48	6.56	5.79	10.76	6.41
	4.48	3.98	0.91	1.88	4.98	4.48	6.19	4.19	15.29	5.83
	3.82	2.82	1.50	4.19	6.54	4.19	6.30	5.14	17.93	3.48
	2.98	5.02	1.08	3.82	5.60	4.19	6.38	6.58	19.99	5.73
	4.48	2.75	1.05	5.23	4.98	4.19	4.48	5.41	16.76	6.33
	4.19	3.25	1.35	2.38	6.46	3.98	6.37	6.38	22.25	6.03
	5.14	5.15	1.35	4.19	4.48	4.19	3.08	6.43	19.93	5.33
	4.98	5.07	1.53	2.27	5.46	3.98	3.58	5.88	20.81	2.51
	3.82	5.22	1.50	4.19	5.29	4.19	6.17	5.21	19.93	3.69
	2.04	3.69	1.35	2.48	6.13	3.98	2.19	5.36	9.44	5.99
	3.32	3.58	1.35	2.42	5.06	4.19	2.69	6.38	21.37	5.77

Thin Section #	A	B	C	D	E	F	G	H	I	J
Grain Size (ϕ)	3.13	3.98	1.35	3.48	6.64	3.98	5.85	5.29	22.44	6.19
	4.19	3.58	1.50	3.32	3.82	3.98	4.98	3.82	21.56	5.33
	4.98	5.06	1.11	2.40	6.39	4.48	5.93	6.32	17.93	6.33
	4.98	4.48	0.24	4.98	4.19	4.48	6.01	5.46	22.13	3.19
	3.32	3.48	1.53	4.98	5.42	4.48	5.66	4.48	17.93	5.31
	3.69	4.48	1.35	4.98	5.03	4.48	4.48	5.80	22.28	4.98
	2.46	2.72	1.35	5.04	6.30	4.48	6.33	6.51	12.76	5.94
	4.98	2.90	1.50	2.63	3.40	4.19	6.31	6.51	21.23	2.46
	4.48	2.94	1.56	4.98	5.07	4.19	6.52	6.23	14.76	5.02
	4.98	2.79	1.53	4.98	5.34	3.32	5.97	6.19	16.76	6.27
	4.48	3.19	1.26	3.25	6.10	4.48	5.92	6.43	21.47	5.07
	4.98	1.70	0.64	1.71	5.19	3.82	5.70	6.45	20.69	5.55
	3.98	5.15	1.20	4.48	5.73	4.19	6.42	4.48	22.01	6.50
	2.79	2.53	0.64	5.15	6.35	4.48	4.19	5.98	15.93	6.45
	3.58	4.48	1.50	3.82	6.06	3.13	5.59	6.40	15.29	4.48
	3.58	2.98	1.52	2.51	6.23	4.48	6.43	5.55	15.93	6.19
	5.11	4.98	0.93	3.82	4.98	4.19	5.20	5.54	17.93	2.34
	4.48	4.48	1.57	3.98	5.91	4.48	6.35	6.24	22.24	5.03
	4.19	5.06	1.35	3.98	4.48	3.82	3.98	6.33	15.93	6.52
	1.72	3.40	0.81	4.98	4.19	4.48	4.48	6.38	11.29	6.63
	5.06	3.25	1.35	4.19	3.25	4.19	6.35	6.07	21.47	5.74
	4.98	4.98	1.15	4.19	6.29	3.98	6.05	5.30	20.00	5.06
	4.98	4.48	1.53	5.17	4.48	4.48	5.20	6.53	14.76	6.05
	4.19	3.69	1.51	2.79	6.10	3.82	6.07	6.60	13.29	4.48
	2.46	2.82	0.68	5.03	3.08	4.48	5.72	6.19	17.93	6.09
	5.17	3.69	1.50	4.19	4.98	4.48	5.73	5.29	22.57	6.05
	2.34	2.55	1.15	4.98	5.93	4.48	5.07	6.62	21.49	6.62
	1.98	2.86	1.53	3.82	6.20	4.19	6.57	6.30	15.93	6.46
	2.72	4.48	1.50	4.98	6.20	4.19	5.25	5.92	14.32	6.38
	4.48	2.72	0.98	2.86	6.46	3.98	5.90	6.45	21.98	5.33
	4.19	3.19	1.26	4.98	3.69	4.48	5.34	4.99	17.93	6.62
	2.79	4.98	1.57	3.82	5.05	3.48	3.98	6.51	21.84	6.53
	4.48	3.19	1.35	2.16	6.02	4.48	6.46	5.55	11.59	6.25
	3.98	2.90	1.20	2.75	6.15	4.48	4.48	6.56	14.76	5.95
	5.16	3.32	0.88	4.98	5.92	4.48	2.90	6.53	20.19	5.81

Thin Section #	A	B	C	D	E	F	G	H	I	J
Grain Size (ϕ)	3.13	4.98	1.50	3.40	6.46	4.19	5.90	6.42	22.06	5.18
	3.98	3.69	1.50	2.94	6.35	4.19	4.19	6.16	13.93	5.80
	4.98	1.99	1.35	2.42	3.98	4.19	5.14	6.04	22.51	6.53
	5.23	4.98	1.15	3.03	5.68	4.48	4.98	6.00	20.72	6.25
	5.10	5.10	1.02	4.48	6.60	4.48	3.69	6.26	14.32	5.56
	4.19	5.16	1.08	5.08	6.56	4.48	5.77	5.94	14.76	5.43
	4.98	4.19	1.35	4.98	5.83	3.98	4.19	6.43	19.93	6.55
	2.30	2.58	1.53	3.48	4.98	4.48	6.30	5.49	22.49	4.98
	4.48	4.48	0.93	4.98	5.60	4.48	3.69	6.45	17.93	6.63
	4.48	3.25	1.50	5.05	3.58	4.19	5.74	2.94	15.29	6.53
	5.15	4.19	1.50	5.20	5.25	3.69	6.12	6.58	13.59	5.82
	2.86	3.48	0.68	2.22	6.12	3.82	5.73	6.19	22.10	5.81
	4.48	2.98	1.05	1.99	4.48	4.19	6.07	4.98	22.26	5.66
	2.55	4.48	1.52	4.48	6.04	4.48	5.02	5.82	12.12	4.98
	4.98	4.19	1.50	4.98	6.04	4.19	6.50	5.13	16.76	6.03
	2.86	4.48	1.08	2.82	3.82	3.69	5.04	4.48	19.93	5.95
	3.69	2.82	1.53	5.22	6.21	4.19	4.48	6.49	22.56	6.44
	1.97	3.40	1.15	4.48	3.82	3.98	5.80	6.07	15.29	3.32
	3.82	5.10	1.15	2.86	6.50	3.69	5.23	4.48	20.72	6.56
	5.12	3.40	1.50	2.98	6.62	4.48	6.17	5.63	13.59	6.52
	4.98	4.19	0.90	3.25	5.60	4.19	6.39	6.00	16.76	6.50
	4.98	4.19	0.67	5.07	6.35	4.19	5.65	6.12	20.16	6.62
	3.40	3.48	1.08	5.23	5.27	4.48	4.98	5.62	19.93	6.43
	4.98	2.86	1.51	4.48	4.98	4.48	5.49	6.23	17.93	6.25
	2.07	4.98	0.57	2.21	6.21	4.48	5.97	5.73	15.29	5.85
	1.57	3.48	1.50	3.98	3.58	3.82	5.72	5.99	22.22	6.32
	4.19	3.19	1.50	4.98	6.51	4.19	3.48	6.36	11.93	6.30
	4.48	3.40	1.35	2.51	6.28	3.98	6.24	6.43	17.93	6.34
	3.40	3.48	0.93	2.15	6.04	3.69	5.66	6.62	19.93	5.91
	1.76	2.58	0.76	2.24	6.00	4.48	6.27	6.24	21.02	6.27
	5.17	3.25	1.26	5.08	5.69	4.48	6.56	6.49	17.93	5.46
	2.61	3.82	1.50	5.11	6.36	4.48	6.49	5.36	22.12	6.58
	4.98	4.48	1.50	4.98	5.17	4.48	5.47	5.57	17.93	6.44
	4.19	4.98	1.50	3.98	5.64	3.40	5.97	6.27	22.18	6.58
	2.03	2.61	1.20	5.02	6.57	4.48	6.05	6.29	21.05	6.27
	2.04	5.06	1.57	3.48	4.19	3.69	6.46	5.76	12.76	6.50

Thin Section #	A	B	C	D	E	F	G	H	I	J
Grain Size (ϕ)	2.72	4.48	1.35	3.48	5.98	4.48	6.23	5.19	17.93	6.53
	5.12	3.08	0.98	3.82	3.58	3.98	5.08	5.07	13.93	4.19
	3.13	2.66	0.93	4.48	6.44	4.19	3.98	5.94	17.93	3.98
	4.98	4.48	1.52	4.19	6.28	3.32	6.35	6.56	22.44	6.42
	4.98	4.19	1.50	4.48	6.19	3.98	5.21	5.71	11.76	6.21
	4.19	4.19	0.74	4.19	4.48	3.69	6.25	6.14	19.93	6.09
	2.02	2.90	1.35	4.98	3.98	3.48	4.98	5.31	17.93	6.07
	5.03	3.25	1.26	5.00	6.23	3.82	5.52	2.90	21.29	4.48
	3.58	4.98	1.00	4.98	6.16	4.48	3.82	6.23	21.96	5.81
	3.82	4.48	1.35	3.69	6.30	4.19	3.08	6.16	16.76	6.26
	5.14	5.10	0.91	4.48	6.47	3.40	4.48	6.19	14.32	6.59
	3.58	3.48	1.57	3.08	2.27	4.19	3.48	6.21	21.73	6.19
	5.20	4.98	0.72	5.21	6.14	3.98	6.28	5.94	22.41	6.53
	3.82	2.42	0.96	4.99	5.04	3.48	4.48	6.19	20.06	5.62
	2.94	5.16	1.35	2.48	6.10	3.69	6.05	5.34	15.93	6.27
	1.67	4.48	1.35	3.82	5.31	4.48	6.33	6.56	19.93	5.66
	5.05	3.40	1.35	4.48	5.86	4.19	6.17	5.70	17.93	6.35
	4.98	2.90	1.50	3.82	6.17	4.19	5.76	5.86	22.32	5.91
	4.48	5.05	1.00	3.82	5.50	3.19	4.98	6.60	17.93	6.49
	2.98	4.98	1.50	4.98	5.09	3.69	3.25	6.58	12.53	6.20
	4.48	4.48	1.57	5.22	5.73	4.48	6.53	6.06	17.93	6.62
	3.69	4.48	1.20	4.98	3.48	3.98	2.30	5.61	21.60	6.08
	3.82	4.48	1.35	2.34	6.10	3.48	6.17	6.56	16.76	6.56
	5.10	4.19	0.45	4.98	5.48	3.98	2.63	6.60	15.29	5.14
	4.98	3.98	0.79	2.61	4.48	3.82	6.53	6.53	12.32	6.05
	3.98	4.48	0.69	4.98	6.58	4.48	1.47	6.24	22.54	5.65
	4.98	4.19	1.54	2.94	6.22	4.19	4.19	6.45	15.29	6.45
	3.69	3.48	1.54	4.19	4.98	3.82	4.98	5.02	11.44	5.43
	3.08	4.98	1.08	5.05	6.19	4.48	6.61	6.60	17.93	6.34
	2.75	2.72	1.54	3.98	6.43	3.58	3.48	6.15	15.93	6.38
	3.40	4.48	1.11	2.30	5.78	3.98	6.46	4.98	20.52	5.70
	3.82	2.58	1.26	4.48	6.02	3.48	3.13	6.12	20.71	6.58
	4.48	5.14	1.35	3.25	5.95	4.19	5.90	6.33	14.32	5.46
	2.30	2.90	1.50	2.46	6.30	3.19	5.86	6.60	20.45	6.53
	4.48	4.19	0.98	2.63	3.48	3.58	6.27	4.98	21.48	6.38
	5.02	4.48	1.57	5.23	6.26	4.48	3.98	5.37	10.76	5.26

Thin Section #	A	B	C	D	E	F	G	H	I	J
Grain Size (ϕ)	5.02	4.19	0.77	2.25	5.11	3.98	5.97	2.16	8.48	6.44
	4.98	4.19	1.50	4.98	5.36	4.48	3.25	6.56	22.17	6.18
	3.13	4.19	0.78	4.48	5.81	2.98	2.19	5.99	22.15	5.29
	2.02	4.98	1.55	2.79	6.38	4.19	5.77	6.62	10.64	6.21
	2.75	4.98	1.15	2.66	5.49	4.48	6.09	6.35	20.27	3.19
	1.51	3.03	1.20	5.20	5.50	4.48	3.48	6.42	16.76	3.48
	4.98	2.63	1.26	5.21	5.08	3.98	6.19	6.30	15.29	5.73
	2.86	4.98	1.35	4.19	5.72	3.82	6.32	5.95	19.93	5.52
	4.19	5.11	1.35	2.15	4.48	3.98	6.46	5.75	17.93	6.33
	3.40	3.40	0.39	3.98	5.80	3.98	6.40	6.08	17.93	6.37
	4.48	5.22	1.11	5.02	4.48	3.98	6.43	6.10	13.59	6.42
	3.58	3.25	1.15	3.82	6.08	2.79	5.73	6.07	19.93	6.62
	3.82	5.10	0.84	3.98	6.42	4.48	5.26	5.10	21.70	5.91
	3.48	2.25	1.50	4.98	5.95	4.19	6.23	6.56	17.93	4.19
	5.21	4.99	1.57	3.32	4.98	4.19	5.29	6.42	15.93	4.98
	4.19	2.46	0.74	3.82	6.48	3.98	5.76	5.72	19.93	6.43
	3.48	3.58	1.51	3.58	5.43	4.19	6.12	6.47	15.93	5.76
	5.18	4.19	0.87	3.48	6.06	3.32	6.49	5.19	16.76	6.21
	4.48	2.38	1.08	2.86	4.48	3.58	5.27	6.04	22.56	6.09
	2.94	2.75	1.26	5.14	4.98	4.19	5.47	6.56	19.93	6.13
	4.98	4.48	1.55	4.19	6.14	3.82	5.63	5.09	12.32	6.59
	3.98	3.40	0.73	4.98	5.66	3.98	5.88	6.26	22.42	6.29
	4.98	4.99	1.50	4.98	4.19	3.98	6.06	3.98	13.29	6.36
	3.98	3.03	0.75	2.66	6.21	4.48	6.22	5.95	17.93	5.07
	4.48	4.19	0.77	3.25	6.54	4.19	5.83	6.58	21.67	3.69
	4.98	5.01	1.26	2.79	5.66	4.48	5.09	6.19	12.12	4.48
	2.46	3.40	1.56	5.22	5.53	3.82	3.48	6.04	19.93	6.49
	5.06	4.19	1.57	4.98	4.98	3.98	2.42	6.10	21.88	6.55
	3.82	3.13	1.50	4.19	4.19	3.98	6.09	5.09	17.93	3.58
	4.98	3.32	1.26	3.03	6.17	4.19	2.98	4.98	19.93	6.25
	4.48	3.32	0.98	4.48	6.44	4.19	6.56	5.56	20.64	5.79
	3.40	2.90	0.76	2.36	6.37	3.69	5.69	6.01	21.47	6.46
	2.75	3.69	1.20	3.08	6.64	4.19	5.91	6.33	13.29	5.91
	3.58	3.25	1.56	4.19	4.98	4.19	6.62	6.11	20.21	5.73
	4.48	3.19	1.54	2.53	3.98	3.69	6.09	2.79	15.29	3.32
	4.19	5.03	0.79	5.13	2.24	4.48	6.45	6.60	21.35	6.61

Thin Section #	A	B	C	D	E	F	G	H	I	J
Grain Size (ϕ)	3.25	2.86	1.15	4.19	5.56	4.19	6.51	5.49	22.45	5.65
		4.98	1.57	4.19	6.30	4.19	6.57	4.98	20.90	6.18
	5.12	5.05	1.53	3.98	6.29	4.48	6.61	5.29	17.93	5.16
	4.48	2.75	1.54	4.98	6.02	4.48	5.18	3.03	19.93	6.54
	3.98	3.08	1.20	2.58	6.14	3.82	4.98	6.62	16.76	3.40
	3.19	3.98	1.57	2.90	3.69	4.19	5.96	5.05	17.93	6.04
	3.08	3.69	1.51	4.48	5.71	3.13	5.11	4.98	16.76	5.64
	3.82	3.08	0.65	4.19	6.48	4.19	6.02	6.17	14.32	4.19
	2.72	2.79	0.91	4.48	6.64	3.69	6.09	5.99	21.82	6.61
	3.25	4.98	1.05	3.48	5.82	4.48	5.06	6.06	15.93	5.99
	4.98	2.22	1.35	3.03	5.47	4.48	2.63	5.80	21.04	4.98
	3.82	4.98	1.15	3.25	5.04	3.98	6.36	6.06	13.29	5.83
	3.03	3.98	0.75	2.90	5.93	3.82	6.47	6.10	22.24	6.17
	4.98	4.48	1.08	4.98	6.50	3.98	6.08	5.78	22.53	5.68
	3.58	3.25	1.20	1.81	6.60	4.19	6.52	6.51	15.93	6.22
	5.12	4.48	0.41	4.98	5.73	4.19	5.45	5.54	21.57	5.91
	5.17	4.98	1.50	3.08	5.35	4.48	6.52	6.27	20.60	1.68
	4.48	3.82	1.50	5.15	3.98	4.19	6.47	5.76	17.93	5.53
	4.19	4.98	1.50	1.84	6.47	3.48	1.92	5.75	14.76	5.71
	4.48	3.40	1.56	4.98	6.48	4.48	5.73	6.09	19.93	6.04
	3.98	2.63	0.73	5.05	5.16	4.48	6.59	6.49	19.93	5.45
	4.48	3.40	1.50	2.53	5.76	4.48	3.19	6.07	20.14	3.82
	2.94	2.44	1.26	5.01	5.42	4.19	6.35	6.00	16.76	6.14
	4.19	4.19	1.50	3.19	6.04	4.19	6.02	5.27	21.43	5.47
	3.03	3.40	1.05	4.98	5.93	4.19	6.63	5.79	15.93	6.44
	2.58	3.32	1.50	2.79	3.13	4.48	3.58	5.14	21.71	6.51
	3.25	2.94	1.56	4.19	5.93	3.98	6.48	6.36	20.39	5.81
	5.04	4.48	1.55	3.40	6.38	4.19	5.79	6.49	12.53	5.23
	3.58	3.82	1.35	4.48	6.14	4.48	6.55	4.48	22.30	5.92
	2.53	4.98	1.51	4.48	6.43	3.82	5.60	6.43	21.79	6.61
	4.48	4.19	0.88	4.98	5.22	4.19	6.38	2.53	16.76	5.95
	2.46	2.69	1.08	3.98	5.63	4.19	3.32	5.82	16.76	5.80
	2.82	4.48	1.53	3.08	4.48	4.19	6.62	6.58	19.93	5.30
	4.98	3.82	1.50	4.48	4.98	4.48	6.13	6.29	20.73	5.35
	3.40	2.72	1.11	3.69	4.98	3.32	6.19	6.60	15.93	6.05
	3.48	3.58	0.40	2.15	5.34	4.19	6.30	5.66	16.76	6.21

Thin Section #	A	B	C	D	E	F	G	H	I	J
Grain Size (ϕ)	4.48	3.98	1.26	2.86	4.19	3.40	5.45	5.56	11.93	3.58
	5.07	4.48	1.53	3.69	6.58	4.19	6.57	6.08	20.02	6.44
	4.48	3.48	1.58	5.22	6.46	3.98	6.20	5.21	19.95	6.45
	3.48	5.03	1.35	3.82	6.60	4.19	6.20	4.98	19.93	6.52
	3.48	3.32	0.22	3.98	5.70	4.48	6.12	6.40	16.76	2.98
	3.82	4.98	0.79	5.17	5.03	4.19	5.70	6.30	16.76	6.29
	2.98	2.86	0.78	3.40	5.53	4.19	5.94	4.48	11.44	6.03
	4.19	1.90	0.75	5.00	6.45	4.19	4.98	5.90	20.44	4.98
	4.98	2.82	1.52	5.11	6.08	3.98	6.31	5.50	22.14	6.35
	4.98	3.82	1.05	3.48	4.19	4.19	5.47	6.60	22.41	1.55
	3.03	2.90	1.54	3.98	6.03	3.98	6.62	6.26	15.93	3.69
	3.58	4.98	1.50	3.13	5.05	3.58	6.24	6.26	21.45	5.36
	3.98	5.09	1.35	3.40	5.63	3.69	5.88	6.00	19.93	5.64
	2.66	5.12	0.72	5.08	6.00	4.48	6.27	5.17	10.88	5.36
	4.48	4.98	1.50	3.48	5.93	4.48	5.70	3.69	16.76	4.98
	3.58	3.98	1.50	3.40	5.27	4.19	5.89	5.89	10.64	5.39
	4.48	3.03	1.50	5.16	5.52	4.48	5.10	6.60	15.29	6.00
	3.19	3.13	1.54	4.19	6.59	4.19	5.88	4.19	22.57	6.11
	4.19	4.48	1.26	3.98	6.11	4.19	6.46	5.68	21.33	6.47
	2.79	2.90	1.11	3.25	5.48	3.82	6.24	6.45	17.93	5.52
	2.58	2.79	0.75	5.16	5.69	3.98	6.08	6.19	21.72	4.98
	2.58	3.69	0.48	4.98	5.70	4.48	6.20	5.17	21.29	5.93
	4.98	2.11	1.57	4.98	5.98	2.94	4.98	3.69	15.29	6.22
	3.98	4.48	1.15	3.58	4.48	3.08	5.82	6.60	22.35	6.01
	2.94	4.19	1.35	5.07	6.46	3.69	6.60	6.45	21.95	3.58
	4.48	5.13	0.82	3.98	5.15	4.48	5.56	5.47	19.93	5.15
	3.32	2.75	1.15	5.10	5.90	3.82	6.01	6.26	19.93	5.93
	3.19	3.13	1.35	4.98	5.40	4.48	6.01	6.04	20.62	6.15
	3.40	3.25	0.41	5.01	6.52	4.48	6.18	6.24	15.29	6.07
	2.40	3.03	0.84	2.51	5.09	3.98	5.14	6.53	15.93	4.19
	4.19	5.19	0.98	5.08	6.28	3.82	6.44	5.12	19.93	5.43
	3.19	2.66	1.35	5.07	5.46	3.98	2.66	6.43	15.93	6.23
	5.19	5.19	1.50	2.24	6.04	3.98	6.20	5.63	17.93	4.48
	4.98	3.98	1.35	4.98	5.41	4.19	5.94	5.66	17.93	6.04
	2.82	2.82	1.20	2.04	5.35	4.48	5.88	6.14	12.32	6.24
	5.19	4.98	0.98	4.98	6.24	4.19	2.94	4.48	22.24	5.42

Thin Section #	A	B	C	D	E	F	G	H	I	J
Grain Size (ϕ)	3.82	2.66	1.15	4.19	5.29	4.19	4.48	4.98	17.93	6.44
	3.32	3.08	1.20	4.48	5.60	3.82	5.41	6.14	14.76	4.48
	3.25	2.66	1.26	2.03	5.26	4.19	6.33	6.58	16.76	6.21
	5.22	3.48	1.11	2.27	6.60	4.48	5.80	6.01	16.76	5.95
	4.48	2.69	1.35	3.25	3.32	3.48	6.27	5.94	15.29	4.98
	4.48	3.25	1.35	4.98	6.18	2.90	6.48	6.36	21.74	6.60
	3.40	3.82	1.35	2.22	6.46	4.48	6.24	6.53	13.93	6.56
	3.82	4.48	1.20	4.98	6.64	4.48	6.10	6.04	15.29	4.48
	3.98	4.98	1.58	4.98	5.29	4.48	3.25	5.94	15.93	5.08
	5.15	3.08	1.05	3.98	6.28	4.19	6.24	6.23	22.49	5.07
	3.69	2.40	1.35	4.48	5.80	4.48	6.22	5.92	11.93	6.54
	5.13	2.58	1.53	2.32	3.82	4.19	5.55	5.87	20.39	3.98
	5.00	2.82	1.02	4.98	6.49	3.82	6.07	6.58	13.93	6.29
	4.48	5.17	0.64	5.15	4.98	4.48	6.48	6.60	17.93	5.96
	3.32	2.40	0.90	2.46	6.51	4.19	6.00	5.81	20.67	6.55
	3.98	2.98	0.93	2.21	6.08	4.19	6.60	6.30	21.05	5.99
	2.02	4.98	1.50	2.82	4.19	4.19	6.04	6.27	17.93	5.60
	2.94	2.29	0.94	3.69	5.95	4.48	6.44	5.52	22.35	6.47
	5.10	2.63	0.98	5.05	5.90	4.48	6.35	5.82	12.76	6.14
	2.32	4.98	1.51	4.48	3.98	3.69	1.71	6.36	13.59	3.69
	2.90	4.98	1.53	4.98	5.78	3.58	4.98	6.38	16.76	5.04
	4.48	3.69	0.73	4.98	4.98	4.48	4.19	6.58	21.30	5.16
	4.98	4.48	1.50	4.48	6.08	3.98	6.08	4.98	14.76	4.48
	3.48	5.18	1.02	4.98	6.62	4.19	6.04	5.49	16.76	4.19
	4.98	5.07	1.35	2.86	4.48	4.48	6.37	5.39	14.76	5.13
	3.32	3.32	1.50	4.98	6.20	3.82	5.86	2.34	19.93	6.59
	4.98	2.94	1.53	4.48	5.94	4.19	6.36	6.49	22.33	3.08
	3.69	2.29	1.56	5.14	6.54	3.32	3.69	6.10	9.67	5.83
	4.48	3.25	0.93	4.48	5.08	4.48	5.16	3.40	13.29	3.25
	4.48	3.08	1.00	2.24	6.19	3.98	3.40	6.33	17.93	6.39
	5.13	3.98	1.50	3.40	4.98	3.48	4.48	6.35	21.87	6.63
	3.08	5.08	1.26	1.93	6.09	3.98	6.04	2.36	19.93	6.59
	4.48	4.98	0.44	3.69	5.44	4.48	6.30	5.61	22.25	5.08
	5.20	2.30	0.98	5.06	6.48	4.19	5.17	5.95	21.47	6.38
	4.48	2.66	1.50	4.98	6.50	4.48	6.46	5.35	11.93	5.62
	2.63	2.75	1.53	5.20	5.83	4.48	5.59	6.33	14.76	5.98

Thin Section #	A	B	C	D	E	F	G	H	I	J
Grain Size (ϕ)	4.48	2.98	1.53	4.19	5.81	3.98	3.98	6.47	17.93	5.09
	4.98	2.90	1.56	4.48	6.37	4.19	6.48	6.16	17.93	5.28
	3.48	2.42	1.50	4.48	6.59	3.98	3.40	5.59	19.93	4.48
	3.40	5.19	1.51	2.94	5.72	3.48	5.97	6.51	16.76	6.38
	4.19	3.08	1.50	4.98	6.47	4.19	6.09	6.53	17.93	5.25
	5.19	3.13	1.50	5.00	6.03	4.19	5.85	6.26	21.98	6.49
	4.19	2.79	0.44	5.17	6.18	3.82	4.48	4.48	19.96	5.59
	3.98	5.09	0.88	4.48	4.98	4.48	4.98	6.49	11.29	3.98
	4.98	3.40	1.00	4.98	4.98	4.19	5.74	2.69	15.93	5.40
	3.58	2.94	1.05	3.58	5.41	2.86	5.05	5.39	19.93	4.98
	4.48	3.98	1.15	5.17	5.58	4.48	6.03	3.03	21.25	5.77
	4.48	4.48	1.53	1.96	6.35	3.19	6.59	6.49	21.55	4.19
	4.98	2.75	0.65	3.98	5.69	3.98	6.09	5.95	15.93	5.97
	3.08	4.48	0.91	3.98	4.48	3.82	5.09	5.72	21.22	6.49
	3.98	5.19	1.52	5.01	5.70	3.98	6.48	5.92	14.76	6.63
	4.48	3.25	1.54	4.98	6.52	4.19	4.19	6.24	17.93	6.29
	3.82	5.07	1.50	4.19	6.16	3.98	6.21	5.61	17.93	6.54
	3.82	3.32	1.50	3.82	3.19	3.82	6.53	5.88	15.93	6.22
	2.94	3.32	1.57	5.10	3.69	3.82	5.91	6.02	14.76	6.04
	5.06	4.98	1.11	5.11	3.40	3.98	5.61	4.48	17.93	5.60
	4.48	3.69	1.55	5.00	4.98	3.82	2.18	6.49	22.53	6.18
	4.98	3.19	1.50	4.19	6.20	4.19	6.07	5.60	12.53	5.27
	3.98	2.82	0.76	5.12	6.31	3.98	5.02	6.40	19.93	3.58
	3.32	4.19	1.35	4.98	5.70	4.48	6.21	6.29	22.22	6.28
	1.13	5.20	1.20	5.20	4.19	3.58	5.17	5.58	16.76	6.15
	3.13	3.08	1.54	3.48	5.83	3.69	6.09	5.87	16.76	5.20
	2.86	2.86	1.57	2.46	6.40	4.19	2.38	6.53	22.02	5.66
	1.83	4.48	1.50	5.09	5.43	3.82	6.13	5.37	19.93	6.33
	3.40	2.63	1.50	3.69	5.42	4.48	6.30	5.52	22.31	6.38
	4.48	3.13	1.54	3.03	5.98	4.19	6.13	6.45	21.19	6.30
	3.98	3.19	1.50	2.90	6.26	4.19	6.55	6.23	20.53	5.99
	5.05	5.12	1.52	2.07	5.42	4.19	6.37	6.27	17.93	4.98
	2.98	5.11	1.50	5.10	5.92	3.13	4.98	5.49	17.93	6.24
	2.98	2.90	1.50	5.24	5.99	3.98	6.59	5.97	21.94	4.98
	4.48	2.98	0.85	3.19	6.46	4.19	6.15	3.08	21.73	6.29
	3.48	4.98	1.26	2.24	5.96	3.58	5.31	6.30	17.93	6.23

Thin Section #	A	B	C	D	E	F	G	H	I	J
Grain Size (ϕ)	4.98	3.13	1.02	3.19	5.17	3.82	5.73	4.48	19.93	5.44
	2.36	4.98	1.35	4.98	4.19	3.82	4.98	5.99	15.29	6.54
	5.22	4.48	1.26	4.98	6.24	4.19	6.57	5.85	22.16	5.59
	3.69	5.00	1.52	5.23	6.59	4.48	5.43	6.51	15.93	6.54
	4.19	4.98	0.96	4.48	4.19	4.48	6.50	6.40	22.23	5.85
	3.19	2.46	1.53	4.98	5.73	4.48	6.61	6.60	13.59	6.38
	4.98	2.58	1.15	4.98	4.19	3.82	6.52	6.47	22.06	6.56
	3.82	3.69	1.57	4.98	4.19	3.98	6.32	4.98	21.13	3.58
	5.21	3.82	0.84	5.10	3.58	3.82	5.89	6.40	21.06	3.82
	5.10	4.48	1.55	5.04	5.28	3.82	2.30	6.24	20.34	6.23
	3.69	3.48	0.49	3.08	5.34	4.19	6.60	6.27	12.53	5.79
	2.90	3.25	1.53	3.98	5.40	2.86	2.27	5.05	14.76	6.54
	4.48	4.99	0.12	3.32	5.20	4.48	6.41	2.58	12.32	6.53
	3.19	3.98	1.26	3.69	4.48	3.98	5.00	5.11	20.09	5.35
	2.55	4.19	1.51	5.04	6.34	3.82	6.19	5.68	21.71	6.53
	3.69	3.82	1.26	2.48	5.67	3.82	3.32	3.82	22.07	6.23
	4.19	3.69	1.00	2.22	4.19	4.19	6.44	5.42	8.32	6.54
	4.19	2.94	1.52	4.48	6.25	3.98	5.98	3.98	20.23	5.88
	1.36	2.86	0.72	3.82	5.33	4.48	3.32	6.49	10.76	5.32
	5.23	4.19	1.50	3.58	6.53	3.32	5.55	5.19	15.29	5.53
	4.48	2.79	1.50	3.48	3.98	3.98	5.77	6.15	17.93	6.50
	5.16	4.48	1.56	2.40	5.44	4.19	4.98	4.48	19.99	6.02
	0.79	2.98	1.50	4.98	6.62	4.48	5.60	6.17	16.76	6.10
	3.69	4.48	1.02	4.48	6.29	4.48	5.02	5.35	22.25	6.47
	2.86	3.98	1.35	4.98	6.01	3.98	5.54	5.58	19.93	2.82
	4.98	4.19	0.93	2.40	6.47	3.98	5.58	6.26	20.81	3.98
	2.79	2.55	0.84	2.69	2.63	3.82	6.13	6.42	19.93	5.70
	0.62	2.42	0.87	2.29	5.45	4.19	6.54	6.43	9.44	5.23
	3.98	4.48	0.70	3.69	6.35	3.82	4.98	5.76	21.37	4.98
	4.19	3.98	0.70	4.48	3.58	4.48	2.79	4.19	22.44	5.35
	4.99	5.15	0.84	3.98	4.48	4.19	6.29	6.07	21.56	6.59
	4.19	4.19	1.35	4.19	5.41	3.82	5.44	6.10	17.93	6.26
	4.48	4.98	1.35	2.63	5.05	3.58	5.74	6.49	22.13	6.58
	5.14	2.42	1.54	3.25	5.97	3.98	6.46	6.04	17.93	6.28
	5.01	3.13	1.35	4.19	6.54	3.69	6.24	6.43	22.28	6.38
	5.01	5.12	1.50	4.48	6.34	4.48	6.08	6.29	12.76	6.14

Thin Section #	A	B	C	D	E	F	G	H	I	J
Grain Size (ϕ)	3.58	4.99	0.64	4.98	5.73	3.48	6.62	6.29	21.23	3.69
	5.02	4.98	1.53	4.19	6.07	4.19	5.64	5.38	14.76	5.14
	3.82	5.02	1.35	3.13	5.28	3.98	5.02	5.86	16.76	5.90
	3.58	4.98	1.05	2.86	6.60	3.82	6.59	6.35	21.47	6.45
	3.48	3.98	1.15	5.18	5.54	3.69	5.96	5.95	20.69	4.98
	3.69	4.99	1.50	4.98	6.32	3.25	5.45	6.42	22.01	5.27
	4.98	2.69	1.55	3.03	6.19	3.19	4.98	4.19	15.93	6.36
	3.58	4.98	1.56	5.06	6.03	3.98	4.19	4.48	15.29	4.48
	5.15	2.40	1.26	4.98	5.56	3.48	5.78	5.62	15.93	6.52
	4.19	5.08	1.54	5.09	6.08	4.19	5.04	6.45	17.93	6.15
	4.19	3.13	1.35	4.98	4.98	4.19	6.54	6.60	22.24	4.48
	4.48	3.03	1.35	5.07	4.98	3.48	6.35	6.60	15.93	6.23
	2.86	4.98	0.93	2.46	5.42	3.98	4.98	4.48	11.29	5.13
	3.98	4.48	1.05	5.18	5.39	4.19	6.46	6.01	21.47	2.58
	2.16	3.25	1.02	4.48	4.98	4.19	6.00	6.23	20.00	5.62
	5.10	2.40	0.88	2.94	6.58	4.19	5.39	6.20	14.76	6.06
	2.90	3.98	1.57	4.98	6.17	3.69	3.48	5.96	13.29	4.98
	5.24	4.19	0.88	2.69	3.69	4.19	3.58	6.62	17.93	6.37
	4.48	2.63	1.56	3.58	6.58	4.48	6.09	6.23	22.57	3.13
	3.82	3.98	1.26	5.14	6.54	4.19	6.40	6.30	21.49	5.20
	4.98	4.48	1.26	2.90	5.72	4.48	6.13	4.48	15.93	5.71
	4.19	3.48	1.50	2.02	6.46	4.48	6.63	6.62	14.32	4.48
	4.19	3.40	0.93	4.98	6.40	3.82	3.03	5.72	21.98	4.98
	4.98	4.98	1.26	5.03	5.93	4.48	5.20	6.58	17.93	4.48
	2.82	5.21	1.51	5.15	5.85	4.19	4.98	5.07	21.84	4.19
	4.48	5.22	1.20	4.48	6.41	3.98	6.43	6.32	11.59	4.98
	4.48	5.17	1.11	5.23	4.48	3.82	6.11	5.06	14.76	4.48
	4.98	4.98	1.02	5.03	3.58	4.19	3.40	6.43	20.19	4.48
	3.69	4.98	1.50	4.48	6.52	4.19	4.98	5.74	22.06	3.48
	4.98	5.22	0.77	2.75	6.58	3.82	5.99	5.27	17.93	5.87
	3.82	5.17	1.50	5.03	6.32	4.48	5.54	6.16	13.93	3.25
	5.11	3.82	0.72	4.98	5.36	4.48	6.30	5.86	22.51	5.95
	2.53	4.19	1.35	5.09	3.19	4.48	6.48	1.42	20.72	5.62
	3.48	3.08	1.50	4.98	5.88	4.48	5.74	4.48	14.32	6.55
	4.98	3.13	1.35	3.69	4.48	3.03	5.64	3.25	14.76	6.61
	2.29	5.18	1.11	4.98	6.57	4.19	5.82	6.20	19.93	4.98

Thin Section #	A	B	C	D	E	F	G	H	I	J
Grain Size (ϕ)	3.58	5.02	1.15	4.48	4.19	4.19	6.48	5.82	22.49	5.95
	2.86	3.98	0.74	2.46	3.98	3.48	6.63	4.98	17.93	4.48
	3.82	4.98	1.53	4.98	5.76	4.48	6.49	6.32	15.29	3.98
	2.98	2.75	1.20	5.14	6.37	4.48	5.96	5.91	13.59	6.63
	5.21	3.08	1.20	5.16	3.98	4.19	6.32	4.48	22.10	4.48
	2.48	4.98	0.45	2.42	4.19	4.48	6.23	6.33	22.26	6.56
	2.08	4.98	1.54	4.48	5.41	3.48	5.74	2.61	12.12	4.19
	5.12	4.98	1.35	3.82	4.98	3.69	6.28	6.33	16.76	4.19

Appendix F-Point Count Data

Table 10. Point count data derived from thin section A from the Carthage Gas Unit No.9-4A at 2012 ft.

Thin Section A: Carthage Gas Unit No.9-4A, 2012ft					
	Calcite Cement	**Quartz**	**Chalcedonic Quartz**	**Pellets**	**Pore Spaces**
	1				
	1				
	1				
		1			
	1				
	1				
		1			
	1				
	1				
					1
	1				
		1			
				1	
					1
					1
		1			
	1				
		1			
				1	

Thin Section A: Carthage Gas Unit No.9-4A, 2012ft					
	Calcite Cement	**Quartz**	**Chalcedonic Quartz**	**Pellets**	**Pore Spaces**
		1			
	1				
	1				
		1			
		1			
			1		
	1				
				1	
	1				
					1
		1			
				1	
		1			
	1				
		1			
		1			
		1			
	1				
	1				
		1			
		1			
		1			
					1

Thin Section A: Carthage Gas Unit No.9-4A, 2012ft					
	Calcite Cement	**Quartz**	**Chalcedonic Quartz**	**Pellets**	**Pore Spaces**
				1	
		1			
		1			
					1
		1			
		1			
				1	
		1			
	1				
	1				
	1				
		1			
					1
	1				
		1			
		1			
		1			
				1	
	1				
		1			
					1
	1				
	1				

Thin Section A: Carthage Gas Unit No.9-4A, 2012ft					
	Calcite Cement	**Quartz**	**Chalcedonic Quartz**	**Pellets**	**Pore Spaces**
	1				
		1			
		1			
		1			
		1			
		1			
			1		
	1				
		1			
	1				
		1			
		1			
		1			
					1
	1				
		1			
					1
					1
		1			
					1
		1			

Thin Section A: Carthage Gas Unit No.9-4A, 2012ft					
	Calcite Cement	**Quartz**	**Chalcedonic Quartz**	**Pellets**	**Pore Spaces**
		1			
		1			
	1				
	1				
	1				
				1	
	1				
		1			
	1				
	1				
	1				
		1			
Total	35	42	1	9	13

Table 11. Point count data derived from thin section B from the Carthage Gas Unit No.9-4A at 2016 ft.

Thin Section B: Carthage Gas Unit No.9-4A, 2016 ft						
	Calcite Cement	**Quartz**	**Chalcedonic Quartz**	**Pellets**	**Pore Spaces**	**Hematite**
			1			
		1				
	1					
	1					
		1				
				1		
		1				
	1					
				1		
		1				
	1					
	1					
		1				
		1				
	1					
		1				
		1				
		1				
	1					
					1	
		1				

Thin Section B: Carthage Gas Unit No.9-4A, 2016 ft						
	Calcite Cement	**Quartz**	**Chalcedonic Quartz**	**Pellets**	**Pore Spaces**	**Hematite**
	1					
		1				
		1				
		1				
		1				
		1				
		1				
				1		
				1		
		1				
					1	
		1				
		1				
		1				
	1					
		1				
	1					
					1	
					1	
		1				
	1					
		1				
		1				

Thin Section B: Carthage Gas Unit No.9-4A, 2016 ft						
	Calcite Cement	**Quartz**	**Chalcedonic Quartz**	**Pellets**	**Pore Spaces**	**Hematite**
		1				
		1				
	1					
		1				
		1				
		1				
						1
	1					
		1				
		1				
					1	
		1				
		1				
	1					
		1				
		1				
		1				
	1					
	1					
	1					
		1				
		1				
		1				

Thin Section B: Carthage Gas Unit No.9-4A, 2016 ft						
	Calcite Cement	**Quartz**	**Chalcedonic Quartz**	**Pellets**	**Pore Spaces**	**Hematite**
		1				
		1				
		1				
		1				
	1					
		1				
		1				
		1				
		1				
		1				
		1				
					1	
	1					
						1
		1				
		1				
		1				
		1				
		1				
	1					
					1	
	1					
	1					

Thin Section B: Carthage Gas Unit No.9-4A, 2016 ft						
	Calcite Cement	**Quartz**	**Chalcedonic Quartz**	**Pellets**	**Pore Spaces**	**Hematite**
		1				
		1				
		1				
	1					
	1					
	1					
		1				
		1				
		1				
		1				
Total	25	61	1	4	7	2

Table 12. Point count data derived from thin section C from the Carthage Gas Unit No.9-4A at 2022 ft.

Thin Section C: Carthage Gas Unit No.9-4A, 2022 ft						
	Matrix	**Quartz**	**Chalcedonic Quartz**	**Pellets**	**Pore Spaces**	**Hematite**
	1					
		1				
		1				
	1					
	1					
		1				
		1				
		1				
		1				
		1				
		1				
		1				
		1				
				1		
	1					
			1			
			1			
				1		
				1		
	1					
				1		

Thin Section C: Carthage Gas Unit No.9-4A, 2022 ft						
	Matrix	**Quartz**	**Chalcedonic Quartz**	**Pellets**	**Pore Spaces**	**Hematite**
			1			
		1				
				1		
		1				
				1		
			1			
			1			
		1				
		1				
		1				
		1				
		1				
						1
						1
						1
			1			
						1
		1				
		1				
						1
		1				
		1				

Thin Section C: Carthage Gas Unit No.9-4A, 2022 ft						
	Matrix	**Quartz**	**Chalcedonic Quartz**	**Pellets**	**Pore Spaces**	**Hematite**
		1				
		1				
		1				
		1				
		1				
	1					
	1					
				1		
		1				
	1					
	1					
		1				
		1				
		1				
			1			
		1				
		1				
			1			
		1				
		1				
		1				
				1		
	1					

Thin Section C: Carthage Gas Unit No.9-4A, 2022 ft						
	Matrix	**Quartz**	**Chalcedonic Quartz**	**Pellets**	**Pore Spaces**	**Hematite**
	1					
		1				
		1				
	1					
		1				
	1					
						1
						1
		1				
		1				
						1
						1
						1
						1
						1
						1
	1					
	1	1				
					1	
		1				
		1				

Thin Section C: Carthage Gas Unit No.9-4A, 2022 ft						
	Matrix	**Quartz**	**Chalcedonic Quartz**	**Pellets**	**Pore Spaces**	**Hematite**
			1			
			1			
		1				
					1	
		1				
		1				
		1				
		1				
		1				
		1				
	1					
					1	
Total	16	50	10	8	3	13

Thin Section D: Carthage Gas Unit No.9-4A, 2037 ft					
	Matrix	**Quartz**	**Chalcedonic Quartz**	**Pellets**	**Pore Spaces**
		1			
	1				
	1				
	1				
				1	
				1	
	1				
		1			
		1			
		1			
		1			
	1				
		1			
		1			
		1			
		1			
		1			
		1			
	1				
			1		
			1		
			1		

Table 13. Point count data derived from thin section D from the Carthage Gas Unit No.9-4A at 2037 ft.

Thin Section D: Carthage Gas Unit No.9-4A, 2037 ft					
	Matrix	**Quartz**	**Chalcedonic Quartz**	**Pellets**	**Pore Spaces**
	1				
	1				
	1				
	1				
		1			
		1			
		1			
	1				
	1				
		1			
		1			
		1			
	1				
	1				
		1			
		1			
	1				
		1			
		1			
	1				
		1			

Thin Section D: Carthage Gas Unit No.9-4A, 2037 ft					
	Matrix	**Quartz**	**Chalcedonic Quartz**	**Pellets**	**Pore Spaces**
		1			
	1				
	1				
		1			
		1			
		1			
		1			
	1				
	1				
	1				
	1				
		1			
		1			
		1			
		1			
	1				
	1				
		1			
	1				
	1				
		1			
		1			
		1			

Thin Section D: Carthage Gas Unit No.9-4A, 2037 ft					
	Matrix	**Quartz**	**Chalcedonic Quartz**	**Pellets**	**Pore Spaces**
	1				
		1			
	1				
	1				
	1				
			1		
	1				
	1				
	1				
		1			
		1			
			1		
			1		
			1		
	1				
	1				
		1			
	1				
		1			
			1		
	1				
	1				

Thin Section D: Carthage Gas Unit No.9-4A, 2037 ft					
	Matrix	**Quartz**	**Chalcedonic Quartz**	**Pellets**	**Pore Spaces**
		1			
	1				
		1			
		1			
		1			
			1		
			1		
	1				
	1				
			1		
	1				
	1				
Total	43	44	11	2	0

Table 14. Point count data derived from thin section E from the Carthage Gas Unit No.9-4A at 2043 ft.

Thin Section E: Carthage Gas Unit No.9-4A, 2043 ft					
	Calcite Cement	**Quartz**	**Chalcedonic Quartz**	**Pellets**	**Pore Spaces**
				1	
	1				
	1				
		1			
	1				
	1				
	1				
	1				
		1			
		1			
	1				
				1	
				1	
				1	
			1		
	1				
				1	
		1			
		1			
		1			
		1			

Thin Section E: Carthage Gas Unit No.9-4A, 2043 ft					
	Calcite Cement	**Quartz**	**Chalcedonic Quartz**	**Pellets**	**Pore Spaces**
		1			
		1			
		1			
	1				
		1			
		1			
		1			
	1				
	1				
			1		
		1			
		1			
		1			
	1				
				1	
		1			
	1				
	1				
		1			
		1			
	1				
		1			
	1	1			

Thin Section E: Carthage Gas Unit No.9-4A, 2043 ft					
	Calcite Cement	**Quartz**	**Chalcedonic Quartz**	**Pellets**	**Pore Spaces**
		1			
		1			
	1				
	1				
		1			
		1			
		1			
		1			
	1				
	1				
				1	
				1	
	1				
	1				
		1			
	1				
		1			
		1			
		1			
		1			
				1	
	1				

Thin Section E: Carthage Gas Unit No.9-4A, 2043 ft					
	Calcite Cement	**Quartz**	**Chalcedonic Quartz**	**Pellets**	**Pore Spaces**
		1			
				1	
				1	
		1			
		1			
		1			
	1				
	1				
				1	
	1				
	1				
			1		
	1				
	1				
		1			
				1	
		1			
	1				
		1			
		1			
		1			
	1				

Thin Section E: Carthage Gas Unit No.9-4A, 2043 ft					
	Calcite Cement	**Quartz**	**Chalcedonic Quartz**	**Pellets**	**Pore Spaces**
		1			
		1			
		1			
		1			
		1			
		1			
		1			
		1			
		1			
		1			
		1			
		1			
Total	32	53	3	13	0

Table 15. Point count data derived from thin section F from the Werner Smith No.1-A at 2011 ft.

Thin Section F: Werner Smith No.1-A, 2011 ft					
	Matrix	**Quartz**	**Chalcedonic Quartz**	**Pellets**	**Pore Spaces**
		1			
		1			
		1			
		1			
		1			
		1			
		1			
		1			
		1			
		1			
		1			
		1			
	1				
		1			
		1			
	1				
				1	
		1			
		1			
		1			
	1				

Thin Section F: Werner Smith No.1-A, 2011 ft					
	Matrix	**Quartz**	**Chalcedonic Quartz**	**Pellets**	**Pore Spaces**
	1				
	1				
		1			
		1			
		1			
		1			
				1	
		1			
		1			
		1			
	1				
		1			
		1			
		1			
		1			
				1	
	1				
	1				
		1			
		1			
		1			
		1			
		1			

Thin Section F: Werner Smith No.1-A, 2011 ft					
	Matrix	**Quartz**	**Chalcedonic Quartz**	**Pellets**	**Pore Spaces**
		1			
		1			
		1			
	1				
		1			
		1			
		1			
		1			
		1			
		1			
		1			
	1				
	1				
	1				
		1			
		1			
		1			
		1			
		1			
		1			
		1			
		1			

Thin Section F: Werner Smith No.1-A, 2011 ft					
	Matrix	**Quartz**	**Chalcedonic Quartz**	**Pellets**	**Pore Spaces**
		1			
		1			
		1			
	1				
	1				
	1				
	1				
	1				
	1				
		1			
		1			
	1				
		1			
	1				
		1			
		1			
	1				
	1				
	1				
	1				
	1				
	1				

Thin Section F: Werner Smith No.1-A, 2011 ft					
	Matrix	**Quartz**	**Chalcedonic Quartz**	**Pellets**	**Pore Spaces**
	1				
		1			
	1				
	1				
	1				
	1				
	1				
	1				
	1				
	1	1			
Total	35	62	0	3	0

Table 16. Point count data derived from thin section G from the Werner Smith No.1-A at 2026 ft.

Thin Section G: Werner Smith No.1-A, 2026 ft						
	Calcite Cement	**Quartz**	**Chalcedonic Quartz**	**Pellets**	**Pore Spaces**	**Plagioclase**
				1		
	1					
				1		
		1				
		1				
		1				
		1				
		1				
		1				
				1		
				1		
		1				
	1					
				1		
	1					
		1				
		1				
	1					
		1				
	1					
	1					

Thin Section G: Werner Smith No.1-A, 2026 ft						
	Calcite Cement	**Quartz**	**Chalcedonic Quartz**	**Pellets**	**Pore Spaces**	**Plagioclase**
				1		
				1		
		1				
				1		
						1
				1		
				1		
		1				
	1					
				1		
				1		
				1		
	1					
		1				
	1					
	1					
	1					
	1					
	1					
	1					
	1					
	1					
				1		

Thin Section G: Werner Smith No.1-A, 2026 ft						
	Calcite Cement	**Quartz**	**Chalcedonic Quartz**	**Pellets**	**Pore Spaces**	**Plagioclase**
	1					
	1					
	1					
		1				
	1					
	1					
				1		
	1					
				1		
	1					
	1					
		1				
		1				
		1				
				1		
	1					
	1					
	1					
	1					
	1					
	1					
	1					

Thin Section G: Werner Smith No.1-A, 2026 ft						
	Calcite Cement	**Quartz**	**Chalcedonic Quartz**	**Pellets**	**Pore Spaces**	**Plagioclase**
		1				
						1
			1			
				1		
		1				
		1				
		1				
				1		
	1					
		1				
	1					
		1				
		1				
				1		
		1				
		1				
	1					
	1					
		1				
				1		
	1					
						1

Thin Section G: Werner Smith No.1-A, 2026 ft						
	Calcite Cement	**Quartz**	**Chalcedonic Quartz**	**Pellets**	**Pore Spaces**	**Plagioclase**
		1				
	1					
	1					
	1					
		1				
	1					
	1					
	1					
	1					
	1					
		1				
	1					
Total	45	30	2	20	0	3

Table 17. Point count data derived from thin section H from the Werner Smith No.1-A at 2028 ft.

Thin Section H: Werner Smith No.1-A, 2028 ft						
	Matrix	**Quartz**	**Chalcedonic Quartz**	**Pellets**	**Pore Spaces**	**Plagioclase**
	1					
	1					
		1				
	1					
	1					
		1				
		1				
			1			
	1					
		1				
		1				
		1				
	1					
		1				
	1					
	1					
		1				
		1				
			1			
		1				
		1				

Thin Section H: Werner Smith No.1-A, 2028 ft						
	Matrix	**Quartz**	**Chalcedonic Quartz**	**Pellets**	**Pore Spaces**	**Plagioclase**
						1
				1		
	1					
		1				
		1				
					1	
						1
	1					
		1				
	1					
	1					
	1					
	1					
		1				
		1				
		1				
		1				
		1				
		1				
						1
		1				
	1					
				1		

Thin Section H: Werner Smith No.1-A, 2028 ft						
	Matrix	**Quartz**	**Chalcedonic Quartz**	**Pellets**	**Pore Spaces**	**Plagioclase**
		1				
						1
		1				
	1					
	1					
	1					
		1				
	1					
	1					
		1				
		1				
		1				
	1					
	1					
				1		
	1					
		1				
		1				
	1					
		1				
		1				
		1				

Thin Section H: Werner Smith No.1-A, 2028 ft						
	Matrix	**Quartz**	**Chalcedonic Quartz**	**Pellets**	**Pore Spaces**	**Plagioclase**
		1				
	1					
		1				
	1					
	1					
	1					
	1					
		1				
		1				
		1				
		1				
		1				
	1					
		1				
		1				
		1				
		1				
	1					
		1				
	1					
		1				
		1				

Thin Section H: Werner Smith No.1-A, 2028 ft						
	Matrix	**Quartz**	**Chalcedonic Quartz**	**Pellets**	**Pore Spaces**	**Plagioclase**
		1				
		1				
	1					
	1					
				1		
		1				
	1					
		1				
	1					
		1				
	1					
	1					
Total	38	51	3	4	0	4

Table 18. Point count data derived from thin section I from the No.3-A Gena Williamson at 2037 ft.

Thin Section I: No.3-A Gena Williamson, 2037 ft					
	Matrix	**Quartz**	**Chalcedonic Quartz**	**Pellets**	**Pore Spaces**
	1				
	1				
		1			
		1			
		1			
	1				
		1			
		1			
		1			
		1			
		1			
		1			
		1			
	1				
		1			
	1				
	1				
	1				
		1			
		1			
	1				

Thin Section I: No.3-A Gena Williamson, 2037 ft					
	Matrix	**Quartz**	**Chalcedonic Quartz**	**Pellets**	**Pore Spaces**
		1			
	1				
		1			
	1				
	1				
		1			
	1				
				1	
		1			
	1				
		1			
		1			
	1				
	1				
		1			
	1				
			1		
		1			
	1				
		1			
		1			
		1			
	1				

Thin Section I: No.3-A Gena Williamson, 2037 ft					
	Matrix	**Quartz**	**Chalcedonic Quartz**	**Pellets**	**Pore Spaces**
	1				
	1				
	1				
	1				
		1			
		1			
	1				
	1				
	1				
	1				
	1				
		1			
		1			
		1			
		1			
			1		
	1				
		1			
	1				
	1				
				1	
	1				
		1			

Thin Section I: No.3-A Gena Williamson, 2037 ft					
	Matrix	**Quartz**	**Chalcedonic Quartz**	**Pellets**	**Pore Spaces**
		1			
	1				
	1				
		1			
		1			
		1			
		1			
	1				
		1			
		1			
		1			
		1			
		1			
		1			
	1				
		1			
		1			
	1				
	1				
		1			
	1				
		1			
		1			

Thin Section I: No.3-A Gena Williamson, 2037 ft					
	Matrix	**Quartz**	**Chalcedonic Quartz**	**Pellets**	**Pore Spaces**
	1				
	1				
	1				
		1			
	1				
		1			
		1			
		1			
		1			
		1			
Total	42	54	2	2	0

Table 19. Point count data derived from thin section J from the No.1 Borders Smith at 2059 ft.

Thin Section J: No.1 Borders Smith, 2059 ft						
	Calcite Cement	**Quartz**	**Chalcedonic Quartz**	**Pellets**	**Pore Spaces**	**Plagioclase**
	1					
			1			
	1					
			1			
			1			
		1				
		1				
				1		
	1					
		1				
	1					
		1				
	1					
		1				
		1				
		1				
			1			
		1				
		1				
		1				
			1			

Thin Section J: No.1 Borders Smith, 2059 ft						
	Calcite Cement	**Quartz**	**Chalcedonic Quartz**	**Pellets**	**Pore Spaces**	**Plagioclase**
		1				
		1				
		1				
	1					
		1				
		1				
	1					
		1				
			1			
		1				
	1					
				1		
		1				
		1				
	1					
		1				
					1	
	1					
			1			
		1				
		1				
	1					
		1				

Thin Section J: No.1 Borders Smith, 2059 ft						
	Calcite Cement	**Quartz**	**Chalcedonic Quartz**	**Pellets**	**Pore Spaces**	**Plagioclase**
		1				
		1				
		1				
			1			
			1			
		1				
		1				
		1				
		1				
		1				
			1			
	1					
		1				
			1			
		1				
			1			
			1			
				1		
						1
	1					
						1
					1	

Thin Section J: No.1 Borders Smith, 2059 ft						
	Calcite Cement	**Quartz**	**Chalcedonic Quartz**	**Pellets**	**Pore Spaces**	**Plagioclase**
		1				
	1					
	1					
		1				
		1				
	1					
		1				
		1				
		1				
		1				
		1				
		1				
		1				
		1				
		1				
		1				
		1				
	1					
	1					
		1				
	1					
		1				
		1				
	1					

Thin Section J: No.1 Borders Smith, 2059 ft						
	Calcite Cement	**Quartz**	**Chalcedonic Quartz**	**Pellets**	**Pore Spaces**	**Plagioclase**
	1					
				1		
		1				
	1					
		1				
		1				
		1				
		1				
		1				
	1					
	1					
		1				
Total	24	55	13	4	2	2

Appendix G – Core Descriptions

Table 20. Core description of the Carthage Gas Unit No.9-4A.

Carthage Gas Unit No.9-4A							
Depth (Ft)	**~Grain Size (mm)**	**Lithology**	**Structures**	**Fossils**	**Other Structures**	**Notes**	**Formation**
1985	0.0625	Shale	Planar laminated			micaceous fissile, green, weathers dingy brown	Brownstown Marl
1985.5	0.0625	Shale	Planar laminated				Brownstown Marl
1986	0.0625	Shale	Planar laminated			micaceous fissile, green, weathers dingy brown	Brownstown Marl
1986.5	0.0625	Shale	Planar laminated				Brownstown Marl
1987	0.0625	Siltstone	Planar laminated			micaceous fissile, green	Blossom Sand
1987.5	0.125	Siltstone	Wavy bedding				Blossom Sand
1988	0.0625	Siltstone	Wavy bedding		scoured surface^ & load cast	fossils in ~1.5 in caclite layer	Blossom Sand
1988.5	0.125	Siltstone	Wavy bedding			calcite nodule ~ 1998.5	Blossom Sand
1989	0.125	Sandstone	Wavy bedding			fine sand interbedded w/ clay. Can see green pellets in microscope	Blossom Sand
1989.5	0.125	Sandstone	Wavy bedding				Blossom Sand

Carthage Gas Unit No.9-4A							
Depth (Ft)	**~Grain Size (mm)**	**Lithology**	**Structures**	**Fossils**	**Other Structures**	**Notes**	**Formation**
1990	0.125	Sandstone	Wavy bedding			heavily bioturbated less clay and pellets	Blossom Sand
1990.5	0.125	Sandstone	Wavy bedding				Blossom Sand
1991	0.125	Sandstone	Wavy bedding			fine sand becomes more homogenous going to 1992, pellets	Blossom Sand
1991.5	0.125	Sandstone	Wavy bedding				Blossom Sand
1992	0.125	Sandstone	Wavy bedding				Blossom Sand
1992.5	0.125	Sandstone	Wavy bedding				Blossom Sand
1993	0.125	Sandstone	Wavy bedding			pellets bit more wavy bedding	Blossom Sand
1993.5	0.125	Sandstone	Wavy bedding				Blossom Sand
1994	0.125	Sandstone	Wavy bedding			~1 in calcite cemented nodule, pellets	Blossom Sand
1994.5	0.125	Sandstone	Wavy bedding				Blossom Sand
1995	0.125	Sandstone	Wavy bedding			pellets	Blossom Sand

Carthage Gas Unit No.9-4A							
Depth (Ft)	**~Grain Size (mm)**	**Lithology**	**Structures**	**Fossils**	**Other Structures**	**Notes**	**Formation**
1995.5	0.125	Sandstone	Wavy bedding				Blossom Sand
1996	0.125	Sandstone	Wavy bedding			calcite cemented, pellets, almost looks like a micrite	Blossom Sand
1996.5	0.125	Sandstone	Wavy bedding				Blossom Sand
1997	0.125	Sandstone	Wavy bedding			calcite cemented burrows, pellets	Blossom Sand
1997.5	0.125	Sandstone	Wavy bedding			calcite cement around burrows too	Blossom Sand
1998	0.125	Sandstone	Wavy bedding			few burrows more pellets, homogenous	Blossom Sand
1998.5	0.125	Sandstone	Wavy bedding			calcite cemented to 1999	Blossom Sand
1999	0.125	Sandstone	Wavy bedding			very friable sands, darker green than the others, pellets	Blossom Sand
1999.5	0.125	Sandstone	Wavy bedding				Blossom Sand
2000	0.125	Sandstone	Wavy bedding			wavy bedding gradually increases from 2000 to 2001	Blossom Sand

Carthage Gas Unit No.9-4A							
Depth (Ft)	**Depth (Ft)**	**Depth (Ft)**	**Depth (Ft)**	**Depth (Ft)**	**Depth (Ft)**	**Depth (Ft)**	**Depth (Ft)**
2000.5	0.125	Sandstone	Wavy bedding				Blossom Sand
2001	0.0625	Sandstone	Wavy bedding			looks like an even distribution of sand and shale	Blossom Sand
2001.5	0.0625	Sandstone	Wavy bedding				Blossom Sand

Carthage Gas Unit No.9-4A							
Depth (Ft)	**~Grain Size (mm)**	**Lithology**	**Structures**	**Fossils**	**Other Structures**	**Notes**	**Formation**
2002.5	0.0625	Sandstone	Wavy bedding				Blossom Sand
2003	0.0625	Sandstone	Wavy bedding	Small burrows			Blossom Sand
2003.5	0.0625	Sandstone	Wavy bedding				Blossom Sand
2004	0.0625	Sandstone	Wavy bedding			fine sand content increasing moving toward 2005	Blossom Sand
2004.5	0.125	Sandstone	Wavy bedding				Blossom Sand
2005	Not Recovered						Blossom Sand
2005.5	Not Recovered						Blossom Sand
2006	Not Recovered						Blossom Sand
2006.5	Not Recovered						Blossom Sand
2007	Not Recovered						Blossom Sand
2007.5	Not Recovered						Blossom Sand
2008	Not Recovered						Blossom Sand
2008.5	Not Recovered						Blossom Sand
2009	Not Recovered						Blossom Sand
2009.5	Not Recovered						Blossom Sand
2010	Not Recovered						Blossom Sand

Carthage Gas Unit No.9-4A							
Depth (Ft)	**~Grain Size (mm)**	**Lithology**	**Structures**	**Fossils**	**Other Structures**	**Notes**	**Formation**
2011	0.0625	Sandstone	Horizontal bedding			calcite cemented, fine sand, pellets	Blossom Sand
2011.5	0.0625	Sandstone	Horizontal bedding				Blossom Sand
2012	0.0625	Sandstone	Horizontal bedding			calcite cemented, fine sand, pellets	Blossom Sand
2012.5	0.0625	Sandstone	Horizontal bedding				Blossom Sand
2013	0.125	Sandstone	Horizontal bedding			calcite cement, pellets	Blossom Sand
2013.5	0.125	Sandstone	Horizontal bedding			pellets	Blossom Sand
2014	0.125	Sandstone	Horizontal bedding			pellets	Blossom Sand
2014.5	0.125	Sandstone	Horizontal bedding				Blossom Sand
2015	0.125	Sandstone	Horizontal bedding			thin shale laminae, pellets	Blossom Sand
2015.5	0.125	Sandstone	Horizontal bedding			no structures	Blossom Sand
2016	0.125	Sandstone	Horizontal bedding			pellets, dime size calcitic nodule ~2016.83	Blossom Sand
2016.5	0.125	Sandstone	Horizontal bedding				Blossom Sand
2017	0.125	Sandstone	Horizontal bedding			pellets	Blossom Sand

Carthage Gas Unit No.9-4A							
Depth (Ft)	**~Grain Size (mm)**	**Lithology**	**Structures**	**Fossils**	**Other Structures**	**Notes**	**Formation**
2018	0.125	Sandstone	Wavy bedding			micaceous, pellets	Blossom Sand
2018.5	0.125	Sandstone	Wavy bedding				Blossom Sand
2019	0.125	Sandstone	Wavy bedding			micaceous, pellets	Blossom Sand
2019.5	0.125	Sandstone	Wavy bedding				Blossom Sand
2020	0.125	Sandstone	Wavy bedding			pellets	Blossom Sand
2020.5	0.125	Sandstone	Wavy bedding			Calcite cemented spot ~3.81 cm	Blossom Sand
2021	0.125	Sandstone	Wavy bedding			sand interbedded with shale	Blossom Sand
2021.5	0.125	Sandstone	Wavy bedding				Blossom Sand
2022	0.125	Sandstone	Wavy bedding			sand interbedded with shale, pyrite in burrows under microscope	Blossom Sand
2022.5	0.125	Shale	Planar laminated	Burrows			Blossom Sand
2023	0.00006	Sandstone	Wavy bedding			First 3 in, are sand with wavy 3-6 in fissile shale	Blossom Sand
2023.5	0.125	Sandstone	Wavy bedding		scoured surface	Go from silt to calcite cemented, laminated sand	Blossom Sand

Carthage Gas Unit No.9-4A							
Depth (Ft)	**~Grain Size (mm)**	**Lithology**	**Structures**	**Fossils**	**Other Structures**	**Notes**	**Formation**
2024	0.125	Sandstone	Horizontal bedding			Right at 2024, calcite cemented, sand/clay	Blossom Sand
2024.5	0.125	Sandstone	Wavy bedding			cemented sand conact	Blossom Sand
2025	0.00006	Sandstone	Wavy bedding			~1 in shale layer at 2025, clay cement	Blossom Sand
2025.5	0.125	Sandstone	Wavy bedding				Blossom Sand
2026	0.125	Sandstone	Wavy bedding			Sand interbedded with clay, clay cement	Blossom Sand
2026.5	0.125	Sandstone	Wavy bedding				Blossom Sand
2027	0.125	Sandstone	Wavy bedding			Tiny Black streaks, look like organic material	Blossom Sand
2027.5	0.125	Sandstone	Wavy bedding	Plant Fragments?		3mm of rip up clasts in somewhat calcitic matrix	Blossom Sand
2028	0.125	Sandstone	Wavy bedding	Burrows		contact @ 2028	Blossom Sand
2028.5	0.125	Sandstone	Wavy bedding				Blossom Sand
2029	0.125	Sandstone	Wavy bedding				Blossom Sand
2029.5	0.125	Sandstone	Wavy bedding				Blossom Sand
2030	0.0625	Sandstone	Wavy bedding	Small burrows			Blossom Sand

Carthage Gas Unit No.9-4A							
Depth (Ft)	**~Grain Size (mm)**	**Lithology**	**Structures**	**Fossils**	**Other Structures**	**Notes**	**Formation**
2030.5	0.0625	Sandstone	Wavy bedding				Blossom Sand
2031	0.00006	Sandstone	Wavy bedding	Small burrows			Blossom Sand
2031.5	0.0625	Shale	Planar laminated			~1 in shale layer @ 2031.5	Blossom Sand
2032	0.0625	Sandstone	Wavy bedding	Small burrows			Blossom Sand
2032.5	0.00006	Shale	Planar laminated				Blossom Sand
2033	0.0625	Sandstone	Wavy bedding	Burrows			Blossom Sand
2033.5	0.0625	Sandstone	Wavy bedding	Small burrows			Blossom Sand
2034	0.0625	Sandstone	Wavy bedding	Small burrows			Blossom Sand
2034.5	0.0625	Sandstone	Wavy bedding	Small burrows			Blossom Sand
2035	0.0625	Sandstone	Wavy bedding	Small burrows		wavy bedding by 2035.5	Blossom Sand
2035.5	0.125	Sandstone	Wavy bedding	Small burrows			Blossom Sand
2036	0.125	Sandstone	Wavy bedding	Burrows		begin seeing siderite nodules ~5mm in diam cc	Blossom Sand
2036.5	0.125	Sandstone	Wavy bedding	Burrows			Blossom Sand
2037	0.125	Sandstone	Wavy bedding	Burrows		siderite nodule ~2cm in diam	Blossom Sand

Carthage Gas Unit No.9-4A							
Depth (Ft)	**~Grain Size (mm)**	**Lithology**	**Structures**	**Fossils**	**Other Structures**	**Notes**	**Formation**
2038	0.125	Sandstone	Wavy bedding	Burrows	scoured surface^ & load cast	siderite streaks with pyrite associated calcite cement	Blossom Sand
2038.5	0.125	Sandstone	Cross bedding		scoured surface^	~2 in of mudstone siderite nodules	Blossom Sand
2039	0.125	Sandstone	Wavy bedding	Burrows			Blossom Sand
2039.5	0.125	Sandstone	Wavy bedding	Burrows		siderite nodules and steaks	Blossom Sand
2040	0.125	Sandstone	Wavy bedding	Burrows		siderite nodule & lookis like there might be a flame cast	Blossom Sand
2040.5	0.125	Sandstone	Wavy bedding	Burrows		primarily clay cement with some calcite	Blossom Sand
2041	0.125	Sandstone	Wavy bedding			grades into silt, cc	Blossom Sand
2041.5	0.031	Sandstone	Wavy bedding	Small burrows			Blossom Sand
2042	0.031	Sandstone	Wavy bedding	Small burrows		random calcite cement	Blossom Sand
2042.5	0.031	Sandstone	Wavy bedding	Small burrows			Blossom Sand
2043	0.031	Sandstone	Wavy bedding	Burrows		calcite cement, siderite, lots of pellets	Blossom Sand

Carthage Gas Unit No.9-4A							
Depth (Ft)	**~Grain Size (mm)**	**Lithology**	**Structures**	**Fossils**	**Other Structures**	**Notes**	**Formation**
2043.5	0.031	Sandstone	Wavy bedding	Burrows		calcite cement siderite	Blossom Sand
2044	0.125	Sandstone	Wavy bedding	Burrows		calcite cement	Blossom Sand

Table 21. Core description of the No.3-A Gena Williamson.

No.3-A Gena Williamson							
Depth (Ft)	**~Grain Size (mm)**	**Lithology**	**Structures**	**Fossils**	**Other Structures**	**Notes**	**Formation**
2026	0.25	Sandstone	Wavy Bedding			Sand interbedded with clay	Blossom Sand
2026.5	0.25	Sandstone	Wavy Bedding				Blossom Sand
2027	0.25	Sandstone	Wavy Bedding			about a foot of this box is missing	Blossom Sand
2027.5	0.25	Sandstone	Wavy Bedding				Blossom Sand
2028	0.25	Sandstone	Wavy Bedding				Blossom Sand
2028.5	0.25	Sandstone	Wavy Bedding			very friable	Blossom Sand
2029	0.125	Sandstone	Wavy Bedding				Blossom Sand
2029.5	0.125	Sandstone	Wavy Bedding			very friable	Blossom Sand
2030	0.125	Sandstone	Wavy Bedding				Blossom Sand
2030.5	0.25	Sandstone	Wavy Bedding			cemented much better,	Blossom Sand
2031	0.25	Sandstone	Wavy Bedding				Blossom Sand
2031.5	0.25	Sandstone	Wavy Bedding			See wavy bedding get more intense	Blossom Sand
2032	0.25	Sandstone	Wavy Bedding			Vertical burrows	Blossom Sand
2032.5	0.25	Sandstone	Wavy Bedding			1 'spot' with calcite cement	Blossom Sand
2033.5	0.25	Sandstone	Wavy Bedding				Blossom Sand

No.3-A Gena Williamson							
Depth (Ft)	**~Grain Size (mm)**	**Lithology**	**Structures**	**Fossils**	**Other Structures**	**Notes**	**Formation**
2034	0.25	Sandstone	Wavy Bedding			still pretty homogenous aside from a burrow or two	Blossom Sand
2034.5		Sandstone	Wavy Bedding				Blossom Sand
2035	0.25	Sandstone	Wavy Bedding			14cm long cal cemented interva, everything else is clay	Blossom Sand
2035.5	0.25	Sandstone	Wavy Bedding				Blossom Sand
2036	0.25	Sandstone	Wavy Bedding				Blossom Sand
2036.5	0.25	Sandstone	Wavy Bedding				Blossom Sand
2037	0.25	Sandstone	Wavy Bedding				Blossom Sand
2037.5	0.25	Sandstone	Wavy Bedding				Blossom Sand
2038	0.25	Sandstone				No distiguishable burrows	Blossom Sand
2038.5	0.25	Sandstone					Blossom Sand
2039	0.25	Sandstone					Blossom Sand
2039.5	0.25	Sandstone					Blossom Sand
2040	0.25	Sandstone	Wavy Bedding			Vertical burrow	Blossom Sand

No.3-A Gena Williamson							
Depth (Ft)	**~Grain Size (mm)**	**Lithology**	**Structures**	**Fossils**	**Other Structures**	**Notes**	**Formation**
2040.5	0.25	Sandstone	Wavy Bedding			with some calcite cement next to the hole left by a plug	Blossom Sand
2041	0.25	Sandstone	Wavy Bedding				Blossom Sand
2041.5	0.25	Sandstone	Wavy Bedding				Blossom Sand
2042	0.25	Sandstone					Blossom Sand
2042.5	0.25	Sandstone					Blossom Sand
2043	0.25	Sandstone					Blossom Sand
2043.5	0.25	Sandstone					Blossom Sand
2044	0.25	Sandstone					Blossom Sand
2044.5	0.25	Sandstone					Blossom Sand
2045	0.25	Sandstone					Blossom Sand
2045.5	0.25	Sandstone				Sand with interbedded shale	Blossom Sand
2046	0.25	Sandstone	Wavy Bedding				Blossom Sand
2046.5	0.25	Sandstone	Wavy Bedding				Blossom Sand
2047	0.25	Sandstone	Wavy Bedding			Calcite cement	Blossom Sand
2047.5	0.25	Sandstone	Wavy Bedding				Blossom Sand

No.3-A Gena Williamson							
Depth (Ft)	**~Grain Size (mm)**	**Lithology**	**Structures**	**Fossils**	**Other Structures**	**Notes**	**Formation**
2048	0.25	Sandstone	Wavy Bedding			Calcite cement	Blossom Sand
2048.5	0.25	Sandstone	Wavy Bedding				Blossom Sand
2049	0.25	Sandstone	Wavy Bedding			Kinda random calcite cement mainly associated with burrows, prolly	Blossom Sand
2049.5	0.25	Sandstone	Wavy Bedding				Blossom Sand
2050	0.25	Sandstone	Wavy Bedding			somewhat random calcite cement	Blossom Sand
2050.5	0.25	Sandstone	Wavy Bedding				Blossom Sand
2051	0.25	Sandstone	Wavy Bedding				Blossom Sand
2051.5	0.25	Sandstone	Wavy Bedding				Blossom Sand
2052	0.25	Sandstone	Wavy Bedding	bivalves		calcite cement	Blossom Sand
2052.5	0.25	Sandstone	Wavy Bedding				Blossom Sand
2053	0.25	Sandstone	Wavy Bedding			interbedded shale	Blossom Sand
2053.5	0.25	Sandstone	Wavy Bedding				Blossom Sand
2054	0.25	Sandstone	Wavy Bedding			tight calcite cement, bivalves 10 mm wide	Blossom Sand

No.3-A Gena Williamson							
Depth (Ft)	**~Grain Size (mm)**	**Lithology**	**Structures**	**Fossils**	**Other Structures**	**Notes**	**Formation**
2054.5	0.25	Sandstone	Wavy Bedding				Blossom Sand
2055	0.25	Sandstone	Wavy Bedding	bivalves			Blossom Sand
2055.5	0.25	Sandstone	Wavy Bedding				Blossom Sand
2056	0.25	Sandstone	Wavy Bedding				Blossom Sand
2056.5	0.25	Sandstone	Wavy Bedding				Blossom Sand
2057	0.25	Sandstone	Wavy Bedding			Calcite cement	Blossom Sand
2057.5	0.25	Sandstone	Wavy Bedding				Blossom Sand
2058	0.25	Sandstone	Wavy Bedding	bivalves		tight calcite cement	Blossom Sand
2058.5	0.25	Sandstone	Wavy Bedding			lost the calcite cement	Blossom Sand
2059	0.25	Sandstone					Blossom Sand
2059.5	0.25	Sandstone	Wavy Bedding				Blossom Sand
2060	0.25	Sandstone	Wavy Bedding			no calcite cement, sand interbedded with shale	Blossom Sand
2060.5	0.25	Sandstone	Wavy Bedding				Blossom Sand
2061	0.25	Sandstone	Wavy Bedding				Blossom Sand
2061.5	0.25	Sandstone	Wavy Bedding				Blossom Sand

No.3-A Gena Williamson							
Depth (Ft)	**~Grain Size (mm)**	**Lithology**	**Structures**	**Fossils**	**Other Structures**	**Notes**	**Formation**
2062	0.25	Sandstone	Wavy Bedding			Some calcite associated with burrows	Blossom Sand

Table 22. Core description of the Werner Smith No.1-A.

Werner Smith No.1-A							
Depth (Ft)	**~Grain Size (mm)**	**Lithology**	**Structures**	**Fossils**	**Other Structures**	**Notes**	**Formation**
2007	0.031	Siltstone	Laminae	Burrows		Laminated	Brownstown
2007.5	0.031	Siltstone	Laminae	Burrows			Brownstown
2008	0.031	Siltstone	Laminae	Bivalves		Laminated	Brownstown
2008.5	0.031	Siltstone	Laminae	Burrows			Brownstown
2009	0.031	Siltstone	Laminae	Burrows		laminated, one large calcite cemented burrow	Brownstown
2009.5	0.031	Siltstone	Laminae	Burrows			Brownstown
2010	0.031	Siltstone	Laminae	Burrows		no bioturbation to speak of but there is a burrow	Brownstown
2010.5	0.031	Siltstone	Laminae	Burrows			Brownstown
2011	0.031	Siltstone	Laminae	Burrows		Laminated	Brownstown
2011.5	0.031	Siltstone	Laminae	Burrows			Brownstown
2012	0.031	Siltstone	Laminae	Burrows		Laminated	Brownstown
2012.5	0.031	Siltstone	Laminae	Burrows			Brownstown
2013	0.031	Siltstone	Laminae	Burrows		Laminated	Brownstown
2013.5	0.031	Siltstone	Laminae	Burrows			Brownstown
2014	0.031	Siltstone	Laminae	Burrows		Less laminated, wavier	Brownstown
2014.5	0.031	Siltstone	Laminae	Burrows		probably fewer pellets	Brownstown
2015	0.031	Siltstone	Wavy bedding	Inoceramus		less lam	Brownstown
2015.5	0.031	Siltstone	Wavy bedding	Burrows		Inoceramus	Brownstown

Werner Smith No.1-A							
Depth (Ft)	**~Grain Size (mm)**	**Lithology**	**Structures**	**Fossils**	**Other Structures**	**Notes**	**Formation**
2016	0.031	Siltstone	Wavy bedding	Shark tooth			Brownstown
2016.5	0.031	Siltstone	Wavy bedding	Burrows			Brownstown
2017	0.125	Sandstone	Wavy bedding	Burrows		Probably some wavy bedding, no lam, maybe a few burrows, hard to tell with uncut butt ends, no calcite cement	Blossom Sand
2017.5	0.125	Sandstone	Wavy bedding	Burrows			Blossom Sand
2018	0.125	Sandstone	Wavy bedding	Burrows		Same thing here, uncut buttend, clay cement	Blossom Sand
2018.5	0.125	Sandstone	Wavy bedding	Burrows			Blossom Sand
2019	0.125	Sandstone	Wavy bedding	Burrows		Same thing here, uncut buttend	Blossom Sand
2019.5	0.125	Sandstone	Wavy bedding	Burrows			Blossom Sand
2020	0.125	Sandstone	Wavy bedding	Burrows		Clay interbedded with sand	Blossom Sand
2020.5	0.125	Sandstone	Wavy bedding	Burrows			Blossom Sand
2021	0.125	Sandstone	Wavy bedding	Burrows		Clay interbedded with sand clay cement	Blossom Sand

Werner Smith No.1-A							
Depth (Ft)	**~Grain Size (mm)**	**Lithology**	**Structures**	**Fossils**	**Other Structures**	**Notes**	**Formation**
2021.5	0.125	Sandstone	Wavy bedding	Burrows			Blossom Sand
2022	0.125	Sandstone	Wavy bedding	Burrows		clay interbedded with sand caly cement	Blossom Sand
2022.5	0.125	Sandstone	Wavy bedding	Burrows		picks up calcite cement at ~2022.83	Blossom Sand
2023	0.125	Sandstone	Wavy bedding	Burrows		Calcite cement	Blossom Sand
2023.5	0.125	Sandstone	Wavy bedding	Burrows			Blossom Sand
2024	0.125	Sandstone	Wavy bedding	Burrows		Big clay filled burrows, calcite cement	Blossom Sand
2024.5	0.125	Sandstone	Wavy bedding	Burrows		Fecal pellets	Blossom Sand
2025	0.25	Sandstone	Wavy bedding	Burrows		LOTS of burrows	Blossom Sand
2025.5	0.25	Sandstone	Wavy bedding	Burrows		sand interbedded with mon	Blossom Sand
2026	0.25	Sandstone	Wavy bedding	Burrows		Calcite cement, sand interbedded with clay	Blossom Sand
2026.5	0.25	Sandstone	Wavy bedding	Burrows		lose calcite ~2006.5	Blossom Sand
2027	0.25	Sandstone	Wavy bedding	Burrows		still heavy bioturbation	Blossom Sand
2027.5	0.25	Sandstone	Wavy bedding	Burrows			Blossom Sand

Werner Smith No.1-A							
Depth (Ft)	**~Grain Size (mm)**	**Lithology**	**Structures**	**Fossils**	**Other Structures**	**Notes**	**Formation**
2028	0.25	Sandstone	Wavy bedding	Burrows		still heavy bioturbation	Blossom Sand
2028.5	0.25	Sandstone	Wavy bedding	Burrows			Blossom Sand
2029	0.25	Sandstone	Wavy bedding	Burrows			Blossom Sand
2029.5	0.25	Sandstone	Wavy bedding	Burrows		Fecal pellets aren't green, brownish orange instead	Blossom Sand
2030	0.25	Sandstone	Wavy bedding	Burrows			Blossom Sand
2030.5	0.25	Sandstone	Wavy bedding	Burrows			Blossom Sand
2031	0.25	Sandstone	Wavy bedding	Burrows		some clay interbedded with sand	Blossom Sand
2031.5	0.25	Sandstone	Wavy bedding	Burrows			Blossom Sand
2032	0.25	Sandstone	Wavy bedding	Burrows		clay interbedded with sand	Blossom Sand
2032.5	0.25	Sandstone	Wavy bedding	Burrows		clay interbedded with sand	Blossom Sand
2033	0.25	Sandstone	Wavy bedding	Burrows		clay interbedded with sand	Blossom Sand
2033.5	0.125	Sandstone	Wavy bedding	Burrows		clay interbedded with sand	Blossom Sand
2034	0.125	Sandstone	Wavy bedding	Burrows		clay interbedded with sand	Blossom Sand

Werner Smith No.1-A							
Depth (Ft)	**~Grain Size (mm)**	**Lithology**	**Structures**	**Fossils**	**Other Structures**	**Notes**	**Formation**
2034.5	0.125	Sandstone	Wavy bedding	Burrows		clay interbedded with sand	Blossom Sand
2035	0.125	Sandstone	Wavy bedding	Burrows		clay interbedded with sand	Blossom Sand
2035.5	0.125	Sandstone	Wavy bedding	Burrows		clay interbedded with sand	Blossom Sand
2036	0.125	Sandstone	Wavy bedding	Burrows		clay interbedded with sand	Blossom Sand
2036.5	0.125	Sandstone	Wavy bedding	Burrows		Losing the micas @ 2036	Blossom Sand
2037	0.25	Sandstone	Wavy bedding	Burrows		clay interbedded with sandstone	Blossom Sand
2037.5	0.5	Sandstone	Wavy bedding	Burrows			Blossom Sand
2038	0.5	Sandstone	Wavy bedding	Burrows		Pretty homogenous, Except for a few burrows	Blossom Sand
2038.5	0.5	Sandstone	Wavy bedding	Burrows			Blossom Sand
2039	0.5	Sandstone	Wavy bedding	Burrows		Again, pretty homogenous, exc for a burrow or two	Blossom Sand
2039.5	0.5	Sandstone	Wavy bedding	Burrows			Blossom Sand
2040	0.5	Sandstone		Burrows		Homogenous sands, 1 burrow	Blossom Sand

Werner Smith No.1-A							
Depth (Ft)	**~Grain Size (mm)**	**Lithology**	**Structures**	**Fossils**	**Other Structures**	**Notes**	**Formation**
2040.5	0.5	Sandstone		Burrows		5.5 mm diam calcite cemented spot	Blossom Sand
2041	0.5	Sandstone				Homogenous sands	Blossom Sand
2041.5	0.5	Sandstone					Blossom Sand
2042	0.5	Sandstone	Wavy bedding	Burrows		very little calcite cement	Blossom Sand
2042.5	0.5	Sandstone		Burrows			Blossom Sand
2043	0.5	Sandstone				Calcite cement	Blossom Sand
2043.5	0.5	Sandstone				back to clay	Blossom Sand
2044	0.25	Sandstone	Wavy bedding	Burrows		2 in wide calcite cemented vein	Blossom Sand
2044.5	0.25	Sandstone	Wavy bedding	Burrows			Blossom Sand
2045	0.25	Sandstone	Wavy bedding	Burrows		~1 in shale layer right above 2045	Blossom Sand
2045.5	0.25	Sandstone	Wavy bedding	Burrows			Blossom Sand
2046	0.125	Sandstone	Wavy bedding	Burrows		calcite cement	Blossom Sand

Table 23. Core description of the No.1 Borders Smith.

No.1 Borders Smith							
Depth (Ft)	**~Grain Size (mm)**	**Lithology**	**Structures**	**Fossils**	**Other Structures**	**Notes**	**Formation**
2010	0.031	Sandstone	Wavy Bedding			Clay cement, calcareous concretion ~8 cm in diameter	Blossom Sand
2010.5	0.031	Sandstone	Wavy Bedding			Fossil shaped like a crab clay & calcitic	Blossom Sand
2011	0.031	Sandstone	Wavy Bedding			clay cement	Blossom Sand
2011.5	0.031	Sandstone	Wavy Bedding				Blossom Sand
2012	0.031	Sandstone	Wavy Bedding			calcite concretion, clay cement	Blossom Sand
2012.5	0.031	Sandstone	Wavy Bedding				Blossom Sand
2013	0.031	Sandstone	Wavy Bedding				Blossom Sand
2013.5	0.031	Sandstone	Wavy Bedding				Blossom Sand
2014	0.031	Sandstone	Wavy Bedding				Blossom Sand
2014.5	0.031	Sandstone	Wavy Bedding				Blossom Sand
2015	0.031	Sandstone	Wavy Bedding				Blossom Sand
2015.5	0.031	Sandstone	Wavy Bedding				Blossom Sand
2016	0.031	Sandstone	Wavy Bedding				Blossom Sand
2016.5	0.031	Sandstone	Wavy Bedding			No idea what this fossil is	Blossom Sand

No.1 Borders Smith							
Depth (Ft)	**~Grain Size (mm)**	**Lithology**	**Structures**	**Fossils**	**Other Structures**	**Notes**	**Formation**
2017	0.031	Sandstone	Wavy Bedding				Blossom Sand
2017.5	0.031	Sandstone	Wavy Bedding				Blossom Sand
2018	0.031	Sandstone	Wavy Bedding				Blossom Sand
2018.5	0.031	Sandstone	Wavy Bedding				Blossom Sand
2019	0.031	Sandstone	Wavy Bedding				Blossom Sand
2019.5	0.031	Sandstone	Wavy Bedding				Blossom Sand
2020	0.031	Sandstone	Wavy Bedding			super fine sand interbedded with clays	Blossom Sand
2020.5	0.031	Sandstone	Wavy Bedding	Bivs, Shark tooth		Tooth ~6mm long, 3-4 bivs that I can't ID	Blossom Sand
2021	0.031	Sandstone	Wavy Bedding	Bivalves		Super fine sand, interbedded with clay	Blossom Sand
2021.5	0.031	Sandstone	Wavy Bedding				Blossom Sand
2022	0.1	Sandstone	Wavy Bedding	Bivalves			Blossom Sand
2022.5	0.1	Sandstone	Wavy Bedding				Blossom Sand
2023	0.1	Sandstone	Wavy Bedding				Blossom Sand
2023.5	0.1	Sandstone	Wavy Bedding				Blossom Sand

No.1 Borders Smith							
Depth (Ft)	**~Grain Size (mm)**	**Lithology**	**Structures**	**Fossils**	**Other Structures**	**Notes**	**Formation**
2024	0.1	Sandstone	Wavy Bedding	Inoceramus		starting to see some of these clay filled burrows	Blossom Sand
2024.5	0.1	Sandstone	Wavy Bedding				Blossom Sand
2025	0.1	Sandstone	Wavy Bedding	Burrows			Blossom Sand
2025.5	0.125	Sandstone	Wavy Bedding	Burrows		sand interbedded with shale	Blossom Sand
2026	0.125	Sandstone	Wavy Bedding	Burrows		sand interbedded with shale	Blossom Sand
2026.5		Not Recovered					Blossom Sand
2027	0.125	Sandstone	Wavy Bedding	Burrows			Blossom Sand
2027.5	0.125	Sandstone	Wavy Bedding	Burrows			Blossom Sand
2028	0.125	Sandstone	Wavy Bedding	Burrows			Blossom Sand
2028.5	0.125	Sandstone	Wavy Bedding	Burrows		Shale interbedded with sand	Blossom Sand
2029	0.125	Sandstone	Wavy Bedding	Burrows		Same as above, hard to tell if its wavy bedded or bioturbation	Blossom Sand
2029.5	0.125	Sandstone	Wavy Bedding	Burrows			Blossom Sand
2030	0.25	Sandstone	Wavy Bedding	Burrows		same as above	Blossom Sand

No.1 Borders Smith							
Depth (Ft)	**~Grain Size (mm)**	**Lithology**	**Structures**	**Fossils**	**Other Structures**	**Notes**	**Formation**
2030.5	0.25	Sandstone	Wavy Bedding	Burrows			Blossom Sand
2031	0.25	Sandstone	Wavy Bedding	Burrows		Calcite cement	Blossom Sand
2031.5	0.25	Sandstone	Wavy Bedding	Burrows			Blossom Sand
2032	0.25	Sandstone	Wavy Bedding	Burrows		Calcite cement	Blossom Sand
2032.5	0.25	Sandstone	Wavy Bedding	Burrows		lost the calcite cement	Blossom Sand
2033	0.25	Sandstone	Wavy Bedding	Burrows		two 2-3 cm wide shale layers	Blossom Sand
2033.5	0.25	Sandstone	Wavy Bedding	Burrows			Blossom Sand
2034	0.25	Sandstone	Wavy Bedding	Inoceramus			Blossom Sand
2034.5	0.25	Sandstone	Wavy Bedding	Burrows			Blossom Sand
2035	0.25	Sandstone	Wavy Bedding	Burrows			Blossom Sand
2035.5	0.25	Sandstone	Wavy Bedding	Burrows			Blossom Sand
2036	0.25	Sandstone	Wavy Bedding	Burrows		Calcite cemented ~8cm wide	Blossom Sand
2036.5	0.25	Sandstone	Wavy Bedding	Burrows			Blossom Sand
2037	0.25	Sandstone	Wavy Bedding	Burrows		sand with interbedded shale	Blossom Sand
2037.5	0.25	Sandstone	Wavy Bedding	Burrows			Blossom Sand

No.1 Borders Smith							
Depth (Ft)	**~Grain Size (mm)**	**Lithology**	**Structures**	**Fossils**	**Other Structures**	**Notes**	**Formation**
2038	0.25	Sandstone	Wavy Bedding	Burrows		sand with interbedded shale	Blossom Sand
2038.5	0.25	Sandstone	Wavy Bedding	Burrows			Blossom Sand
2039	0.25	Sandstone	Wavy Bedding	Burrows		sand with interbedded shale	Blossom Sand
2039.5	0.25	Sandstone	Wavy Bedding	Burrows			Blossom Sand
2040	0.25	Sandstone	Wavy Bedding	Burrows		11cm wide calcite cemented sand at 2040	Blossom Sand
2040.5	0.25	Sandstone	Wavy Bedding	Burrows		Calcite cement	Blossom Sand
2041	0.25	Sandstone	Wavy Bedding	Burrows		Calcite cement	Blossom Sand
2041.5	0.25	Sandstone	Wavy Bedding	Burrows		Calcite cement	Blossom Sand
2042	0.25	Sandstone	Wavy Bedding	Burrows		calcite cement @ ~2042.33	Blossom Sand
2042.5	0.25	Sandstone	Wavy Bedding	Burrows		lose calcite back to clay	Blossom Sand
2043	0.25	Sandstone	Wavy Bedding	Burrows			Blossom Sand
2043.5	0.25	Sandstone	Wavy Bedding	Burrows			Blossom Sand
2044	0.25	Sandstone	Wavy Bedding	Burrows			Blossom Sand
2044.5	0.25	Sandstone	Wavy Bedding	Burrows			Blossom Sand

No.1 Borders Smith							
Depth (Ft)	**~Grain Size (mm)**	**Lithology**	**Structures**	**Fossils**	**Other Structures**	**Notes**	**Formation**
2045	0.25	Sandstone	Wavy Bedding	Burrows			Blossom Sand
2045.5	0.25	Sandstone	Wavy Bedding	Burrows			Blossom Sand
2046	0.25	Sandstone	Wavy Bedding	Burrows			Blossom Sand
2046.5	0.25	Sandstone	Wavy Bedding	Burrows			Blossom Sand
2047	0.25	Sandstone	Wavy Bedding	Burrows		Big clay filled burrows and random calcite cemented,	Blossom Sand
2047.5	0.25	Sandstone	Wavy Bedding	Burrows			Blossom Sand
2048	0.25	Sandstone	Wavy Bedding	Burrows			Blossom Sand
2048.5	0.25	Sandstone	Wavy Bedding	Burrows		ramonly calcite cemented	Blossom Sand
2049	0.25	Sandstone	Wavy Bedding	Burrows		Calcite cement	Blossom Sand
2049.5	0.25	Sandstone	Wavy Bedding	Burrows			Blossom Sand
2050	0.25	Sandstone	Wavy Bedding	Burrows		Calcite cement	Blossom Sand
2050.5	0.25	Sandstone	Wavy Bedding	Burrows			Blossom Sand
2051	0.25	Sandstone	Wavy Bedding	Burrows			Blossom Sand
2051.5	0.25	Sandstone	Wavy Bedding	Burrows			Blossom Sand
2052	0.25	Sandstone	Wavy Bedding	Burrows		calcite cement	Blossom Sand

No.1 Borders Smith							
Depth (Ft)	**~Grain Size (mm)**	**Lithology**	**Structures**	**Fossils**	**Other Structures**	**Notes**	**Formation**
2052.5	0.25	Sandstone	Wavy Bedding	Burrows			Blossom Sand
2053	0.25	Sandstone	Wavy Bedding	Burrows		calcite cement	Blossom Sand
2053.5	0.25	Sandstone	Wavy Bedding	Burrows			Blossom Sand
2054	0.25	Sandstone	Wavy Bedding	Burrows		Calcite cement	Blossom Sand
2054.5	0.25	Sandstone	Wavy Bedding	Burrows			Blossom Sand
2055	0.25	Sandstone	Wavy Bedding	Burrows			Blossom Sand
2055.5	0.25	Sandstone	Wavy Bedding	Burrows			Blossom Sand
2056	0.25	Sandstone	Wavy Bedding	Burrows			Blossom Sand
2056.5	0.25	Sandstone	Wavy Bedding	Burrows			Blossom Sand
2057	0.25	Sandstone	Wavy Bedding	Burrows			Blossom Sand
2057.5	0.25	Sandstone	Wavy Bedding	Burrows			Blossom Sand
2058	0.25	Sandstone	Wavy Bedding	Burrows			Blossom Sand
2058.5	0.25	Sandstone	Wavy Bedding	Burrows			Blossom Sand
2059	0.25	Sandstone	Wavy Bedding	Burrows			Blossom Sand
2059.5	0.25	Sandstone	Wavy Bedding	Burrows		Calcite cement	Blossom Sand
2060	0.25	Sandstone	Wavy Bedding	Burrows		Calcite cement	Blossom Sand

No.1 Borders Smith							
Depth (Ft)	**~Grain Size (mm)**	**Lithology**	**Structures**	**Fossils**	**Other Structures**	**Notes**	**Formation**
2060.5	0.25	Sandstone	Wavy Bedding	Burrows			Blossom Sand
2061	0.25	Sandstone	Wavy Bedding	Burrows			Blossom Sand
2061.5	0.25	Sandstone	Wavy Bedding	Burrows			Blossom Sand
2062	0.25	Sandstone	Wavy Bedding	Burrows			Blossom Sand
2062.5	0.25	Sandstone	Wavy Bedding	Burrows			Blossom Sand
2063	0.25	Sandstone	Wavy Bedding	Burrows			Blossom Sand
2063.5	0.25	Sandstone	Wavy Bedding	Burrows		Calcite cement	Blossom Sand

Table 24. Core description of the Carthage Gas Unit No.9-5A.

Carthage Gas Unit No.9-5A							
Depth (Ft)	**~Grain Size (mm)**	**Lithology**	**Structures**	**Fossils**	**Other Structures**	**Notes**	**Formation**
1986	0.0006	Siltstone	Laminae	Bivalve		1 tiny bivalve	Blossom Sand
1986.5	0.0625	Siltstone	Wavy Bedding	Burrows			Blossom Sand
1987	0.0625	Siltstone	Wavy Bedding	Bivalves & Burrows		5cm diameter bivalves clay cement until this point	Blossom Sand
1987.5	0.0625	Siltstone	Wavy Bedding			~5 cm diameter clay nodule	Blossom Sand
1988	0.0625	Siltstone	Wavy Bedding	Bivalves & Burrows			Blossom Sand
1988.5	0.0625	Siltstone	Wavy Bedding				Blossom Sand
1989	0.0625	Siltstone	Wavy Bedding	Bivalves & Burrows		sand interbedded with shale	Blossom Sand
1989.5	0.125	Sandstone	Wavy Bedding	Burrows		sand interbedded with shale	Blossom Sand
1990	0.125	Sandstone	Wavy Bedding	Burrows		sand interbedded with shale	Blossom Sand
1990.5	0.125	Sandstone	Wavy Bedding	Burrows			Blossom Sand
1991	0.125	Sandstone	Wavy Bedding	Burrows		sand interbedded with shale	Blossom Sand
1991.5	0.125	Sandstone	Wavy Bedding	Burrows		sand interbedded with shale	Blossom Sand
1992	0.125	Sandstone	Wavy Bedding	Burrows		sand interbedded with shale	Blossom Sand

Carthage Gas Unit No.9-5A							
Depth (Ft)	**~Grain Size (mm)**	**Lithology**	**Structures**	**Fossils**	**Other Structures**	**Notes**	**Formation**
1992.5	0.125	Sandstone	Wavy Bedding	Burrows		sand interbedded with shale	Blossom Sand
1993	0.125	Sandstone	Wavy Bedding	Burrows		sand interbedded with shale	Blossom Sand
1993.5	0.125	Sandstone	Wavy Bedding	Burrows		calcite cemented nodule @ 1992.83 ~6cm wide.	Blossom Sand
1994	0.125	Sandstone	Wavy Bedding	Burrows		sand interbedded with shale	Blossom Sand
1994.5	0.125	Sandstone	Wavy Bedding	Burrows		calcite cemented nodule with giant burrow	Blossom Sand
1995	0.125	Sandstone	Wavy Bedding	Burrows		lots of horizontal burrows	Blossom Sand
1995.5	0.125	Sandstone	Wavy Bedding	Burrows			Blossom Sand
1996	0.125	Sandstone	Wavy Bedding	Burrows		little less wavy bedding	Blossom Sand
1996.5	0.125	Sandstone	Wavy Bedding	Burrows			Blossom Sand
1997	0.5	Sandstone	Wavy Bedding	Burrows		large burrows full of green clay	Blossom Sand
1997.5	0.5	Sandstone	Wavy Bedding	Burrows		sand is a little coarser	Blossom Sand
1998	0.5	Sandstone	Wavy Bedding	Burrows		large burrows full of clay	Blossom Sand
1998.5	0.5	Sandstone	Wavy Bedding	Burrows			Blossom Sand

Carthage Gas Unit No.9-5A							
Depth (Ft)	**~Grain Size (mm)**	**Lithology**	**Structures**	**Fossils**	**Other Structures**	**Notes**	**Formation**
1999	0.5	Sandstone	Wavy Bedding	Burrows		some large burrows, calcite cement,	Blossom Sand
1999.5	0.5	Sandstone	Wavy Bedding	Burrows			Blossom Sand
2000	0.5	Sandstone	Wavy Bedding	Burrows		large burrows, calcite cement	Blossom Sand
2000.5	0.5	Sandstone	Wavy Bedding	Burrows			Blossom Sand
2001	0.5	Sandstone	Wavy Bedding	Burrows		clay filled burrows calcite cemented	Blossom Sand
2001.5	0.5	Sandstone	Wavy Bedding	Burrows			Blossom Sand
2002	0.5	Sandstone	Wavy Bedding	Burrows		clay filled, burrows, calcite cement	Blossom Sand
2002.5	0.0625	Siltstone	Wavy Bedding	Burrows		small burrows	Blossom Sand
2003	0.0625	Siltstone	Wavy Bedding	Burrows		small burrows	Blossom Sand
2003.5	0.0625	Siltstone	Wavy Bedding	Burrows			Blossom Sand
2004	0.0625	Siltstone	Wavy Bedding	Burrows		small burrows	Blossom Sand

Appendix H– Stratigraphy of the Austin Group

The lowermost of these formations is the Early Coniacian Ector. This formation consists of chalk deposited on a shallow marine inner shelf (Pearson, 2012; Rogers, 1968; Young, 1963). While clean chalk is the primary component of the Ector, it is interbedded with brown to grey, fissile shales as well as shaly, glauconitic chalks containing *Gryphaea aucella* and *Radiolites austinensis* fossils (Rogers, 1968).

The Late Coniacian to Early Santonian offshore shales of the Bonham Clay conformably overly the Ector (Rogers, 1968; Young, 1963). This 150 to 200 feet thick formation is primarily composed of fissile shales, and grey, calcareous shales. Interbedded with the primary lithologies of the Bonham Clay are beds of medium to fine-grained glauconitic sandstones (Rogers, 1968). The Bonham Clay contains *Inoceramus*, *Ostrea congesta*, *Baculites asper*, and *Gryphaea aucella* fossils (Stephenson, 1918).

The uppermost formation of the Austin Group is the Late Santonian to Early Campanian Brownstown Marl that conformably overlies the Blossom Sand (Rogers, 1968; Young, 1963). This unit can be as thick as 155 feet. The uppermost section of the Brownstown Marl is composed of offshore marls followed by grey, fissile, calcareous shales, which can be locally fossiliferous (Rogers, 1968). Fossils found in the Brownstown Marl include primarily bivalve mollusks such as *Exogyra ponderosa*, *Turritella quadrilla*, and *Paranomia scabra* (Stephenson, 1918). The primary sediments of this formation are interbedded with lenses of fine grained, glauconitic, calcareous sandstones, as well as brown sandy shales (Rogers, 1968).

Appendix I – Detailed Methods

A combination of XRD, XRF, SEM, petrophysical analysis, and core analysis were used in this study to determine depositional and diagenetic history, along with controls on porosity and permeability. The primary source of data are five cores collected from Panola County, TX and archived in the East Texas Core Repository, Stephen F. Austin State University, Nacogdoches, TX (Table 1). The cores have a combined length of 216 feet. All five of the cores include butt ends, with one of the five containing an interval of seven slab packs.

A detailed description of each core noted sedimentary structures, grain sizes, fossils and lithologies, which were used to determine the Blossom Sand's depositional environment. Lithofacies were correlated across the five cores.

Ten thin sections were made by National Petrographic to analyze grain size distribution, identify porosity types and sedimentary petrography. Locations for thin sections were chosen based on XRD and XRF data. The thin sections were impregnated with blue epoxy to highlight porosity. The thin sections were analyzed using a Labomed Lx POL Polarizing microscope.

To obtain grain size distributions, a photo of each thin section was taken under 400x magnification in cross polarized light. ImageJ was used to perform particle analysis and point counting on each of the photos. The scale was set in each photo and using the gridding tool, 500 points were placed on the images. At each point the mineralogy was noted which helped to identify accessory minerals whose percentages would have been

too inadequate to have been recognized by the XRD. The grids were removed from the images that were then converted to a 16-bit image. The converted images were then processed to highlight individual grains to make polygons that could be measured for area in square millimeters. Each image yielded areas for approximately 500 polygons. The areas were uploaded into Excel where the square root was taken for each measurement to obtain grain sizes in mm which were then converted to ϕ scale. Each thin section was analyzed under 400x magnification under cross polarized light and plane polarized light to observe primary and secondary porosity and any secondary minerals precipitated in pore spaces that were seen constricting porosity.

XRD was used to identify the bulk mineralogy on four samples. Samples for XRD were chosen based on lithologic changes, and sample prep followed Eberl (2008). The samples were ground using a porcelain mortar and pestle and then sieved using a 250 µm mesh sieve. Two grams of the sieved sample were added to 0.5 grams of ground corundum. The combined sample and corundum were milled in a McCrone Micronizing mill along with 5 ml of isopropyl alcohol for five minutes. The sample was placed into an oven at 80°C for 24 hours or until all of the isopropyl alcohol evaporated. The dried sample was gently ground back into a powder using an agate mortar and pestle, and placed into a test tube with 0.5 ml of hexane and shaken for ten minutes. Afterward, the sample was sieved once more using a 250 µm sieve. The sample was placed into a custom side-loading holder, with a piece of plexiglass with 600 grit sandpaper affixed to the opening. The samples were run on a Bruker D8 Advance diffractometer with an angle

range from 5 to 65 2Θ, a step size of 0.02 2Θ, 2 seconds per step, and a voltage/amp of 40 kV/40 mA. The resulting data was analyzed for mineral content and quantity using RockJock from the USGS (Eberl, 2008).

Trace elemental analysis was conducted using the Thermo Fisher Scientific Niton XL3t GOLDD^{+} XRF Analyzer. The device was set to the Test All Geo setting and used to sample each of the five cores at a resolution of four inches for a total of 180 seconds (30 seconds main, low and high each, and 90 seconds on light). Prior to sampling, any debris on the core was brushed off and each core was rinsed with deionized water and dried overnight. To ensure that measurements properly represented the lithologies and minerals present in any given location, anomalies such as lone body fossils, and small concretions (<10 cm in diameter) were avoided. A specific location was recorded for each reading to reference at any later time.The resulting geochemical data was processed in Excel. Areas containing abundances of Fe, Al and Mg were identified as areas of high clay content. Areas containing high concentrations of Ca were identified as areas of high calcite content. Having determined the clay and calcite content throughout the core, locations were chosen for porosity and permeability measurements to be taken.

Eleven plugs were extracted from the core to obtain porosity and permeability measurements by Stratum Reservoir, Houston, TX. Locations for the plugs were chosen based on the varying amount of clay minerals throughout the core that were identified from the geochemical data. The eleven plugs were taken from areas exhibiting high, moderate and low clay content. Samples were convection dried at 140°C. The porosity

and permeability were then taken at a net confining stress of 800 psi, following protocols at Stratum Reservoir. The permeability measurements were corrected using the Klinkenberg method.

Sampling locations for SEM were chosen based on the concentration of Fe, Ca, Al, Si and Mg from the XRF data. To obtain higher quality images, chips of samples were coated with gold and vanadium to increase their conductivity. Using a JEOL Scanning Electron Microscope, SEM was conducted on four samples to help provide insight as to the origin of the glauconite and the order of events that occurred as diagenesis progressed within the Blossom Sand. These images displayed the orientation of the sand grains, clay minerals, pore spaces, and any other clays that were present.

Vita

Hannah Chambers is a graduate of Mississippi State University where she received her B.S. in geology in 2019. Hannah is currently a graduate student at Stephen F. Austin State University where she will graduate with an M.S. in geology in May 2021. Her thesis research focuses on defining the depositional environment and diagenetic features of the Blossom Sand in Panola County, Texas. Hannah is a member of AAPG and SGE and is recognized as a Geologist-In-Training by the Mississippi Board of Registered Professional Geologists.

Permanent Address: 6233 MS Hwy 12
Ackerman, MS 39735

This thesis was typed by Hannah C. Chambers in accordance with GSA guidelines